Line Trier Aslesen
Stian Hollund
Artur Szymon Zebrowski

# Pre-feasability study for hybridization of Achwa 2 hydropower plant with usage of PV-system

Bachelor's project in Renewable Energy Engineering
Supervisor: Kjell Kolsaker
May 2019

Bachelor's project

NTNU
Norwegian University of Science and Technology
Faculty of Engineering
Department of Energy and Process Engineering

NTNU
Norwegian University of
Science and Technology

Norwegian University of Science and Technology
Department of Energy and Process Engineering

| **Project title:** | **Submission deadline:** |
| --- | --- |
| Pre-feasibility study for hybridization of Achwa 2 hydropower plant with usage of PV-system | 24.05.2019 |
| **Oppgavenes tittel:** | **Number of pages/appendices:** |
| Forstudie for hybridisering av Achwa 2 vannkraftverk med bruk av PV-anlegg | 84/6 |
| **Project participants:** | **Supervisor:** |
| Line Trier Aslesen<br>Stian Hollund<br>Artur Szymon Żebrowski | Kjell Kolsaker<br>email: kjell.kolsaker@ntnu.no<br>tel.: 735 92 509 |
| **Program of study:** | **Project number:** |
| Renewable energy engineering | FEN1908 |
| **Client:** | **Assignment provider:** |
| Multiconsult ASA | Stanislas Merlet<br>email: stanislas.merlet@multiconsult.no<br>tel.: 911 31 493 |

Free for publication [X]

Fritt tilgjengelig [X]

## Preamble

This thesis is the final project in the bachelor's degree in renewable energy engineering at the Norwegian University of Science and Technology (NTNU), written by Stian Hollund, Line Trier Aslesen and Artur Szymon Żebrowski. The scope of the thesis is 20 ECTS, equivalent of 500 work hours per student.

The bachelor thesis concerns a hybrid solution between the existing hydropower plant, Achwa 2, and a simulated PV plant. The assignment was given by the Norwegian consulting company Multiconsult. Feasible solutions for hybridization by analyzing various technologies were investigated, resulting in a proposal for the best case.

The group would like to thank the external mentor from Multiconsult, Stanislas Merlet, for sharing information and knowledge, and for good help along the way. Furthermore, we would like to give our thanks to Edgar Ogume Buza, working for ARPE Limited, representing Achwa 2 HPP, for much needed and important data. Finally we would like to thank our internal mentor, Kjell Kolsaker, for guidance and knowledgeable input during this project period.

Trondheim, May 23, 2019

Line Trier Aslesen

Stian Hollund

Artur Szymon Żebrowski

# Abstract

As of 2019, Uganda relies on further power capacity expansion to satisfy the increasing demand for electricity. In this report, the possibility of hybridization of a hydropower plant with a photovoltaic plant in northern Uganda is being reviewed.

To investigate this, literature searches have been conducted to acquire knowledge of the necessary theory and later used to propose a solution. In situations where information could not be obtained, several assumptions have been made in consultation with supervisors to minimize potential errors. Based on simulated annual production data and water flow information from Achwa river, a model has been created describing hydropower production in the Achwa 2 hydropower plant. Additionally, a load profile estimate has been created, to find the approximated demand for electricity in Pader, Kitgum and Gulu districts. Based on this, four different cases have been produced, including use of monofacial and bifacial PV panels with different mounting systems and installed capacity. These cases have been simulated using the computer software, PVsyst and Matlab, to find the most optimal alternative. Economical aspects as well as synergy for all cases have been examined to conclude on which one is most suitable for Achwa 2 hydropower plant.

Simulation results indicate that all four cases are feasible with financial profit. The best case involved construction of a 20 MWp solar power plant with bifacial panels and horizontal single axis tracking. Although this case required the largest investment costs, it resulted in the highest net present value after 25 years, with the lowest levelized cost of electricity of 6.48 US cents/kWh, and the shortest energy payback time of 4.48 years. By using Matlab, it was calculated that the average annual production from the hybrid power plant reached 60 MWp in the month of August. The average daily production was produced for the month of June. Combined generation in the 24 hour span increased by 13 MW between 6 AM and 7 PM, and was significantly influenced by the implemented horizontal single axial tracking system. In conclusion, hybridizing Achwa 2 with PV system could contribute to diversifying of the power generation sources, thus stabilizing the energy supply in the area.

# Sammendrag

Per 2019 er Uganda avhengig av videre kraftutbygging for å tilfredsstille det økende behovet for elektrisitet. I denne rapporten blir muligheten for hybridisering av et vannkraftverk med solkraft i nord-Uganda undersøkt.

For å undersøke dette, har det blitt gjennomført litteratursøk for å erverve kunnskap om nødvendig teori og anvende denne til å foreslå en løsning. I situasjoner der informasjon ikke kunne oppdrives har det blitt gjort flere antagelser i samråd med veiledere for å minimere potensielle feilkilder. Basert på årlig simulert produksjonsdata og vannføringsdata i Achwa-elven har det blitt laget en modell som beskriver vannkraftproduksjonen i Achwa 2 vannkraftverk. I tillegg til dette har det blitt laget et estimat for behovet etter elektrisitet i distriktene Pader, Kitgum og Gulu. Forslag til koblingskjema og reguleringssystem har også blitt produsert for dette hybridkraftverket. På bakgrunn av dette, har det blitt utarbeidet fire ulike scenarioer, med en- og dobbelsidige solpaneller med bestemt helning og solfølging og ulik installert kapasitet. Disse scenarioene har blitt simulert i programvarene PVsyst og Matlab, for å finne den mest optimale varianten. Økonomiske aspekter og synergi for alle scenarioene har også blitt undersøkt for å komme fram til en konklusjon om hvilket scenario som egner seg mest for Achwa 2 vannkraftverk.

Simuleringsresultater tilsier at alle fire solkraftscenarioer er gjennomførbare med økonomisk gevinst. Det beste scenarioet innebar utbygging av et 20 MW solkraftverk med dobbeltsidige panel med solfølging. Selv om dette scenarioet innebar den største investeringskostnaden, resulterte det i den høyeste nåverdien etter 25 år, den laveste LCOE på 6.48 US cent/kWh samt den korteste energitilbakebetalingstiden på 4,48 år. Ved bruk av Matlab ble det beregnet at årlig produksjon fra hybridkraftverket nådde 60 MWp i august. Gjennomsnittlig daglig produksjon i juni økte med 13 MW mellom klokken 06:00 og klokken 19:00, og var betydelig påvirket av det implementerte HSAT systemet. Dermed kan det konkluderes med at hybridisering av Achwa 2 med solkraft kan bidra til å mangfoldiggjøre energikildene, og dermed stabilisere energiforsyningen i området.

# List of symbols and abbreviations

### Latin letters

| | | |
|---|---|---|
| $g$ | Gravitational acceleration | [m/s$^2$] |
| $h$ | Elevation difference between inlet and outlet | [m] |
| $I$ | Current | [A] |
| $P$ | Power | [W] |
| $Q$ | Water flow rate | [m$^3$/s] |
| $S$ | Apparent power | [VA] |
| $V$ | Voltage | [V] |
| $W_p$ | Watt peak | [W] |

### Greek letters

| | | |
|---|---|---|
| $\eta$ | Efficiency | [-] |
| $\rho$ | Density | [kg/m$^3$] |

# List of terms

| | |
|---|---|
| **AC** | Alternating current |
| **BOS** | Balance of system |
| **CAPEX** | Capital expenditures |
| **DC** | Direct current |
| **DHI** | Diffuse Horizontal Irradiance |
| **DNI** | Direct Normal Irradiance |
| **EMS** | Energy Management System |
| **EPBT** | Energy payback time |
| **EROI** | Energy return on investment |
| **FIT** | Feed-in tariff |
| **FPV** | Floating Photovoltaic |
| **GHI** | Global Horizontal Irradiance |
| **HPP** | Hydro power plant |
| **HRES** | Hybrid renewable energy system |
| **HSAT** | Horizontal Single Axial Tracking |
| **IEEE** | Institute of Electrical and Electronics Engineers |
| **LCOE** | Levelized cost of energy |
| **LID** | Light induced degradation |
| **MASL** | Meters above sea level |
| **MPPT** | Maximum power point tracking |
| **NPV** | Net present value |
| **NREL** | National Renewable Energy Laboratory |
| **OPEX** | Operation expenditures |
| **O&M** | Operations and maintenance |
| **PED** | Primary energy demand |
| **PID** | Potential induced degradation |
| **PV** | Photovoltaic |
| **REFIT** | Renewable energy feed-in tariff |
| **RPM** | Revolutions per minute |
| **SCADA** | Supervisory control and data acquisition |
| **STC** | Standard test conditions |

# Table of Content

# List of Figures

# List of Tables

# 1 Introduction

## 1.1 Background

Since the industrial revolution, humans have been searching for the best energy source available. For many decades coal and oil were two prime and fundamental materials used to generate electricity worldwide. In the last decade, the focus have changed from fossil to renewable energy sources. Both technological advancements and increasing climate changes in the world, were significant factors in development of new ways to harvest energy.

There are many different ways to incorporate renewable energy sources and one of them is to merge hydro- and solar power. Water can be stored in certain HPP reservoirs thus working as an easily accessible battery to produce energy when needed. Photovoltaic sources rely on the amount of sunlight and therefore cannot produce reliable electricity at command. By combining both suppliers in areas where both dry and wet season occurs, it is possible to level the energy production creating more stable power generation.

Solar power have in recent years ascended on the energy market worldwide. Global annual PV capacity have since 2015 doubled in value and there are currently no signs of it slowing down. Even though global cumulative PV installations are rapidly growing, Africa places last, having the biggest PV potential. This slow development is caused mostly due to lacking amount of resources as well as economical support in the region. Uganda, in contrast to some African states, has a good potential for renewable resources because of its ample fertile land, regular rainfall as well as mineral deposits.[1]

Nevertheless, most recent studies shows that only about 26.7% of population in Uganda has access to electricity.[2] Given that amount, electricity generation contributes to 1.4% of the total national energy balance in the country. The remains are generated through biomass and oil products, that represent 89% and 9.7% of the total energy consumption respectively. Those sources are mainly used in vehicles and thermal power plants.[3]

Uganda has an installed capacity of 957.7 MW, where 743 MW comes from hydropower sources. The demand for electricity has been rising at an average of 10% per annum, mainly due to the fact of a conspicuous GDP growth in the country at approximately 6% over the past two decades.[4] To improve electricity production and advance unstable, renewable energy sources, it has been proposed to combine multiple power harvesting technologies and create hybrid power plants.

## 1.2 Problem definition

Based on the 2017 study from International hydropower association Uganda has one of the lowest electricity consumption in the world despite having a large hydropower potential. By extending electricity access nationwide Uganda's government wants to elevate people from poverty line as well as behold stable economical growth. Investment in hydro sources, which as for 2019 represent $\sim 80\%$ of the total energy production, can result in insufficient delivery of power across the country in dry seasons.[4]

Depending only on hydro sources can be challenging, and that is why implementing PV facility to a hydropower plant can theoretically contribute to increased and more stable power production. Usage of innovative photovoltaic technologies, like bifacial panels and sun trackers, is suggested to improve overall generation in comparison to standard plant designs. This thesis concentrates on the newly built Achwa 2 HPP located in northern Uganda and its potential for PV plant integration with different system designs.

Derived from the previous section, the following questions can be asked:

- Can Achwa 2 HPP be hybridized with economically viable solar power production supplementing?
- Would hybridization minimize annual power generation fluctuations?
- What PV design would be the most efficient based on different technological advancements?

## 1.3 Objectives

This thesis examines the feasibility of hybridization of Achwa 2 Hydroelectric Power Plant in Uganda by integrating a photovoltaic plant. To achieve this, the following objectives have been formed:

1. Analyze meteorological aspects on the site location and how they can influence PV production.
2. Examine Achwa 2 HPP power generation and grid connections.
3. Design an optimized system model of a hybrid power plant to levelize seasonal fluctuation in renewable generation and capacity, based on various photovoltaic systems.
4. Develop a simulation model for hydro/PV hybridization.
5. Analyze power balance for the hybrid plant.
6. Create a techno-economic model.

## 1.4 Thesis outline

**Chapter 1** presents the thesis synopsis, including problem definition as well as established objectives for hybridization of the power plant.

**Chapter 2** provides the relevant theory segment. This chapter is divided in five different sections, each one exploring theory behind multiple aspects of this thesis' main topic.

**Chapter 3** analyzes various features of the hydroelectric Achwa 2 power plant, as well as presenting calculations for its power production.

**Chapter 4** provides a suggestion of photovoltaic power plant designs along with a detailed analysis of meteorological conditions on the site location. This chapter works as a base for further hybrid power plant study.

**Chapter 5** presents case synopsis together with simulations from PVsyst and Matlab. The final results are presented here, in addition to approaches for optimization of the hybrid plant.

**Chapter 6** contains economical assessments of the hybrid power plant; feed-in-tarrifs and cost analysis of the PV plant.

**Chapter 7** is the main discussion section of this thesis. In this chapter evaluation of earlier presented features and results from both power plants are included.

**Chapter 8** gives the final conclusion to the problem statements in the thesis by summing up the discussion chapter, along with suggestions for further work.

## 1.5 Methodology

This thesis is a product of multiple, critical literature reviews, data collections, correspondences and meetings. All methods used to obtain relevant information followed given guidelines to gratify NTNU's standards. Meetings with the university guidance counselor were done to receive continuous feedback and expertise. All data simulations have been reviewed by a mentor from Multiconsult.

# 2 Theory

## 2.1 Meteorology

### 2.1.1 Albedo

The albedo effect is used to evaluate the surface's ability to reflect sunlight on a scale from 0 to 1. Bright surfaces, such as snow or ice, have high albedo between 0.6 and 0.8, whilst dark surfaces, like asphalt or water, absorb the light and therefore have low albedo values.[5] This effect is essential for correct placing of the bifacial solar panels which will be discussed in later sections. Figure 2.1.1 under illustrates albedo on land surfaces.

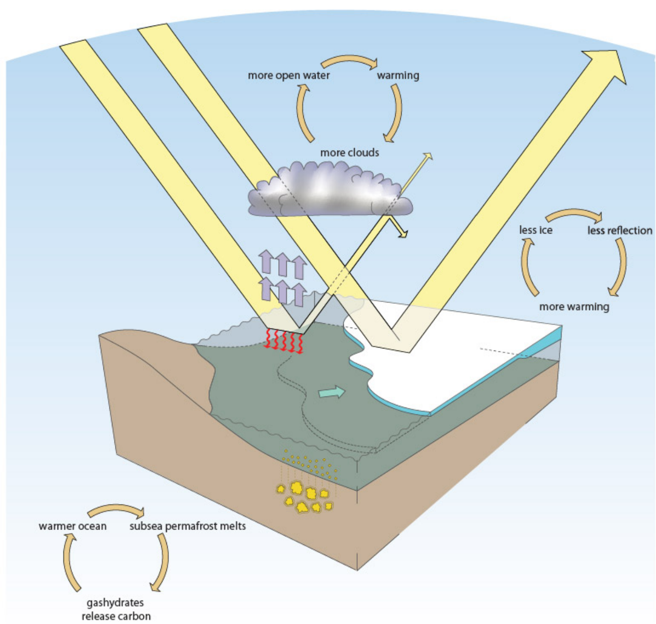


**Figure 2.1.1:** *Illustration of the albedo effect on land.[6]*

### 2.1.2 Solar irradiance

Irradiance can be defined as the amount of flux density of radiant energy from one object that hits one square meter of another surface each second. As an example, the irradiance from the Sun that hits the surface of the Earth, is called solar irradiance, and is measured in the SI unit $kW/m^2$.[7]

Direct Normal Irradiance (DNI) is light energy received per unit area perpendicular to the surface in a direct path from the sun. From a non-direct path perspective, Diffuse Horizontal Irradiance (DHI) is light energy received per unit area from the Sun from all directions, i.e. scattered by molecules in the atmosphere. Global Horizontal Irradiance (GHI) is the total irradiance received on a surface, and can be found using equation 2.1.1 by summing the DNI and DHI, where the $z$ variable represents the zenith angle of the Sun.

$$GHI = DNI + DHI \times cos(z) \tag{2.1.1}$$

### 2.1.3 Sun path

In a spherical coordinate system, the azimuth is an angular measurement along the horizon, while the altitude defines the angle between the horizon and zenith, describing the angle of the Sun. This is illustrated in figure 2.1.2. The azimuth is declared by 0 directly South for the Northern hemisphere and North for the Southern hemisphere. In a direction to the east of due south the azimuth is at -90°, and to the west of due south is +90°. The ratio of azimuth and altitude can also be declared by the horizontal coordinate system, which can be plotted against each other, giving a sun path diagram (iso shading) for a specific location through out a year.[8]

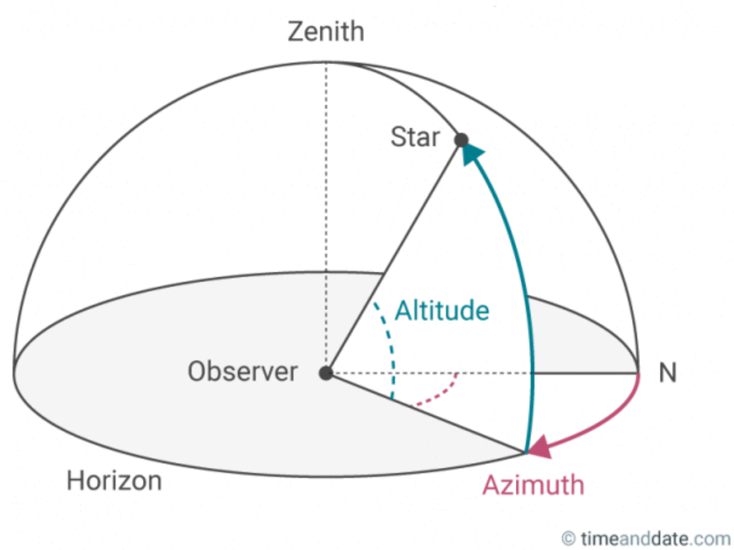


**Figure 2.1.2:** *Illustration of angle measurements.[8]*

## 2.2 Hydropower

### 2.2.1 Principles and types of hydropower

The principle behind electricity generation from hydropower, is using the kinetic energy of flowing water. Achieving this can be done by several different methods. The international hydropower association describes four broad different typologies of hydropower production.[9]

1. Run-of-the-river hydropower
2. Storage hydropower
3. Pumped storage hydropower
4. Offshore hydropower, i.e. power from tidal waves

In this thesis, a run-of-the-river hydropower plant in the Republic of Uganda is examined. Run-of-the-river hydropower plants generates electricity from flowing water that is diverted from a river through a channel or penstock. The diverted water travels through a turbine before it is returned to the river through a tailrace canal. Most of these hydropower plants do not have reservoirs to store the water over longer periods of time, which in turn makes the capacity factor lower compared to storage hydropower plants.

A short term storage, also called pondage, is usually built behind the weir. Pondages are significantly smaller than reservoirs, but serve the same purpose over shorter periods of time, i.e. hours or days. In most cases, pondage stores energy when the demand is low resulting in peaking power plants in dry seasons and base load in wet seasons. The lack of large reservoirs also makes those types of hydropower plants more feasible where the river has a year-round sufficient supply of flowing water.[10] In figure 2.2.1, a simple illustration of a hydropower plant is shown.

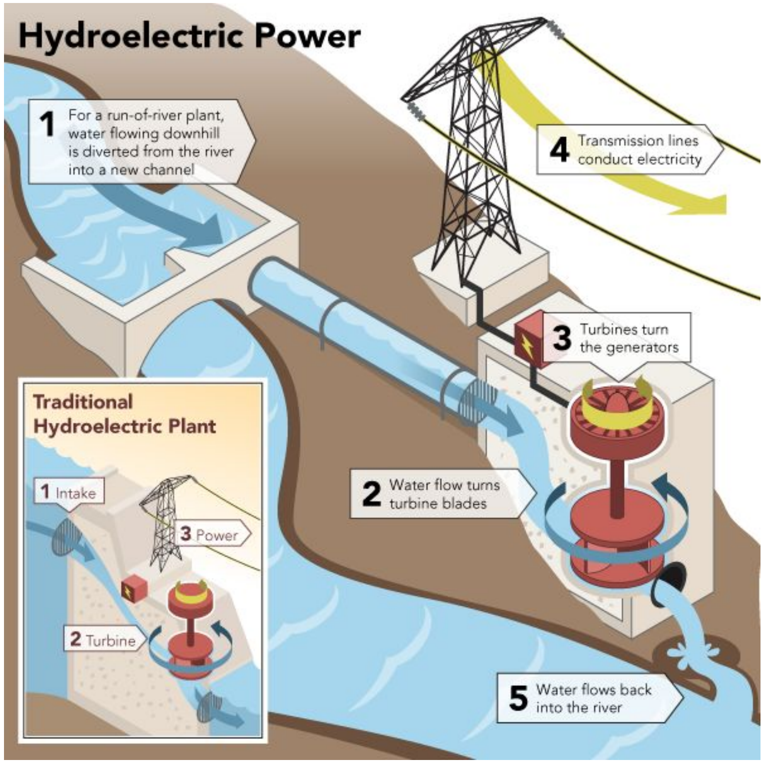


**Figure 2.2.1:** *Illustration of a working system in a run-of-the-river and a traditional hydropower plant.[11]*

Several factors affect the amount of available power in flowing water, and can be calculated from equation 2.2.1. The power is expressed in watts.

$$P = \eta \rho Q g h \tag{2.2.1}$$

Usually, hydropower plants are categorized by size. In this case, size does not represent the area the power plant occupies, but rather the capacity of the power plant given in watts. Large hydropower plants have a capacity of more than 10 MW, while small hydropower plants have a capacity of less than 10 MW. Small hydropower plants can be further divided into mini power plants that have a capacity between 100 kw and 1 MW and micro power plants that have a capacity of less than 100 kW.[12]

One of the benefits of hydropower, is that typically they can handle the variability of photovoltaic power production. PV production will be greatest during the dry season, while hydropower production is greatest during the wet season. This complementing effect, synergy, will be examined further in this thesis.

## 2.3 Photovoltaics

### 2.3.1 Revision of PV panel types

Photovoltaic cells produce energy based on photovoltaic effect where two solar irritated materials, in most cases a mixture of silicon (Si) with boron (B) and phosphorus (P), conduct electrons from one side to another by fulfilling the octet rule raising electrons to the higher energy state. The negative doped side, which is made of a mix of silicon and phosphorus have more negative charged electrons than the opposite positive doped side with boron as a supplement to silicon. Photons from the sunlight hit the n-side with enough energy to force electrons to jump through a membrane to the boron mixed side. Electrons are then conducted back to the original plate, creating electricity and repeating the cycle over again.[13]

There are currently two major ways to structure solar irritated panels by, which are singlejunction and multijunction. Singlejunction cells characterizes in use of only one n- and p-side for each cell, while mulitjunction combines multiple n- and p-doped mix of materials to gain the wider light spectrum which increases efficiency. Monocrystalline-, polycrystalline- and thin film- are currently the three main types of singlejunction cells, widely available on the market. Concentrated PV panels are typical for use of multijunction cells and are usually more expensive to produce.[13] The main differences between those four technologies have been put together in table 2.3.1.

The values in table 2.3.1 can vary significantly from tests in laboratory to real life use outdoors. Based on Fraunhofer data, record efficiency increase for monocrystalline panels, is equal to 11%. In the same test, performance raised up with 76% for thin film, giving the maximal theoretical efficiency of 22.9%.[1]

**Table 2.3.1:** *List of main differences between most common PV cell types.[14]*

| Type of PV cells | Thin film (A-Si) (CdTe) (CIGS) | Polycrystalline (p-Si) | Monocrystalline (Mono-Si) | Concentrated PV (CVP) |
|---|---|---|---|---|
| Junction | Singlejunction | | | Multijunction |
| Efficiency range | ∼7-13% | ∼12-16% | ∼15-24% | ∼46%< |
| Advantages | Low produciton costs, Easy to produce, Flexible | Relative low price | High efficiency rate, Optimized for commercial use, High life-time value | Very high performance, High efficiency rate |
| Disadvantages | Short warranties, Relative short lifespam, Low efficiency range | Sensitive to high temperatures, Medium efficiency range | Expensive to produce | Solar tracker & cooling system needed to reach best results, Expensive to produce |

Each of the PV cell types are based on the same principle of n- and p-doped sides described above, but the main differences are in material usage and components design. This results in different efficiency range, from theoretical 86.8% for concentrated PV cells to 7% for thin film as well as price differences.[14] Visual differences are presented in the figure 2.3.1.

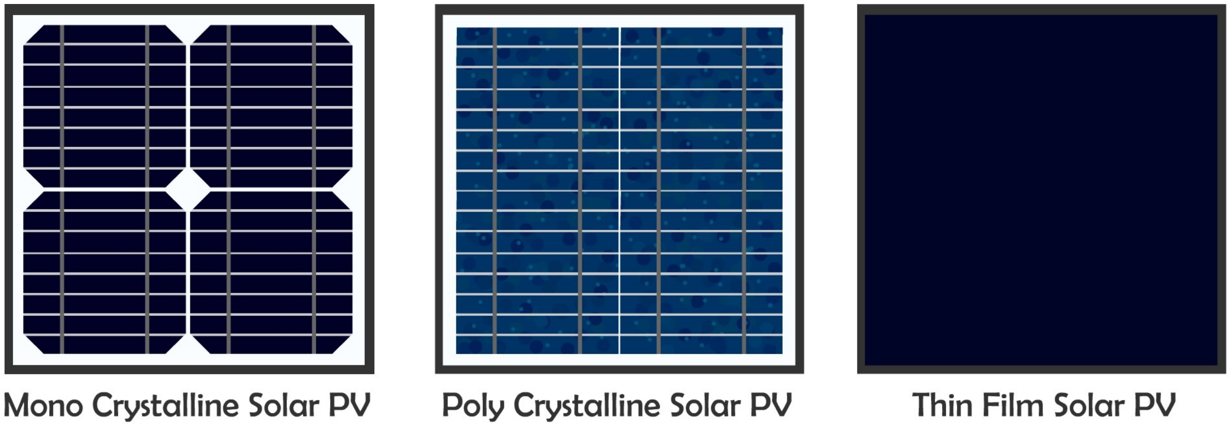


**Figure 2.3.1:** *Most common PV cell types.[15]*

### 2.3.2 Bifacial PV

PV panels are by definition, a collection of photovoltaic modules divided in cells, connected together side by side. PV arrays are sets of multiple panels and most of them consist of one sided PV cells, which absorb sunlight on one side dedicated to this task.

Bifacial PV cells have the advantage of creating direct current from both sides of the same PV unit. Since each surface is sealed with glass, some photons will go through the cell and reflect from the ground possibly hitting the next solar panel. This has been illustrated in figure 2.3.2. Energy production from such panels requires it to effectively obtain sunlight reflected from other surfaces. Implementing bifacial technology to a PV power plant involves wider distances from each PV panel string as well as higher constructed frames above ground level.

This technology relies on surroundings with high albedo effect to produce efficient amount of energy whilst being cost effective. Various studies show that by applying bifacial solar cells in areas with high albedo effect, both LCOE and payback time will decline. It is calculated that albedo between 0.2 and 0.8 can increase power generation by $\sim 15\%$ up to $\sim 30\%$.[16, 17]

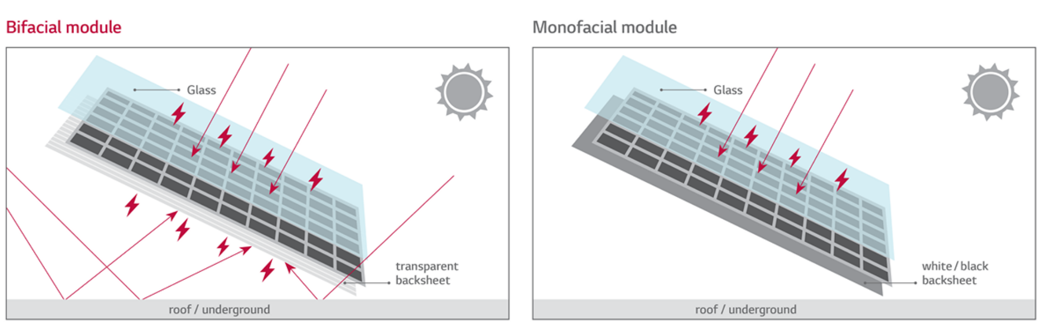


**Figure 2.3.2:** *Difference between light absorption from bi- and monofacial solar modules.[18]*

### 2.3.3 Tilt

The amount of absorbed sunlight that can be transformed into energy depends on the angle between the module and the sun. When the PV is perpendicular to the sun, the power density is at its maximum. In figure 2.3.3 the radiation incident on a tilted surface ($S_{module}$), the horizontal surface($S_{horizontal}$), and the solar radiation perpendicular to the sun($S_{incident}$), are shown.[19]

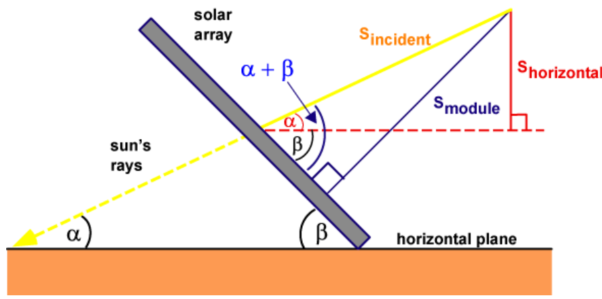


**Figure 2.3.3:** *Illustration of a PV on a tilted surface.[19]*

Equation 2.3.1 and equation 2.3.2 shows the connection between the different radiations.

$$S_{horizontal} = S_{incident} \cdot sin\alpha \qquad (2.3.1)$$

$$S_{module} = S_{incident} \cdot sin(\alpha + \beta) \qquad (2.3.2)$$

### 2.3.4 Tracking

Tracking technology is used to maximize the absorption of sunlight by constantly changing the tilt and position of a PV panel. The change of orientation increases the performance and thus results in higher power generation. Most common tracking systems are based on either single or axial tracker. Possible plant configurations are presented in figure 2.3.4.

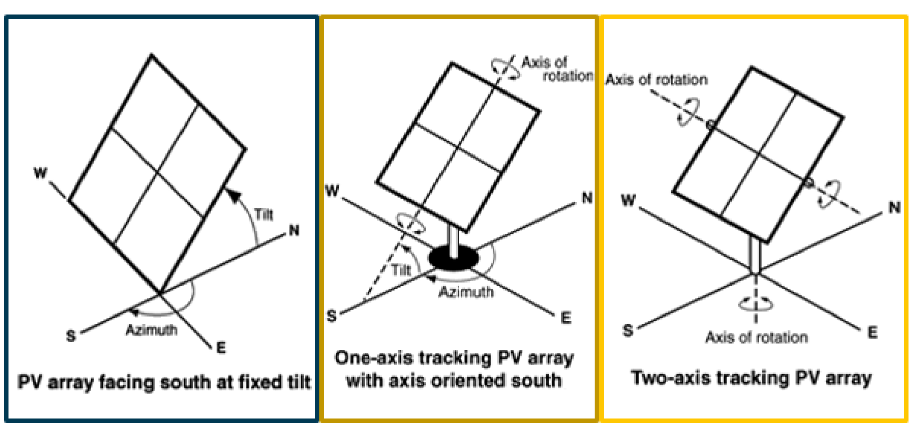


**Figure 2.3.4:** *Illustration of different PV trackers.[20]*

### 2.3.5 PV inverter

As photovoltaics generate DC power and electrical grids demand AC power, an inverter is needed to invert direct current to alternating current. The inverter use semiconductor switches that are periodically connected to a DC input terminal, resulting in AC voltage as the output. Switching causes the current to change direction, thus creating a sine curve. In order to match the frequency of the grid, typically 50 Hz or 60 Hz, this switching has to happen 50 or 60 times per second respectively.[21]

Inverting from DC to AC is not the only task of an inverter. The key tasks for an inverter in a PV system can be divided into the following:

1. Inverting DC to AC
2. Maximum power point tracking (MPPT)
3. Temperature management
4. Sensors for plant monitoring
5. Anti-islanding

Modern inverters may have an efficiency of 98% when operating at maximum efficiency. This means that there will always be a minimum of 2% loss, due to heating. In order to minimize the losses in the inverter, temperature management is important.[22]

MPPT involves the inverter tracking the maximum power point. This point is dependent on several factors, including solar irradiance intensity and temperature, and will therefore change a lot during the day and time of year. Tracking this point is crucial for maximizing the energy output of the PV system.

Depending on the location of the PV system, different topologies or layouts may be utilized in order to achieve maximum power point tracking. The main types of inverters for photovoltaic applications are central, string and micro. Central inverters require that all photovoltaic elements are connected in series thus working as one unit. This type of inverter is typically used in large power plants. String inverters are typically used in smaller plants with photovoltaics connected in series representing a string, with an inverter attached to each string. The micro inverter is an integrated inverter meant for single panel use, and typically has a range of 50 - 400 W.[23]

Islanding is a situation in which the PV plant continue to generate power to the grid when the power from the electric utility does not. This situation becomes dangerous when maintenance workers believing that there is no power present, when in reality it is still powered by other sources than the utility. Islanding may also cause voltage fluctuations causing damages to electrical equipment. Therefore, anti-islanding is an important feature of the inverter.[23]

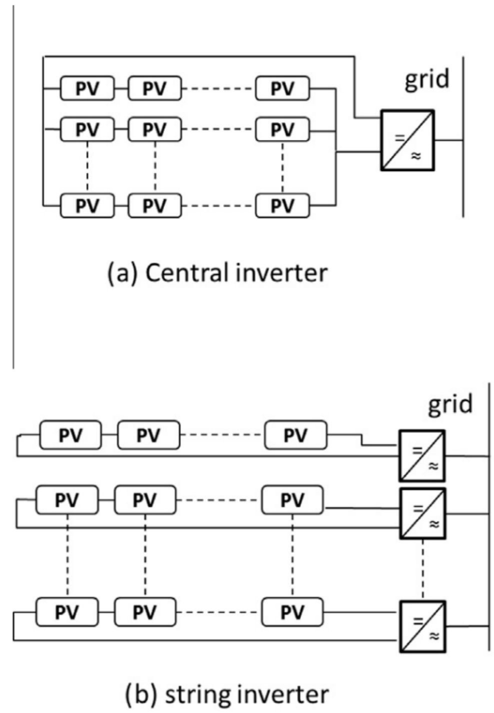


**Figure 2.3.5:** *Illustration of string vs. central inverter layout.[24]*

### 2.3.6 MPPT

Different environmental effects like irradiation on PV cells, the temperature of cells and shading affect the power production from photovoltaics. PV systems possesses different current-voltage (I-V) and power-voltage (P-V) characteristics that vary with these environmental effects. The environmental effects strengthen the non-linearity of these characteristics. Therefore, in order to optimize the power production from photovoltaics, tracking the maximum power point in the different characteristics is of great importance.[23]

As the potential site for the PV-system experience varying weather throughout the year, the needed MPPT system have to be able to account for non-uniform environmental conditions. In order to track the maximum power point, the power-voltage characteristics of the PV can be analyzed. The maximal power point will then be located at the peak of the plot, with decreasing power production to the left and right of this point.[23] Introducing the derivative of the voltage in regard to the derivative of the power, the following statements concerning the location of the maximum power point can be formulated:

$$\frac{dV}{dP} > 0 \tag{2.3.3}$$

Equation 2.3.3 indicates that the given point is located left of the maximum power point.

$$\frac{dV}{dP} = 0 \tag{2.3.4}$$

Equation 2.3.4 indicates that the given point is located at the maximum power point.

$$\frac{dV}{dP} < 0 \tag{2.3.5}$$

Equation 2.3.5 indicates that the given point is located right of the maximum power point.

### 2.3.7 Losses

There are many different factors that can influence efficiency of a solar plant. Each component and connection creates some losses that could affect the final energy production. This subchapter will present following causes of system deficits: DC-losses, inverter clipping, connections between components, low availability of the system, system degradation, soiling, tilt and orientation, incidence angle modifier and environmental conditions.

LID- and PID-losses are two, of several different types of DC-losses. These factors can reduce the amount of DC energy that is produced by the solar plant, before the energy is converted into AC by the inverter. LID-losses occur over the first few days after installation due to exposure to sunlight on the solar cells and only applies for crystalline modules. PID-losses occur when modules operate at high voltages and thus impact the ions negatively. This reduces the power output of a PV-module within the first year of operation. When the maximum DC output is greater than the amount of DC power the inverter can convert, the inverter will operate at a non-optimal point on the IV power curve. The amount of power lost in the production compared to what the system would have produced, if it had not been limited by the rating of the inverter, is called inverter clipping. This phenomenon tends to occur under clear sky conditions when solar irradiation is strong.[25, 26]

Internal resistance in wires depends on the gauge of the cable as well as its length. The resistive losses can be reduced by thickening the gauge although resulting in higher costs. Another cause of decreased production is low availability of the system. Each system has to capture threatening situations that disturb the production negatively, and shut them down if necessary. Examples of some threats include inverter failures and grid outages or disconnections. If specific action is not carried out, the system fails and production is affected by high losses.

Solar cells are built of materials that have to withstand drastic weather conditions throughout their lifespan and with that, lose their efficiency over time. Thermal expansion, UV-light and damage from windblown particles are just few factors that increase production losses over time. When the electrical connections are weakened, losses within the cell are created. Moreover, decreased shunt resistance causes the current to "leak" within a cell instead of being used to power loads. This can damage layers in front of the cells and thus reduce the available light absorption.

Soiling has also an effect on the losses within the PV system. The soiling losses define the amount of sunlight blocked by debris, dirt and bird droppings, which accumulate on the solar panels over time. To prevent major buildup, panels should be cleaned periodically.

The angle of solar panels has an impact on the amount of total irradiance received on the system over a course of a year. IAM- or Incidence Angle Modifier losses, account for lower transmissions of light through the glass when the sunlight enters at a specific angle. To minimize IAM-losses, modules have to be tilted at an angle below latitude value, and be oriented towards equator.

Environmental losses, consist majorly of shading mismatch between modules on the same string and cell temperature losses. The higher the temperature gets, the less efficient solar panels become. The reason for this is that higher cell temperature reduces the amount of available energy from absorbed photons as they flow through the solar panel.[25]

## 2.4 Power evacuation

### 2.4.1 Duck curve

The Duck curve is a graph that shows the timing imbalance between solar energy production and peak demand over the course of a day. In most energy markets, the peak demand occurs early in the mornings and after sunset, which naturally is when the solar power is no longer available, or at its lowest. The duck curve-shape appears reasoning the fact that the graph is composed of a line of demand for electrical power, and a line for the supply of other energy sources when some of the demand is met by solar. When the solar power produces the most, in mid-day, the other energy sources decreases.[27, 28] This is shown in figure 2.4.1, where the upper line (blue) is the electricity demand, the mid-line (orange) is supply of other energy sources and the one at the bottom (grey) is the solar power. The presented graph was made for this thesis as an example model.

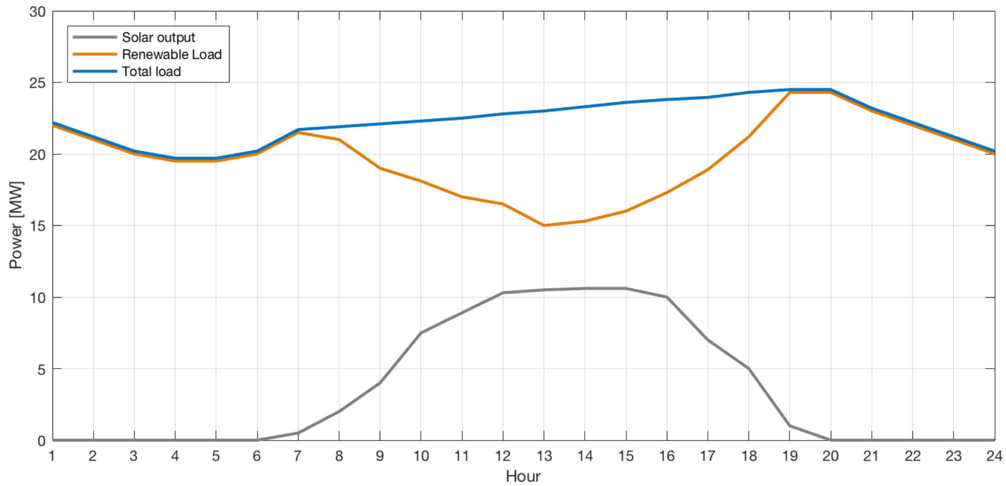


**Figure 2.4.1:** *The Duck curve*

### 2.4.2 Transformer

A transformer is an electrical machine used to transform electrical energy from one energy level to another. By using electromagnetic induction in a specially designed coil with an exact number of wiring turns on each side, transformers can increase or decrease both voltage and current between two systems. This component is connected between inverter or generator and grid to adjust alternating voltage from the power plant, in order for it to be transferred further into the grid network.[29]

### 2.4.3 Grid

The grid compose the link between the producers of power supply and the consumers of electricity, and is an important infrastructure. There are three different types of grid, which are transmission lines, distribution lines and the regional grid. Transmission lines combines large producers and consumers in a nationwide system, as well as distribute foreign relations. The distribution line is the local power line, which provide smaller consumers with power. The regional grid often combine the two previously mentioned, and can include production and consumption radicals at a higher voltage level.[30]

### 2.4.4 Energy storage

Energy can be stored in a variety of ways. Hydroelectric power plants use reservoirs or pondages to stock water for later use, while PV plants are often connected to batteries that serve as power stabilizers. Each form for energy storage can be applied to a power plant, but its type and size depends on multiple factors, like overproduction or devoted tasks.

Electro-chemical batteries are constructed out of a positive charged side called cathode and a negative charged side called anode. The battery is charging when a power supply forces the electrons to flow from the positive to the negative side. When energy is needed, the battery can be discharged by electrons flowing from the anode to the cathode through the load. The higher the nominal voltage of the battery, the more advantageous it is, due to the smaller amount of cells needed for the desired system. Other important factors to consider are energy density and cost. As lead-acid batteries are the least expensive battery technologies, this type has the most widespread use.[31]

### 2.4.5 Modes

There are three different types of modes considering a power plant, which are called base load, peaking power plants, and load following. Power plants running on base load generate maximum output and thus fulfill the minimum level of electricity demand required over a specific period. They only shut down or reduce their power to perform repair or maintenance. Moreover, the peaking power plants only operate during times of peak demand. The peak demands are typical in the middle of the afternoon, so a general power plant running on peaking mode may start up a couple of hours before, and shut down a couple of hours after.[32]

To be able to produce mid-merit electricity, the last mode, load following, adjusts its power output in accordance to the demand for electricity as it fluctuates throughout the day. Those types of power plants are typically somewhere between the two other types in efficiency, capacity factor, speed and construction costs. Load following power plants usually run during the day and early in the evening, and they operate in direct response to changing load profile. When the electricity demand is at its lowest, typically during the night and early morning, they either shut down or greatly curtail the output.[33]

### 2.4.6 Controllers

#### SCADA/EMS

SCADA (Supervisory Control and Data Acquisition) is a software system used in industrial processes like energy production, manufacturing, utilities etc. The main objective for SCADA is controlling, monitoring, analyzing and optimize obtained data from multiple components. The system communicates with controllers on lower levels that execute the actual tasks, for example valves regulating water flow in a hydropower plant or motors decelerating the speed of a production line. The information is then presented in a graphical interface for workers. The SCADA system can interact with controllers and thus log all data for later use, analysis and prediction. For operation of electric utility grids, the SCADA/EMS or Energy monitoring system is used.[34]

#### PPC

The Power plant controller or PPC, is a tool used to regulate certain parameters in a power plant. The task can be either requested by SCADA/EMS, done automatically as a result of safety measurements or by requirement of the grid operator (frequency, voltage, reactive power, etc.). By using a closed loop with multiple input information and data, PPC fulfills given objectives and requirements. A simplified scheme of such loop has been created for this specific thesis and presented in the figure 2.4.2.[35]

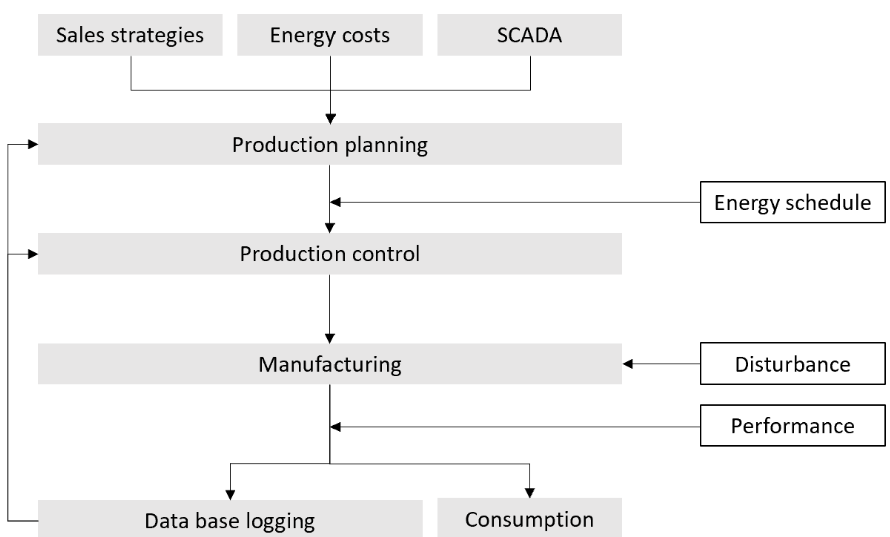


**Figure 2.4.2:** *PPC as closed loop control circuit.*

## 2.5 Economics

### EPBT

Energy payback time is shown in equation 2.5.1, and is the time the unit use to generate all energy needed for its production, including extraction of resources, operation, maintenance and recycling. The Energy Payback Time of PV systems is dependent on the geographical location and the type of the PV technology. In Africa the EPBT is approximately between 0.5 to 1.4 years.[36]

$$EPBT = \frac{E_{mat} + E_{manuf} + E_{trans} + E_{inst} + E_{EOL}}{E_{agen} - E_{aoper}} \tag{2.5.1}$$

Regarding the primary energy demand, $E_{mat}$ is produced materials comprising PV systems, $E_{manuf}$ defines manufactured PV systems, $E_{trans}$ is the transported materials used during the life cycle, $E_{inst}$ describes installment of the system, and $E_{EOL}$ is the end-of-life management. Further on, $E_{agen}$ is the annual electricity generation in primary energy terms, and $E_{aoper}$ is the annual energy demand for operation and maintenance in primary energy terms.

### EROI

Energy return on investment is the technical lifetime of a system divided by the EPBT of the system. In other words, EROI is the ratio of the gained energy from a production process compared to how much of that energy is required to develop and extract. This is shown in equation 2.5.2.[37]

$$EROI = \frac{Energy\ output}{Energy\ input} \tag{2.5.2}$$

### LCOE

Levelized cost of energy measures lifetime costs divided by energy produced. In other words, it calculates the present value of the total cost of both construction and operation of a power plant. It can be calculated using equation 2.5.3. The equation is compiled with respect to $t$ as a year, $r$ as the discount rate and $n$ as the life span. $I_t$ is the investment expenditures, $M_t$ is the operations and maintenance expenditures, $F_t$ is the fuel expenditures and $R_t$ is the net cashflow. $E_t$ is the electricity generation.[38]

$$\frac{\sum_{t=1}^{n} \frac{I_t + M_t + F_t}{(1+r)^t}}{\sum_{t=1}^{n} \frac{E_t}{(1+r)^t}} \tag{2.5.3}$$

### CAPEX & OPEX

Capital expenditures and operation expenses are two different types of business expenses. In respectively order; major purchases which will be used in the future, such as buildings and machinery, and further on day-to-day expenses necessary to keep the business going, such as wages, office supplies and leases. On an income statement only an amortized amount is deducted from revenue regarding CAPEX, while OPEX is fully deducted. Businesses are taxed on revenues minus all OPEX.[39]

### NPV

The net present value of a project is calculated in order to determine the profitability of an investment. A project is considered profitable if NPV>0, and considered unprofitable if NPV<0, and would not be carried out based on a financial perspective. NPV is calculated using equation 2.5.4.[40]

$$NPV = \sum_{t=0}^{n} \frac{R_t}{(1+r)^t} \tag{2.5.4}$$

# 3 Evaluation of existing hydroelectric power plant

## 3.1 Achwa 2 hydropower plant

Achwa 2 is a 42MW hydropower run-of-the-river plant by the Achwa River which marks the border between the northern Uganda districts of Gulu, Pader and Kitgum (03.14822315°$N$, 032.51733589°$E$). This HPP has been constructed as a part of a larger project consisting of three hydroelectric power plants along the Achwa river. The Achwa 2 HPP was finished in late 2018 and is, as of May 2019, in operation. The site can be accessed by a road that stretches around 19 kilometers north-west from a bridge on the Gulu-Kitgum route. Achwa 2 lays approximately 28 km away from nearest settlement of Aswa and 65 km from nearest city of Gulu.[41]

The power plant is being developed and owned by ARPE Limited while the transmission line connecting the construction to the national grid is being built independently by UETCL. The cost of the construction is budgeted at US$ 78.8mill, funded by The African Development Bank and Delta.[42]

**Figure 3.1.1:** *Satellite photo of project site.[43]*

Figure 3.1.1 shows the area in which the Achwa 2 hydropower plant is located. The satellite image is the newest that could be obtained as of the publication date of this thesis, with construction of roads and new water channel, visible in the photo as the lighter colored area.

The topography of the HPP site is common for this region. It is quite uniform, characterized by a flat landscape interrupted only by a few hills. In fact, the powerhouse of the Achwa 2 Hydropower plant is located in the vicinity of a hill with an elevation of 872 m above sea level. The HPP site itself lies 776 m above sea level. Same location site, seen from another angle, is presented in figure 3.1.2.

**Figure 3.1.2:** *Site location from another angle.[44]*

As for the Achwa river, its maximum head water level is approximately 776.18 masl and the minimum is 775.16 masl. which gives an altitude difference of 1m. This thesis will in later chapters describe river water flow and use those values for detailed calculations. The power plant also possess pondage which is able to produce at full load for maximum 3 hours.

Also typical for this district are sandy soils. Due to the fact that the climate alternates between dry and wet seasons, the soil is ferruginous. Due to this, it has a red tint which affects the ability to absorb or reflect sunlight, thus affecting the Albedo effect.[45]

### 3.1.1 Turbine assessment

Achwa 2 HPP has four vertical Francis turbines. Three of them are units rated at 12 MW, with the last one rated at 6 MW, in total 42 MW. As shown in table 3.1.1, the nominal speed of the turbine is at 300 rpm by large unit and 429 rpm by small unit. Rated net head, which will later be used for calculations of power production from HPP, is estimated to be 50.73 m, varying from 59m at its maximum, down to 47 m at its minimum. Each turbine has also an interval discharge it can operate within.

**Table 3.1.1:** *Turbine specifications*

| Parameter | Large unit | Small unit |
|---|---|---|
| Rated net head [m] | 50.73 | |
| Maximum net head [m] | 59 | |
| Minimum net head [m] | 47 | |
| Max. head water level [m.a.s.l.] | 776.18 | |
| Min. head water level [m.a.s.l.] | 775.16 | |
| Max. tail water level [m.a.s.l.] | 730.27 | |
| Min. tail water level [m.a.s.l.] | 723.6 | |
| Max. discharge [$m^3/s$] | 28.667 | 14.434 |
| Min. discharge [$m^3/s$] | 12.68 | 6.60 |
| Turbine nominal speed [rpm] | 300 | 428.57 |

Figures A.0.2 and A.0.3 in the appendix A, present two different hill charts for small and large turbines in the hydropower plant. Those charts visualize efficiency points considering the net head, power, flow and the range for continuous operation. For small units the best efficiency is located between 5000 kW and 5800 kW, with the flow at approximately 11 to 12.5 $m^3$/s and net head between 48 to 51.2 m. At these parameters the efficiency will be upwards to 93%. For larger units the best efficiency is at about 93.5%, with the same head for continuous operating range at 48 to 51.2 m, and flow at approximately 23 - 25 $m^3$/s. With these specifications the power will, at its maximum, be located between 10 000 kW and 12 500 kW for each large turbine and approximately 5 000 kW to 6 300 kW for each small one. The Achwa 2 HPP's efficiency will be used for the purpose of finding the power production as well as optimization of the designed solar plant. To illustrate the size and construction of the turbines, figure 3.1.3 is presented.

**Figure 3.1.3:** *Three major Francis turbines under construction.[41]*

### 3.1.2 Grid and switchyard assessment

The switchyard consists of one 3-pole isolator with earth switch on both sides and one 3-pole sulfur hexafluoride ($SF_6$) insulated circuit breaker. In addition there are three single-phase transformers and three lightning arrestors, which is shown in table A.1 in the appendix A. This information was provided by a representative from ARPE Limited.

Achwa 2 hydropower plant is connected to the Uganda national grid. An overview of how the power plant is currently connected to the grid is shown in figure A.0.1 in the appendix A. The generator of the power plant generates power with an output voltage of 11 kV. A step-up transformer rated at 15/20 MVA increases the voltage from 11 kV to 33 kV. From there, the power is distributed via ACSR 100 transmission lines to Gulu and Kitgum town areas. The power plant is also to be connected to the Lira main high voltage transmission line, which is currently under construction. When finished, it will contribute to a stable power distribution in larger parts of northern Uganda.

In the long term scenario the Achwa 2 HPP will use two 30 MVA transformers to step up voltage to 132 kV and put it on the grid. These transformers are proposed to work for the whole hybrid power plant, including the photovoltaic part. As for the date of publication of this thesis, the 132kV line is not yet complete. Detailed specifications regarding future transformers are shown in table A.2 in the appendix A.

### 3.1.3 Production data

Based on obtained information, the power production from Achwa 2 HPP will at the beginning be constrained by the lower voltage transmission lines of 33 kV. The power plant will provide power to its closest areas of Gulu and Kitgum. Production during the short term will therefore be below the 42 MW capacity.

Due to the fact that Achwa 2 was put in operation in late 2018, the obtained annual production presented in table A.3 in appendix A have been simulated by the HPP's developers. It has been calculated that based on the river's water flow rates in the period 1964-2016, the annual average electricity production from the power plant would be around 177.5 GWh/year. Detailed source and the way the simulations were performed is unknown.

To obtain a complete data set for the entire year, it was necessary to perform own simulations based on the available information about the monthly river flow, which are presented in table A.4 in appendix A.

By readjusting the data from $m^3/s$ to kg/s and establishing assumption for maximal power production at 50.73m as rated net head, as well as estimating the efficiency factor to an average of 86.5%, it was possible to follow the equation 2.2.1 and find available monthly power production. Since the capacity factor was unknown, the value was set to 1. Production restrictions, like functional discharge interval as well as maximal power output were implemented right after, and thus defining capacity factor to around 51.6%. A table with all calculation can be found in the appendix A, figure A.0.4. Results of those calculations are presented as estimated power production data in the table 3.1.2. The average annual production has been calculated in two different ways. The first value of 189.95 GWh is based on average annual productions from 2012 to 2016, whereas 191.16 GWh is a sum of calculated monthly average production. As shown, both numbers correlate with the average result based on original simulations from the same time period. It is worth mentioning that the presented results in the table are in no mean true representation of what the hydropower plant will produce, but is an approximation of what the power output can be expected from the Achwa 2 HPP and thus those values will be used in later chapters.

**Table 3.1.2:** *Calculated approximation of Achwa 2 HPP power production.*

| | Power [MW] | | | | | Avg. capacity [MW] | Avg. production [GWh] |
|---|---|---|---|---|---|---|---|
| Year | 2012 | 2013 | 2014 | 2015 | 2016 | | |
| January | 4.35 | 4.26 | 6.11 | 3.53 | 8.05 | 5.26 | 3.91 |
| February | 0.00 | 0.00 | 0.00 | 0.00 | 0.00 | 0.00 | 0.00 |
| March | 0.00 | 0.00 | 0.00 | 0.00 | 0.00 | 0.00 | 0.00 |
| April | 11.92 | 9.51 | 3.66 | 7.23 | 5.08 | 7.48 | 5.39 |
| May | 42.00 | 26.95 | 13.73 | 35.39 | 34.09 | 30.43 | 22.64 |
| June | 23.85 | 10.72 | 42.00 | 30.74 | 13.78 | 24.22 | 17.44 |
| July | 35.86 | 31.73 | 34.27 | 18.04 | 17.91 | 27.56 | 20.50 |
| August | 42.00 | 42.00 | 42.00 | 42.00 | 42.00 | 42.00 | 31.25 |
| September | 42.00 | 42.00 | 42.00 | 22.69 | 32.11 | 36.16 | 26.04 |
| October | 31.04 | 42.00 | 42.00 | 16.06 | 39.00 | 34.02 | 25.31 |
| November | 42.00 | 42.00 | 35.04 | 42.00 | 9.13 | 34.03 | 24.50 |
| December | 16.70 | 22.77 | 19.16 | 33.45 | 3.14 | 19.04 | 14.17 |

| | | | | | | | |
|---|---|---|---|---|---|---|---|
| Avg. capacity [MW] | 24.31 | 22.83 | 23.33 | 20.93 | 17.02 | Avg. yearly prod. (annualy 2012-2016) [GWh] | Avg. yearly prod. (monthly 2012-2016) [GWh] |
| Avg. production [GWh] | 212.95 | 199.98 | 204.38 | 183.31 | 149.13 | 189.95 | 191.15 |

The visual representation of all average monthly power production power between 2012 and 2016 have been marked in figure 3.1.4. The main average production has been shown with a defined line and later used to produce monthly GWh in figure 3.1.5.

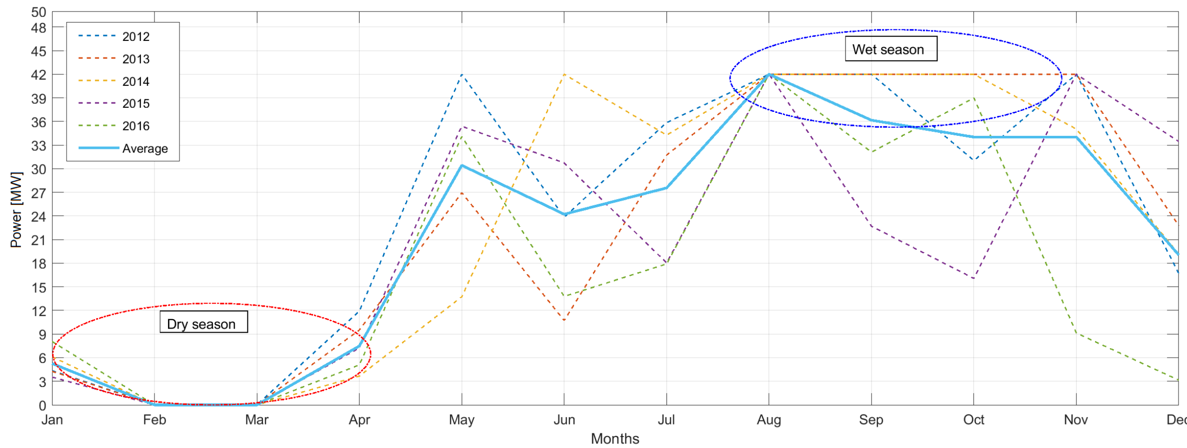


**Figure 3.1.4:** *Potential monthly power production in MW between 2012-2016.*

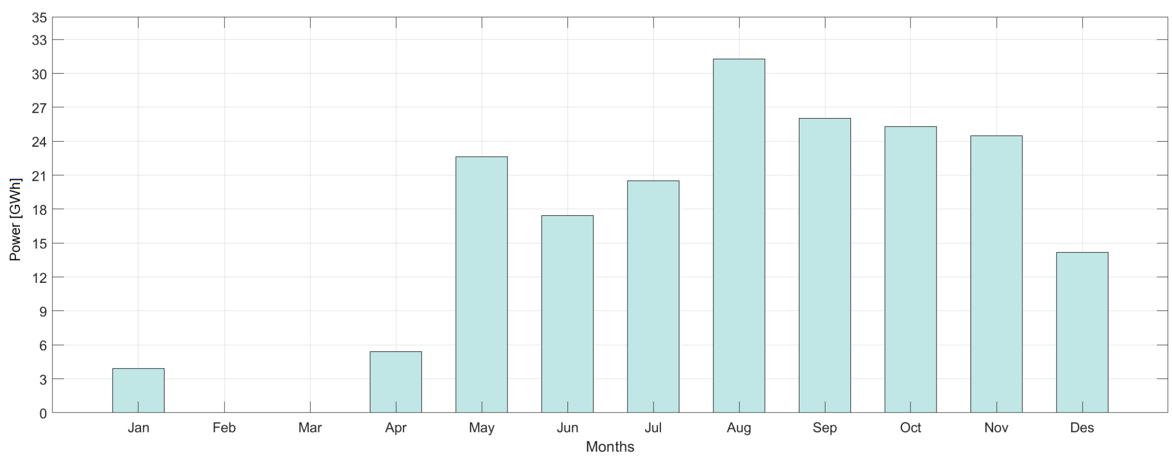


**Figure 3.1.5:** *Potential average monthly production from Achwa 2 HPP in GWh.*

Based on those figures it is clear to identify dry- and wet seasons in Gulu, Pader and Kitgum areas which occur from December to April and July to October, respectively. Production in dry season months will define the PV power size since the benefits of PV production will then be at its greatest. It is also important to mention that power production from HPP will vary based on requests from the Ugandan grid operator. Therefore average values can be lower than presented, even in periods where full production is possible.

# 4 Design and dimensioning of Achwa PV power plant

## 4.1 Topography of site location

This thesis excludes detailed investigation of the site area size and will therefore not take the space approximations into the consideration of the designed PV power plant or simulations in PVsyst software. The following requirements regarding the location site has been determined:

1. No protected wildlife is reported to be present in this area.
2. The location is placed in a stable, government controlled area.
3. There is little to no health hazards related to solar power.

It is also assumed that both vegetation as well as ground quality on the site, is suitable for construction of the photovoltaic power plant. Detailed evaluation of building site, as well as a scheme of the actual photovoltaic plant including component layout with respect to Achwa 2 hydropower plant, will not be presented since this type of information is outside the scope of this thesis.

## 4.2 Analysis of meteorological data

### 4.2.1 Data sources

#### NASA

NASA Langley Research Center (LaRC) created project called POWER funded through the NASA Earth Science/Applied Science Program which provides internet-based meteorological data access as well as parameters for potential energy production from different renewable energy sources. Data sets have been created by using both satellites observations as well as the Goddard Earth Observing System assimilation model.[46]

#### PVGIS

Photovoltaic Geographical Information System (PVGIS) is a free, online tool for climate data for photovoltaic applications, and is developed by the European Commission Joint Research Centre.[47] PVGIS offers a database of solar data for Europe, Africa and Asia.

**Meteonorm**

Meteonorm software generate climate data for any place on Earth, by utilizing more than 8000 weather stations as well as satellite data. In order to provide data for every place on Earth, the program interpolates all obtained values to get most exact results.[48] The weather stations used for interpolating data for the project site are Gulu (48 kilometers away), Paraa (139 kilometers away), Arua (178 kilometers away), Masindi (184 kilometers away) and Soroti (199 kilometers away), in addition to satellite data. The Meteonorm report was provided by Multiconsult.

### 4.2.2 Quality of climate data

To achieve the most reliable simulation results of the designed photovoltaic power plant, a quality check of different climate data sources had to be executed. Due to lack of meteorological stations in the immediate vicinity of the project site, it has been decided to use the most conservative data set for the further simulations. This way, the simulated production data would not be overestimated, thus not making it seem more profitable than it would be in reality.

To conduct a quality check the irradiation data have been selected and compared between from the previously described sources. Irradiation data from Meteonorm has been collected in the time period 1991-2010 with uncertainty stated to be 5%. PVGIS provided monthly solar data from the CM SAF database, in the time period 2007-2016. Then average values for each month were calculated. Data sets from NASA were based on 30 year averages, with meteorological data collected starting in January 1984 and ending in December 2013.

In table 4.2.1, a comparison of deviation from the yearly irradiation average is presented. Based on those values it is clear that Meteonorm has the most protruding deviation from the average, at 9.03%. This is due to the fact that the other sources provide higher estimates for irradiation, thus increasing the average value.

**Table 4.2.1:** *Comparison of deviation from irradiation average.*

| Source | Meteonorm | PVGIS | NASA | Average |
|---|---|---|---|---|
| Yearly GHI [kWh/m$^2$] | 1905 | 2265 | 2114 | 2094 |
| Deviation from average [%] | 9.03 | 8.17 | 0.96 | - |

Figure 4.2.1 shows the average monthly solar irradiation on a horizontal surface on the project site, from the three sources.

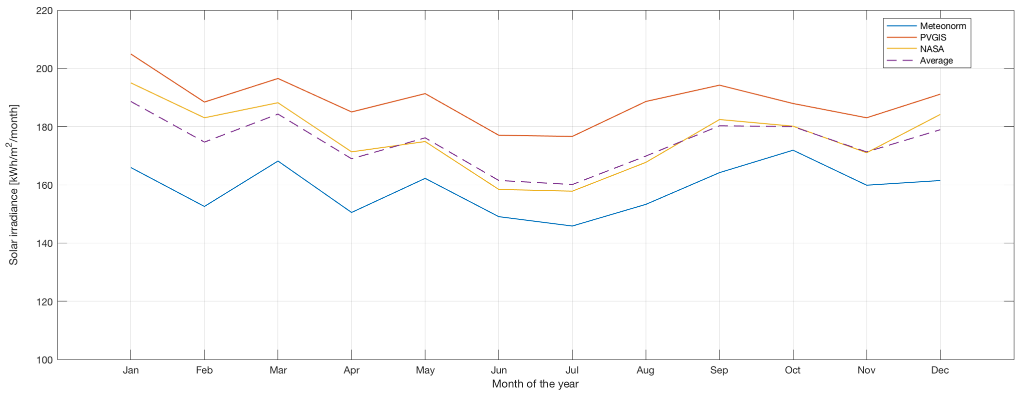


**Figure 4.2.1:** *Average monthly solar irradiance data obtained from multiple sources.*

From figure 4.2.1, it is apparent that Meteonorm provides the most conservative estimate for solar irradiance, while PVGIS provides the most optimistic estimate. NASA is the most similar to the average value from the sources. According to the Meteonorm report, the variability of the global horizontal irradiation is stated to be 2.5%. Even though the three sources estimates the values of solar irradiance to be different, they all share the same overall pattern.

In order to investigate the feasibility of a photovoltaic power plant, the most conservative estimate will be used for further analysis and simulations. Additionally, Meteonorm provided the most complete set of data, thus making it the most appealing for use in the simulation software. In conclusion, researching climate data for the project site was finished.

### 4.2.3 Meteorological data examination

#### Solar irradiance

Solar irradiance helps to define the PV power plant size as well as estimate yearly power production. To present the GHI variations between different areas in Uganda, map from Solargis has been acquired and presented in figure 4.2.2. This source has been used for illustration and all later mentioned GHI values will come from previously chosen source, Meteonorm.

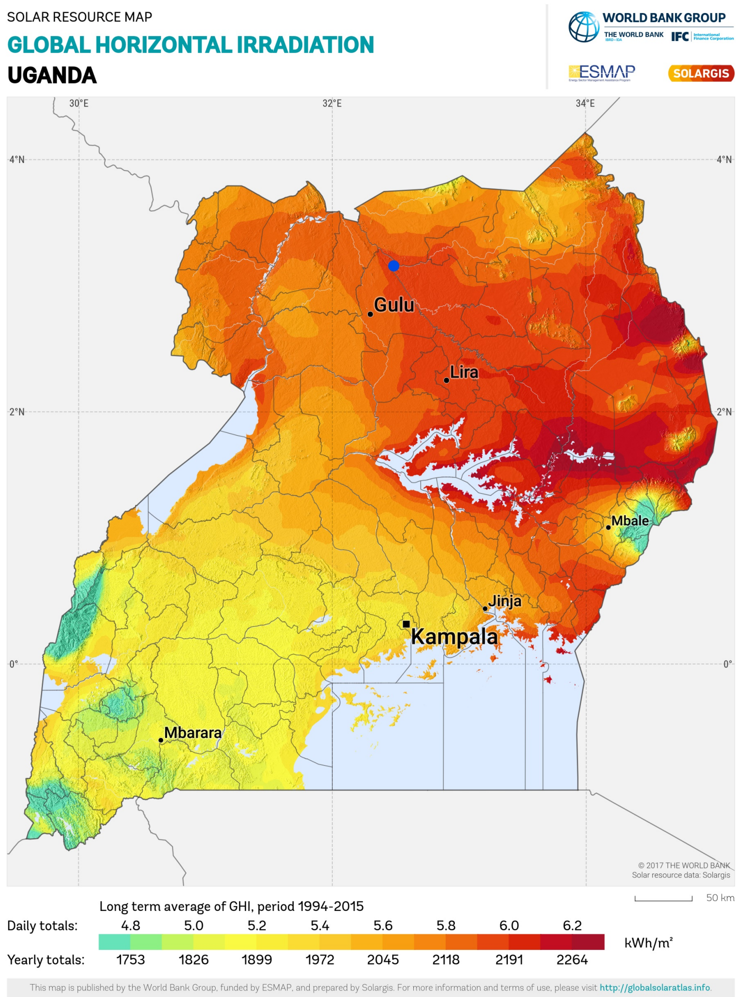


**Figure 4.2.2:** *Global Horizontal Irradiation.[49]*

Achwa 2 hydroelectric power plant is located north of the city of Gulu (blue dot), which figure 4.2.2 reveals to be in an area with a medium high value of GHI, suitable for photovoltaic power production.

The following graph presented in figure 4.2.3 shows simulated solar irradiance profile on the site location for the month of June. Examination of this figure shows how GHI can vary from day to day, thus making energy production from PV harder to forecast.

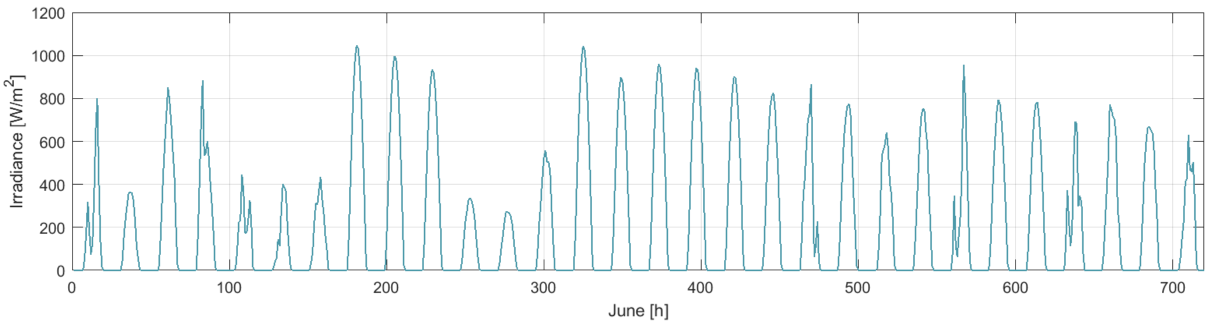


**Figure 4.2.3:** *Irradiance for June*

Based on the water flow in the Achwa river, presented in chapter 3.1.3, wet season starts around July and continues throughout October. The amount of days with precipitation is then higher even though rain fall brings smaller amounts of water. Simplified presentation of the precipitation in the Achwa area is shown in the paragraph "Precipitation". This has been reflected on the obtained irradiance data as June in figure 4.2.3, occurs in the middle of the wet season and has a low average amount of solar irradiance, which can be observed in figure 4.2.4.

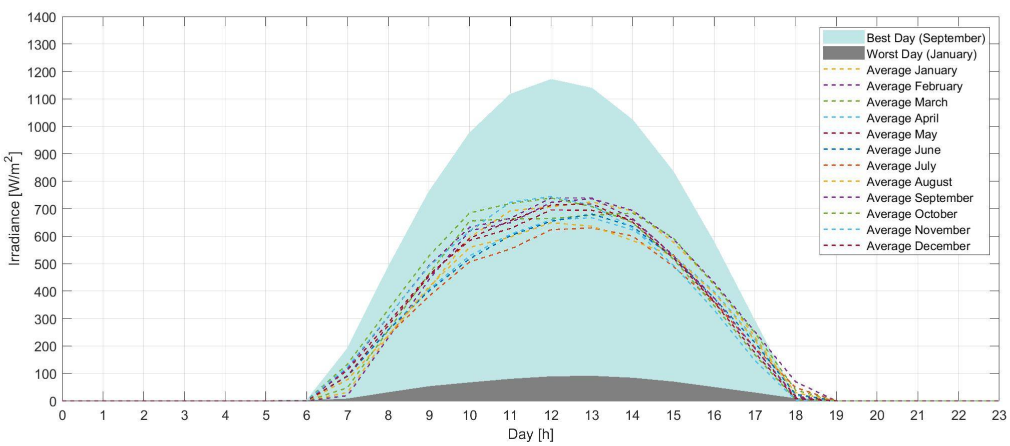


**Figure 4.2.4:** *Daily solar irradiance with average monthly values and worst/best day through the year.*

Figure 4.2.4 visualizes the average simulated irradiance for each month as well as presenting the best and worst days of the whole year. The data behind the plot stems from the Meteonorm climate report and was converted into a Matlab code presented in a shorten version in appendix B, listing 1. The calculation shows that the best day occurs in September and the worst day in January. The amount of solar irradiance can vary drastically from day to day, as shown in previous sections, that is why it is fully possible to have a great amount of solar energy after a rainy day.

### Albedo

The albedo effect is an essential factor that plays a major role in photovoltaic power production. The presented information regarding albedo in this thesis are the only one acquired from another source than Meteonorm, due the lack of detailed monthly values. The obtained data comes from the NASA's POWER project program which is described in detail in chapter 4.2.1.

The graph 4.2.5 below, presents the albedo effect changes over an average year on the location site alongside Achwa river in north Uganda. As shown, the average value lies around 0.18 and can vary with approximately 0.02 throughout the year. Presented under values were later used in system simulations in PVsyst software.

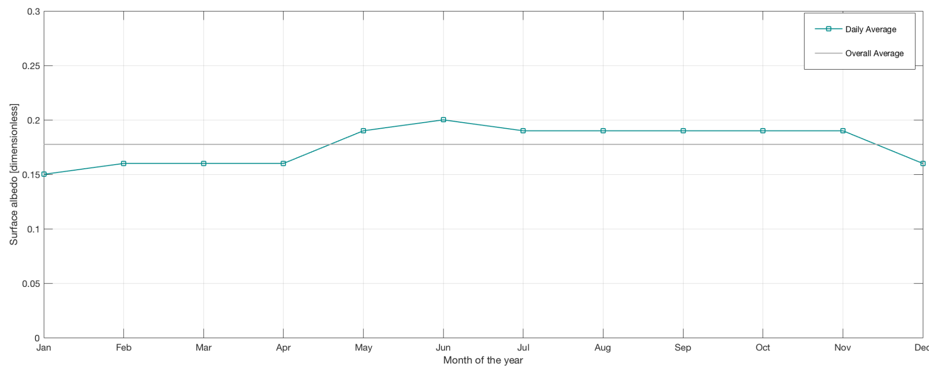


**Figure 4.2.5:** *Surface Albedo*

Based on those findings it reasonable to assume the type of soil in the area as well its reflecting ability. This information can be vital when choosing the right type of photovoltaic cells (monofacial or bifacial PV) as well as calculating thermal losses, which will be discussed in later chapters.

### Sunshine duration

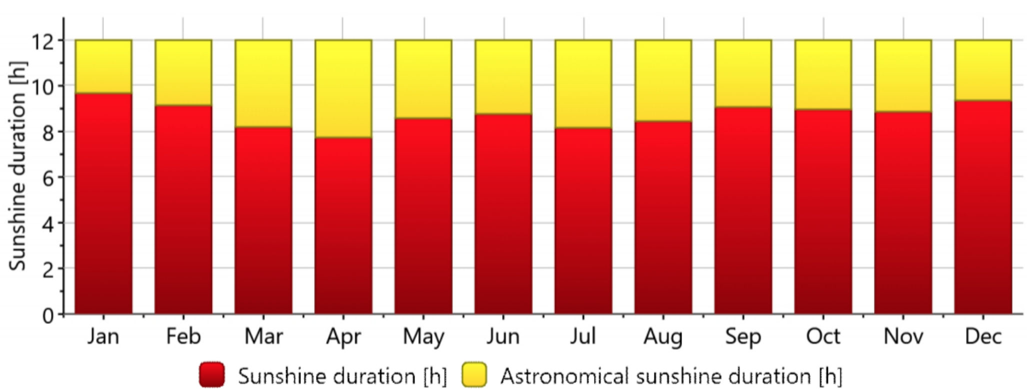


**Figure 4.2.6:** *Sunshine duration.[50]*

Figure 4.2.6 shows the hours of sunshine in the area of the hydropower plant. From the figure, it is apparent that the hours of daylight varies little throughout the year, due to site location near equator. Nevertheless, the maximum difference between monthly sunshine duration values is roughly 2 hours, with longest one reached in January and shortest in April. This figure defines the length of available sunlight in a day by taking into account clouds and other nature caused obstacles that could create a shadow for PV panels and thus lower energy production.

**Collected temperature data**

With a basis in the Meteonorm climate data report for the project site, the average temperatures of the area are presented in this section. As with the solar data, the temperatures are generated through information from satellites and interpolating values from weather stations in the area. The weather stations used for generating temperatures for the project site are Kisumu (437 kilometers away), Eldoret (422 kilometers away), Meru (663 kilometers away), Nakuru (548 kilometers away), Nairobi/Jomo Kenyatt (695 kilometers away) and Garissa (886 kilometers away). Contrary to the weather stations used for solar data, these stations are much further away from the project site. Nevertheless, the uncertainty of the temperature values are reported to be 2.4℃.

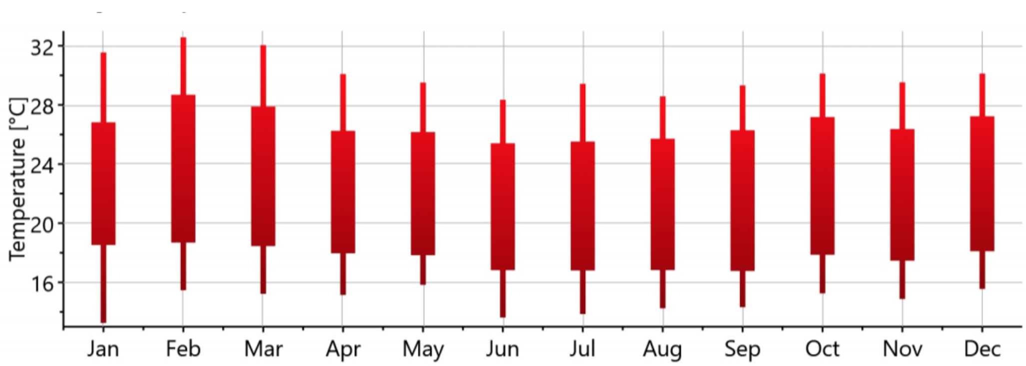


**Figure 4.2.7:** *Monthly temperatures.[50]*

As seen in figure 4.2.7, the temperature varies little throughout the year, with a yearly average temperature of 22.1℃. Although the temperatures are even throughout the year, the period October to March is the hottest.

**Precipitation**

As previously stated, both wet and dry seasons occur in the location of Achwa 2 HPP. The seasons length and intensity varies from year to year, but can be predicted to a certain degree. Precipitation presented in this chapter is an overall estimate simulated by Meteonorm. As shown in the figure 4.2.8 the amount of fallen rain does not have to correlate with the duration of the rain. At the end and beginning of the year, precipitation is more rapid and comes in shorter periods with the same amount of water as it would in the middle of wet season. The given figure serves as an approximation to what precipitation in the area could look like.

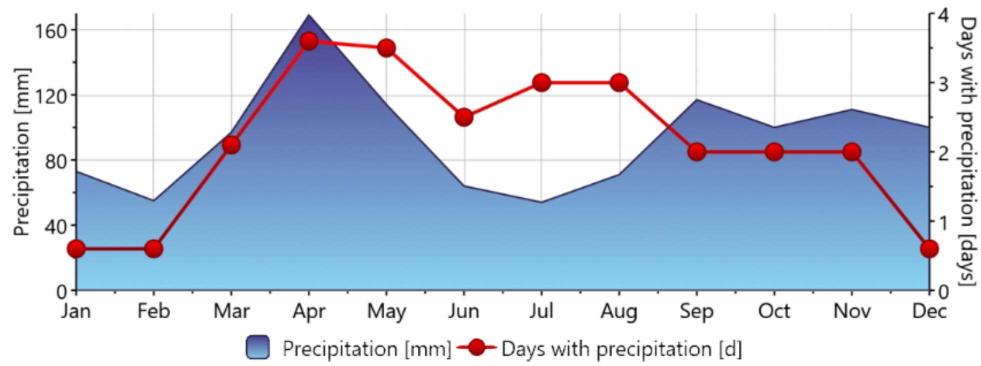


**Figure 4.2.8:** *Precipitation at the location site.[50]*

## 4.3 Adaptation strategies

Given power production from the hydroelectric power plant and earlier stated objectives, it has been decided to create a design for two PV plant sizes: 15 MW and 20 MW at their maximal peak. This resolution will further work as proportion values for chosen components as well as adaptation strategies, presented in this chapter.

### 4.3.1 DC power management

Before analyzing the systems most suitable DC voltage design, it is essential to mention the balance of the system and its importance for economic aspect of a PV plant as well as choosing the right voltage.

The balance of the system components or BOS items, represent all components used at a PV power plant site, excluding PV modules. Examples of such components are: wirings, inverters, batteries, grid connections or even built facilities. Data shows that production prices of PV modules are in continuous decline since the last few decades and with that becoming constantly smaller portion of the whole installation and maintenance costs; as shown in figure 4.3.1. To pull prices even further than they already are, and maintain high production effect, experts concentrate on decreasing the amount of BOS components. To effectively design a PV power plant and lower system costs more, a choice between 1000 volt DC system and 1500 volt DC system, has to be made.

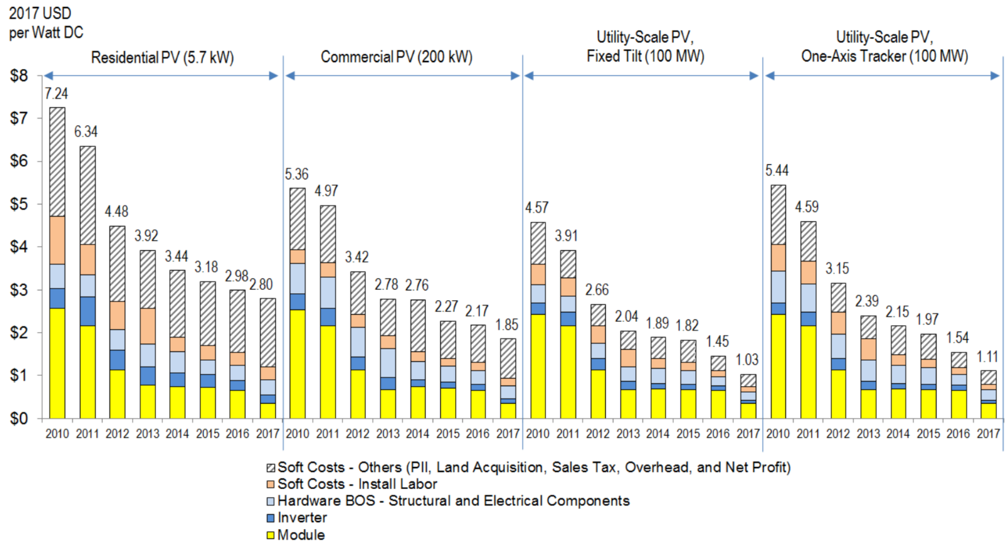


**Figure 4.3.1:** *NREL BOS Benchmarks Costs (2017).[51]*

Solar panels generate direct current (DC) which is unsuitable for transfer through grids that use alternating current (AC). To manage such transmission conversion from DC to AC is required. As of 2019, most producers use 1000 voltage DC inverters to manage distribution of power over PV panels. While those emerged rapidly on the market overthrowing 600 V DC systems, new voltage is considered.

Table 4.3.1, presents simplified differences between each systems voltage design, as well as combining them with the two main types of inverter connections.

**Table 4.3.1:** *Brief overview of advantages and disadvantages for each system type.*

| DC voltage systems | 1000 V system | 1500 V system | 1000 V system + DC string optimizer (1500 V) | 1500 V + DC string optimizer (3000 V) |
|---|---|---|---|---|
| Inverter layout | String | | Central | |
| Advantages | Big component selection on the market | Possible to connect more modules to on inverter, Lower BOS costs | Similiar advantages to 1500 V version, Lower inverter costs | Highest number of modules connected to one inverter, Lower inverter costs |
| Disadvantages | Highest costs [USD/kWh] in the long run | Smaller amount of suitable components on the market | Higher investment costs | Biggest investment, Similar disadvantages to 1500 V system |

Increased maximum voltage from 1000 V to 1500 V makes it possible to connect up to twice as many PV modules to each inverter in a string system, which at the same time cuts the number of combiners and other electrical components by about half, resulting in lower overall prices and EPBT. Based on the 2013 study published on IEEE 39th Photovoltaic Specialists Conference, such voltage change can lead to 15-85% savings in the conductor mass of the cables depending on the size of the plant and modules. Additionally, it is shown that the savings in the number of combiner boxes range between 25–60%. The higher maximum system voltage also improves the performance by reducing resistive losses, thus increasing the system-level energy yield.[52]

Alternatively, investment in DC string optimizer can be made. Strings optimizer enables central type of system to imitate string system functionality as well achieving similar results for 1000 DC voltage systems as for 1500 DC. The trend of 1500 V DC systems has been analyzed and reported by International Technology Roadmap for Photovoltaic (ITRPV), predicted to dominate the PV market in the future. It is hypothesized that 1500 V DC systems will represent 80% of new installations within the next nine years (2028). Based on this analysis it is sensible to favor a 1500 V DC system design, which this thesis will further evaluate and use as a foundation for chosen components in later chapters.[53, 54]

### 4.3.2 Positioning assessment

This subchapter includes a short analysis of how PV panels should be adapted to the location, based on sun path, orientation and size.

#### Sizing

Detailed property ownership, facilities dimensions and detailed positions of those at Achwa 2 HPP are unknown. Although this thesis will not take any proportion limitations regarding the construction site or needed module area, it will present overall dimensions of designed PV power plant in later chapters. Aside from this, the plant size is dependent on the power demand, how much the grid can be burdened, and the topography of the site.

#### Tilt

The location of the Achwa 2 HPP site is positioned on the northern hemisphere with latitude 3.15° which results in the solar panels facing true south to maintain better sun absorption. Based on the 2019 study "Implementation of PV Tracking for Sites Proximate and Away from the Equator", the optimal fixed tilt for Achwa 2 location can be defined to be around 3°.[20, 55] This value represents an annual average optimal angle between PV panel and sun position. Since this number changes throughout the year, closer investigation of solar trackers will be presented in following chapters.

**Tracking**

For this thesis, both fixed tilt modules as well as tracking modules were evaluated. Due to the equatorial location of the PV plant where the angle of the sun is near constant year-round, it was not known whether or not the extra cost of implementing a tracking system would prove profitable.

In general, tracking technology have multiple advantages compared to fixed tilt mounting systems. The amount of harvested sunlight in the 24 hours interval increases substantially in addition to lowering the total LCOE of the system. Both single and dual axis tracking systems require larger area capacity and significantly increases the investment costs. The tracking system that was used for the simulations was horizontal single axis trackers, HSAT.

With fixed tilt the investment costs would be lower compared to single axis tracking. In order to maximize the production yield from the PV plant, it is possible to manually rearrange the modules so that the angle changes a couple times each year. Later in the thesis the optimal solution taking both energy production and investment costs into consideration is investigated.

## 4.4 Components proposal

This subchapter provides recommendations of main components used in a photovoltaic power plant. None of the parts listed under are exclusive to achieve desired results, but have been chosen for system simulations, as described in later chapters. Assumptions regarding construction of ground mounting were inadequate and thus not analyzed in this thesis, as they are not a focus point in this project.

To guarantee a good, long-term performance of the system, given requirements were ratified:

1. All components should be resisted to drastic weather changes, i.e. water resistant
2. All parts have to be financially acquirable
3. A long lasting warranty is available
4. The modules have low potential-induced degradation
5. Cooling system on the transformers to withstand high temperature changes in summertime

### 4.4.1 PV modules

Based on earlier presented factors and several option considerations, the following PV modules have been chosen as example for further development of the PV power plant:

1. Canadian Solar CS3U-375MS 1500 V
2. LG Electronics 395N2T-A5 1500 V (Bifacial)

Both producers deliver panels that fulfill previously mentioned requirements and have easy to obtain data collections which were used in later described simulations. The module's MPPT have been presented in the figure 4.4.1, with monofacial panels to the left and bifacial to the right.

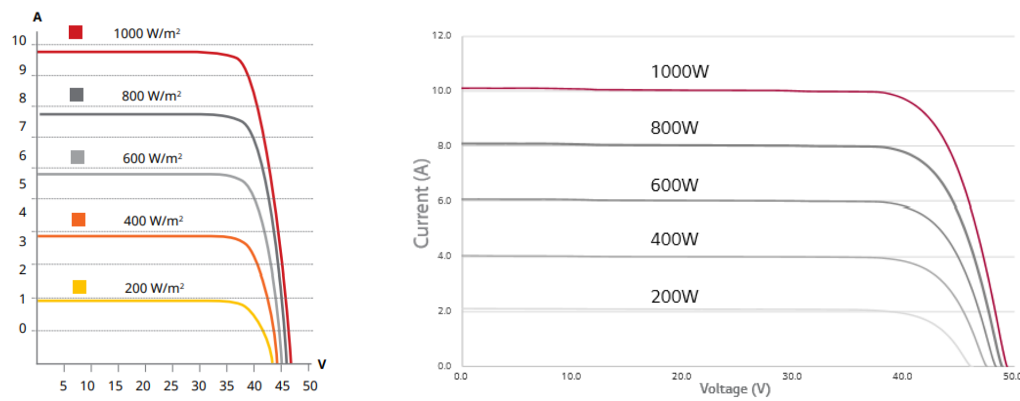


**(a)** *Canadian Solar* **(b)** *LG Electronics*

**Figure 4.4.1:** *MPPT for chosen PV modules.[18, 56]*

In the following tables, data for the chosen PV panels are presented. The values are based on standard test conditions (STC), which means a cell temperature of 25°C and solar irradiance at 1000 W/m$^2$. Table 4.4.1 presents electrical data for a PV module from Canadian Solar. This is the only monofacial module examined in this thesis.

**Table 4.4.1:** *Parameters of Canadian Solar CS3U-375MS 1500 V.[56]*

| PV module | Canadian Solar (Monofacial) |
|---|---|
| Nominal Max. Power [W] | 375 |
| Rated Voltage [V] | 39.8 |
| Rated Current [A] | 9.43 |
| Open-Circuit Voltage [V] | 47.6 |
| Short-Circuit Current [A] | 9.93 |
| Output Voltage [V] | 1500 |
| Panel Efficiency [%] | 18.9 |

**Table 4.4.2:** *Parameters of LG Electronics 395N2T-A5 1500 V.[18]*

| PV module | LG (Bifacial) | | | | |
|---|---|---|---|---|---|
| | Regular | Gain [5%] | Gain [10%] | Gain [20%] | Gain [30%] |
| Nominal Max. Power [W] | 395 | 415 | 435 | 474 | 514 |
| Rated Voltage [V] | 41.8 | 41.8 | 41.8 | 41.9 | 41.9 |
| Rated Current [A] | 9.46 | 9.92 | 10.39 | 11.31 | 12.26 |
| Open-Circuit Voltage [V] | 49.3 | 49.3 | 49.3 | 49.4 | 49.4 |
| Short-Circuit Current [A] | 10.19 | 10.70 | 11.21 | 12.23 | 13.25 |
| Output Voltage [V] | 1500 | 1500 | 1500 | 1500 | 1500 |
| Panel Efficiency [%] | 18.7 | 19.6 | 20.6 | 22.4 | 24.3 |

Table 4.4.2 presents electrical data for a bifacial PV module from LG Electronics. Depending on several factors, like albedo, the gain from using bifacial modules vary. According to the manufacturer, it is possible to gain up to 30% power production.[57] The values for maximum power in different gain situations are presented in the table. More detailed information regarding both PV modules can be found in appendix C.

### 4.4.2 Inverters

For this case, there are two alternatives for inverters to choose from: string or central inverters. Taking the size of the plant into consideration a central inverter has been chosen for the PV system. The reason for this choice, is that central inverters are the most widespread for use in larger, utility-scale grid-connected PV systems. As central inverters consist of fewer devices than string inverters, a higher rate of reliability is accomplished compared to string inverters. However, a central inverter limits the flexibility of PV layout and handles partial shadowing of panels poorer than string inverters.

External components specifications varies with different plant designs. Eight different types of inverters have been chosen for the simulations, depending on the power plant watt peak as well as type of PV panels used.The number of units and types of inverters chosen for each PV module is presented in table 4.5.1 in chapter 4.5.

Regarding the transformers and grid connections, it will be necessary to add an extra transformer after inverters to raise the voltage up to 11 kV. The rated power size of the unit will depend on the chosen inverters. The new transformer will then be connected to the same line as the generator from Achwa 2 HPP and then to larger 30MVA transformers. This approach is presented in later sections in chapter 5.4.

## 4.5 Summary of the system

Based on all previously mentioned components, the different systems specifications have been presented in the table 4.5.1. Two plant sizes, 15 MWp and 20 MWp with both fixed tilt (with 3°tilt) and HSAT as mounting systems has been conducted for monofacial and bifacial PV module designs. Given those nominal peak values, the area sizes and most suitable inverters have been found. All given design systems have been used in PVsyst simulations and work as a base for case scenarios, presented in following chapters.

**Table 4.5.1:** *An overview of the different systems simulated in PVsyst.*

| PV module | Canadian Solar CS3U-375MS | | LG Electronics 395N2T-A5 | |
|---|---|---|---|---|
| Type | Monofacial | | Bifacial | |
| Nominal Max. Power | 375 W | | 395-514 W | |
| Output voltage | 1500 V | | 1500 V | |
| System size | | | | |
| Nominal peak | 15 MW | 20 MW | 15 MW | 20 MW |
| Module area | 79336 $m^2$ | 105813 $m^2$ | 80268 $m^2$ | 107017 $m^2$ |
| Inverters | | | | |
| With fixed tilt (3°) | TMEIC PVH-L2700GR | ABB PVS-800-57-1000kW | ABB PVS-800-57-0875kW | Padcon AMC2500C |
| Number of units | 5 units | 16 units | 14 units | 7 units |
| With tracking system | Siemens Sinvert PVS2000 | Sungrow SG3000HV | KStar GSL2500C | Padcon AMC2500C |
| Number of units | 7 units | 12 units | 10 units | 7 units |
| Transformer | | | | |
| Size | 30 MVA 132/11 kV | | | |
| System frequency | 50 Hz +/- 5% | | | |

As previously stated, all PV plant designs will base their infrastructure on two 30 MVA transformers which will be constructed on the Achwa 2 site in the near future. Additionally, the yet to be built, 132kV grid will be used as a foundation for production from the PV power plant as well as HPP.

Based on the given data, it has been concluded that in order to gain maximal capacity of 15MW and 20MW, it is required to construct a photovoltaic power plant with a module area ranging from 80 000 to 100 000m$^2$. Figure 4.5.1 illustrates those areas in comparison to Achwa 2 HPP, as yellow and red areas. Those numbers do not include space between the arrays, so the final field needed, would be up to twice the size, illustrated in the figure as a white square. This area is assumed to be reasonable in size for this feasibility study. The satelitte image presented in the figure was provided by the representative from Achwa 2 hydropower plant.

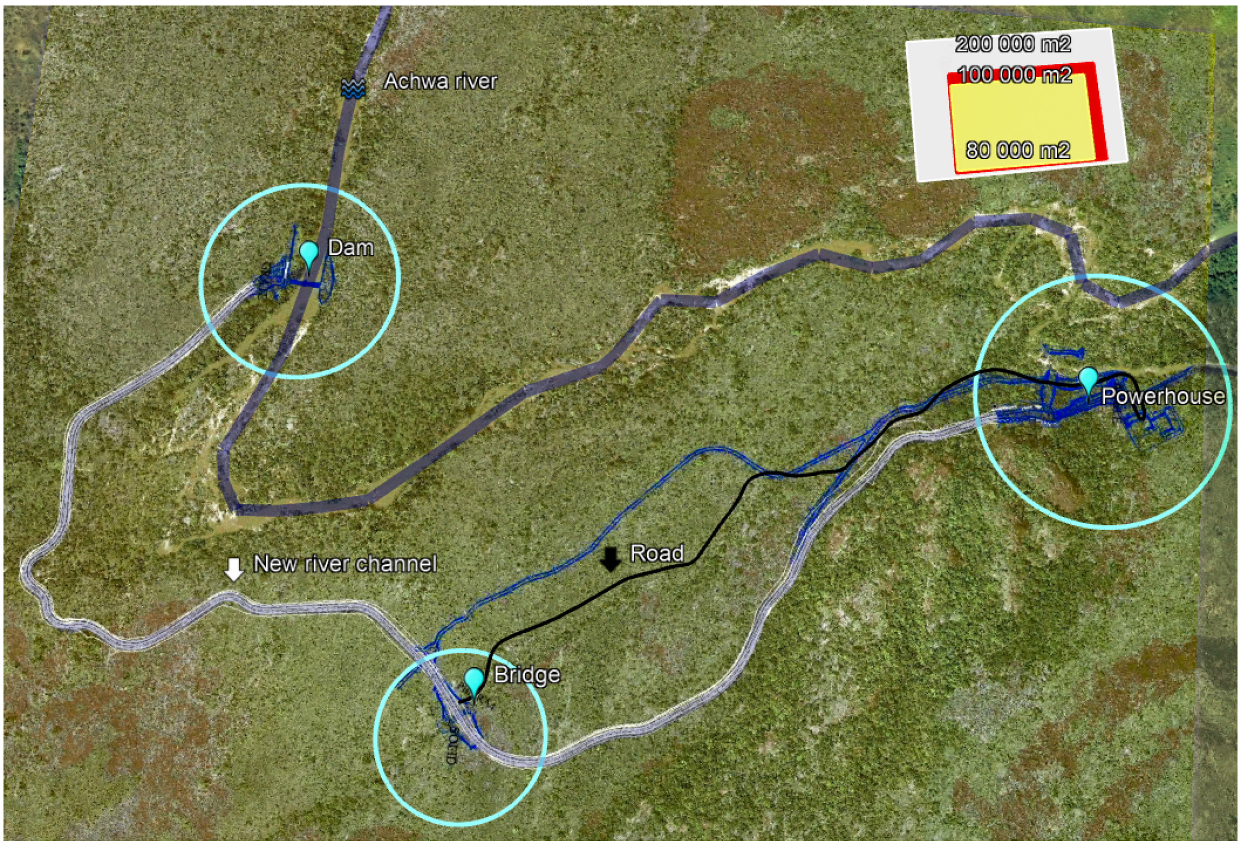


**Figure 4.5.1:** *Illustration of the designed plant areas next to Achwa 2 HPP.*

# 5 Assessment of Hybrid plant

## 5.1 Case synopsis

Based on all presented information regarding the PV power plant design in chapter 4, multiple cases has been determined. All cases are presented in regard to the power production from Achwa 2 HPP in the previously defined average year. The power production of the different cases will be illustrated against the load profile, to get a reasonable overview of the situation.

**Case No. 1**

Determine hybrid power production from the Achwa 2 HPP and 15 MW peak PV power plant constructed out of Canadian Solar CS3U-375MS 1500 V arrays with and without tracking system.

**Case No. 2**

Determine hybrid power production from the Achwa 2 HPP and 15 MW peak power plant constructed out of LG Electronics 395N2T-A5 1500 V (bifacial) arrays with and without tracking system.

**Case No. 3**

Determine hybrid power production from the Achwa 2 HPP and 20 MW peak power plant constructed out of Canadian Solar CS3U-375MS 1500 V arrays with and without tracking system.

**Case No. 4**

Determine hybrid power production from the Achwa 2 HPP and 20 MW peak power plant constructed out of LG Electronics 395N2T-A5 1500 V (bifacial) arrays with and without tracking system.

## 5.2 Simulations

### 5.2.1 PVsyst

#### Approach

The software that was chosen for simulating the PV system was PVsyst. PVsyst is a simulation software developed by scientists at the University of Geneva in Switzerland. The purpose of the software is to design and simulate photovoltaic systems.[58] For this thesis, version 6.7.9 premium education was used, provided by the Norwegian University of Science and Technology. While designing and simulating a photovoltaic system in the software, there are different steps which were followed. These steps are visualized in figure 5.2.1.

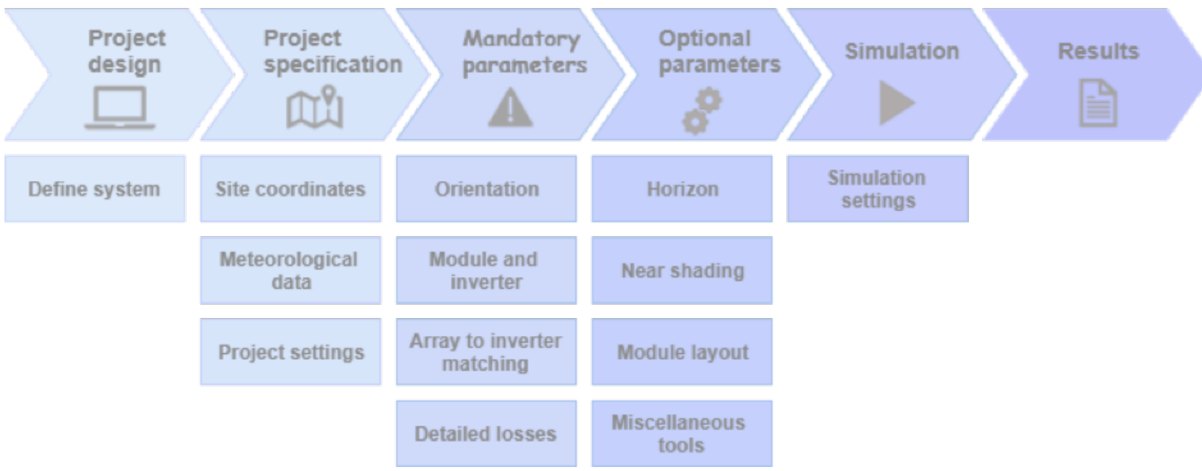


**Figure 5.2.1:** *PVsyst design steps in order.[59]*

The first step was to choose the system that was to be simulated. PVsyst offers the opportunity to simulate grid-connected, stand-alone, pumping and DC grid systems. For this thesis, a grid-connected photovoltaic plant is the system chosen for simulations.

PVsyst has a site database, where the site for PV simulations can be chosen from. The range of this database is quite limited, especially on the African continent. Therefore, using the coordinates for the project site, a new geographical site was defined and added to the database.

Meteorological data in PVsyst are provided by NASA and Meteonorm. The data used for the simulations in this thesis came from the synthetically generated Achwa II HPP report from Meteonorm version 7.3.0.26247, provided by Multiconsult. The settings that were adjusted for the simulations were limited to changing the albedo from default setting at 0.20 to match the albedo data for the project site provided by NASA.

At this point, the project specifications were defined in a satisfactory manner. The next step were to define the mandatory and optional parameters regarding the project. Firstly, the orientation of the PV modules were decided. In this thesis, scenarios with both fixed tilt and horizontal axis tracking were included. For the simulations with fixed tilt, the option "Unlimited sheds" was chosen in the orientation tool. With regular PV panel, the plane tilt was set to 3° and pitch set to 7 m. For the bifacial system with fixed tilt the plane tilt was set to 5° and pitch set to 7 m. For the horizontal axis tracking the setting was set to "Horizontal axis, unlimited trackers", the tracking limits were set to -30°to 30°and pitch set to 6.6 m. An example of what the orientation tool looks like is shown in figure 5.2.2.

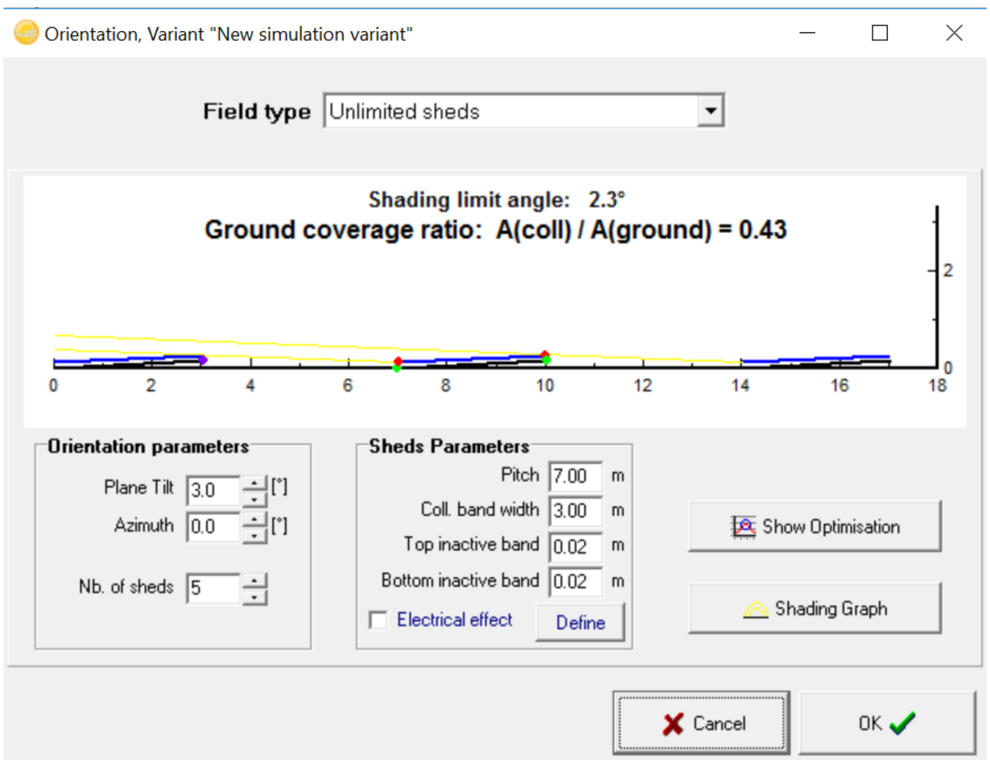


**Figure 5.2.2:** *Screenshot of the orientation in PVsyst.*

In the parameters for detailed losses, thermal parameters and soiling loss were decided. The thermal loss parameters were not defined beforehand, however, PVsyst provides default data for these thermal losses depending on the mounting technology. The mounting was set to "Free mounted modules with air circulation", thus setting the constant loss factor to 29.0 $W/m^2K$ and wind loss factor to 0. The yearly soiling loss factor was also set to a default value of 2.0%.

The next step that was conducted, was to define the size of the plant as well as choosing the components, i.e. PV modules and inverters. An example of what a completely specified system looks like in PVsyst is illustrated in the screenshot figure 5.2.3. The system shown in this figure is a 15MW plant using Canadian Solar monofacial panels with tracking. For bifacial systems, the bifacial menu was opened and the height of the modules were set to 2.0 meters above the ground.

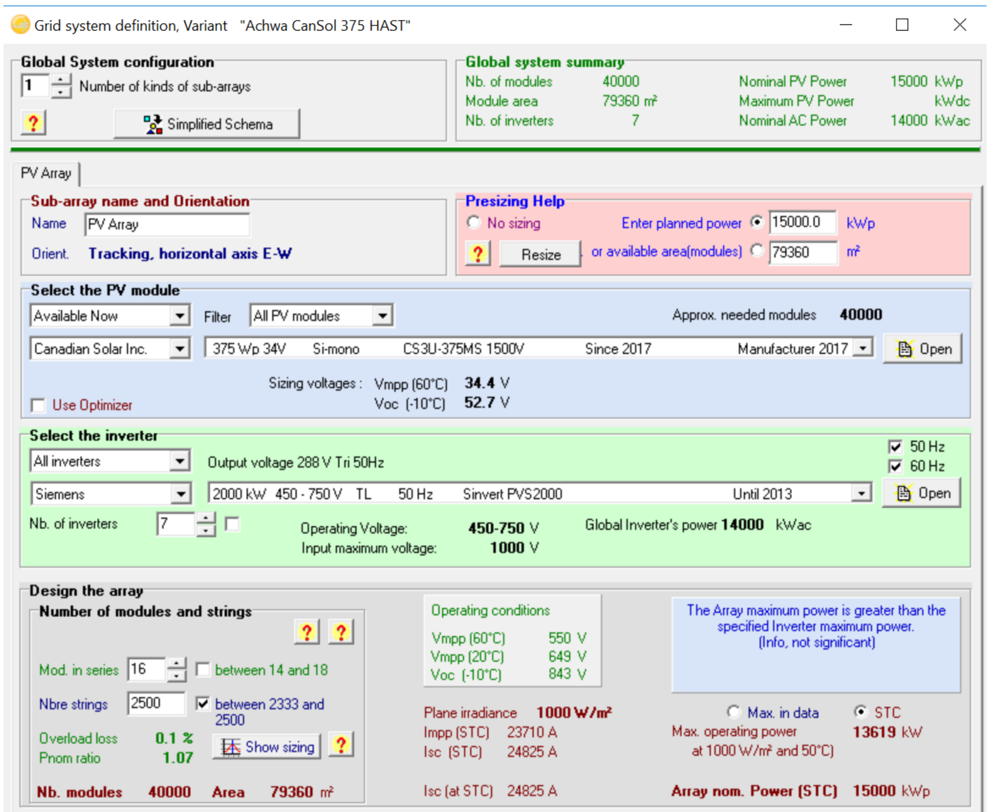


**Figure 5.2.3:** *Screenshot of system specifications in PVsyst.*

Horizon gives the opportunity to simulate shading from far objects. Far shading data was provided by the same Meteonorm report as the climate data.

Near shading simulates shading from objects near the site, for example buildings. In order to do this, a 3D shading construction was made in PVsyst. This can be seen in figure 5.2.4. The model does not have to be identical to the actual system in number of PV modules, but is more meant for modeling how the shading of the modules would behave.

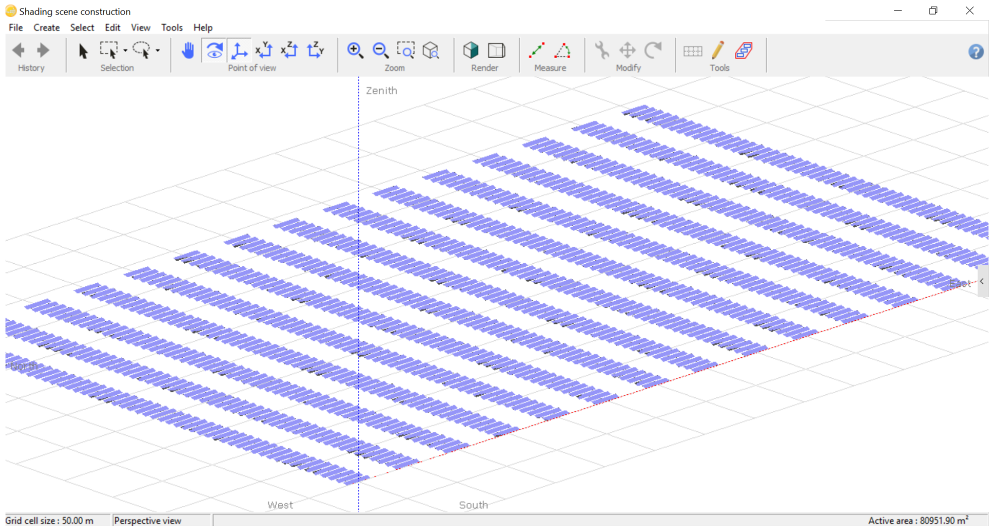


**Figure 5.2.4:** *Screenshot of the near shading model in PVsyst.*

At this point, everything was ready for running the simulations. When PVsyst is ready to simulate the system, green lights on the different parameters indicate that everything is correct. This can be seen in figure 5.2.5. The results of these are presented in table 5.2.1.

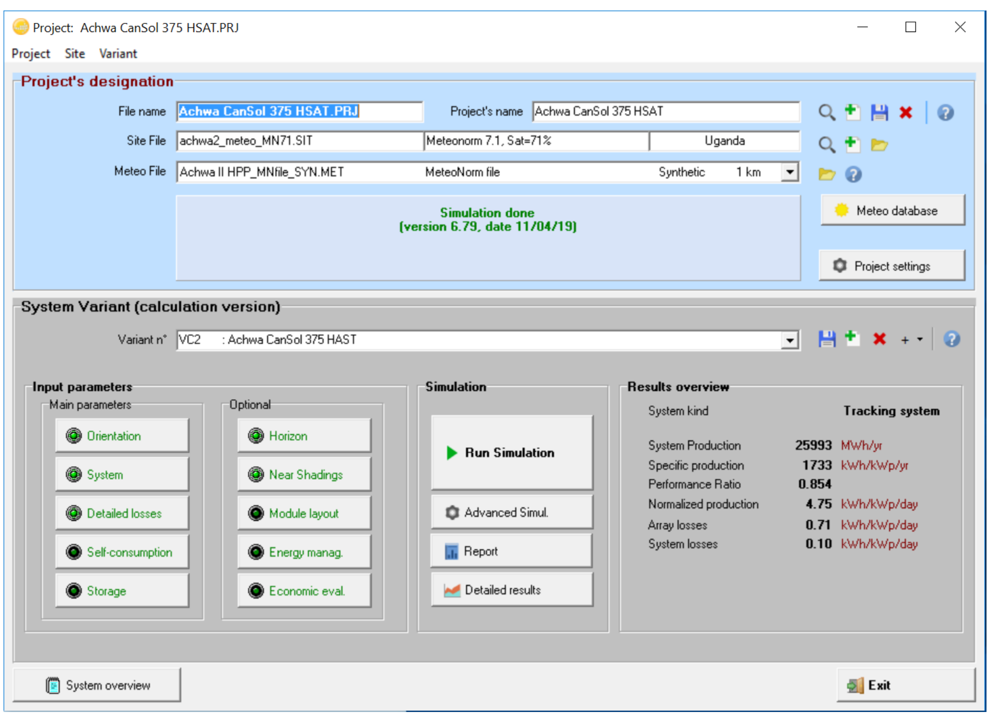


**Figure 5.2.5:** *Screenshot of PVsyst ready for simulation.*

### Information from the PVsyst reports

In table 5.2.1 the overview of the produced energy in GWh from the different cases are shown. All presented data has taken to account later mentioned losses. It is clearly visible that the bifacial LG HSAT with the installed capacity of 20 MW generates the highest power production at 41.4 GWh on an average year.

**Table 5.2.1:** *Selected data from the different PVsyst reports.*

| PV module | LG Electronics (bifacial) | | | | Canadian Solar (monofacial) | | | |
|---|---|---|---|---|---|---|---|---|
| System | Fixed tilt 15 MW | HSAT 15 MW | Fixed tilt 20 MW | HSAT 20 MW | Fixed tilt 15 MW | HSAT 15 MW | Fixed tilt 20 MW | HSAT 20 MW |
| Number of panels | 37 978 | 37 980 | 50 634 | 50 634 | 39 988 | 40 000 | 53 333 | 53 340 |
| Produced energy to grid [GWh] | | | | | | | | |
| Jan | 2.43 | 2.72 | 3.17 | 3.61 | 2.19 | 2.33 | 2.90 | 2.89 |
| Feb | 2.18 | 2.48 | 2.84 | 3.30 | 1.98 | 2.02 | 2.61 | 2.54 |
| Mar | 2.38 | 2.71 | 3.10 | 3.58 | 2.16 | 2.15 | 2.85 | 2.78 |
| Apr | 2.13 | 2.45 | 2.78 | 3.18 | 1.93 | 1.98 | 2.54 | 2.57 |
| May | 2.29 | 2.63 | 2.99 | 3.49 | 2.06 | 2.27 | 2.72 | 2.95 |
| Jun | 2.12 | 2.45 | 2.77 | 3.26 | 1.90 | 2.17 | 2.51 | 2.81 |
| Jul | 2.08 | 2.39 | 2.71 | 3.19 | 1.86 | 2.08 | 2.45 | 2.72 |
| Aug | 2.17 | 2.52 | 2.83 | 3.47 | 1.96 | 2.07 | 2.58 | 2.68 |
| Sep | 2.34 | 2.66 | 3.04 | 3.53 | 2.12 | 2.12 | 2.80 | 2.74 |
| Oct | 2.45 | 2.83 | 3.18 | 3.70 | 2.23 | 2.27 | 2.94 | 2.89 |
| Nov | 2.32 | 2.62 | 3.01 | 3.47 | 2.10 | 2.22 | 2.77 | 2.76 |
| Dec | 2.37 | 2.68 | 3.09 | 3.58 | 2.14 | 2.32 | 2.82 | 2.86 |
| $\Sigma$ [GWh/year] | 27.3 | 31.1 | 35.5 | 41.4 | 24.6 | 26.0 | 32.5 | 33.2 |

Regarding the losses from LG Electronics (bifacial) the fixed tilt and HSAT gives quite different results, considering gained horizontal irradiation. With the fixed tilt the IAM-losses are at about 2.9%, whilst with HSAT they are at about 1.5%. The temperature losses varies between 5.7% to 6.8%, where HSAT generates the most. Wiring losses and mismatch losses keeps relatively constant at about 1.0% - 1.3%. The inverter losses during operation are between 1.2% - 2.0% for 15 MW and approximately 3.6% for 20 MW.

Furthermore, concerning the rear side of the bifacial panels, the ground reflection losses, also called the albedo, are all at 70%. The view factor is approximately between 61% to 66%. The sky diffuse have the biggest positive impact on the HSAT at 15MW, where it is at 31%. At 20 MW it is at 8.3%, and for the fixed tilts they are close to zero. The shading losses on the rear side are all at 5%, and the global irradiance for the HSAT at 15MW and 20 MW is at between 8.7% - 10%. For the fixed tilt at 15 MW and 20 MW, the global irradiance is at about 13%.

Canadian Solar (monofacial) gives a different set off losses. The IAM-losses for the fixed tilt are between 2.4% - 3.2%, whilst for the HSAT they are at approximately 0.7%. The temperature losses are all roughly 6.0%, and the wiring losses and mismatch losses are all respectively 1.0% and 1.1%. The inverter losses during operation are around 1.2% to 2.0%. The irradiance losses, also called near shading, are close to zero for the fixed tilt both with 15 MW and 20 MW. For the HSAT the irradiance losses are 0.7% for 15MW and 6.0% for 20 MW. All the loss variables are estimated over the course of one whole year and collected from the PVsyst reports, which can be viewed in appendix E.

### 5.2.2 Matlab

Matlab is a programming platform allowing the user to create mathematical models and applications, analyze data or develop algorithms. This program uses MATLAB language which has been used to create most of the graphs in this thesis as well as simulating multiple cases and conditions in different environments and scenarios.

#### Approach

All data sets regarding Achwa 2 location site and production as well as information about load profiles in the area were obtained from ARPE Limited. This company is the main developer and owner of the existing Achwa 2 HPP in Uganda.

Most of the files containing requested information for this thesis were simulated by the developer company or based on the accumulated measurements. To produce needed results all data sets had to be controlled and closely investigated to see if there were any irregularities. In order to achieve the most reliable results all materials had to be sorted out and put together in the right order. This approach revealed multiple incidents of missing values and uneven measurements, especially regarding load profile which will be presented in upcoming chapters. Since these given parameters were not accountable for all required time intervals, the approach of finding the average values was chosen. As both hydropower and solar energy depend on the meteorological effects as well as the environment surrounding the power plants, the values can vary significantly each year.

Some estimates had to be taken into the account given the lack of information in the wide spectrum of uncertainties and influential variables in each case. They were chosen after multiple consultations with academics and supervisors.

### Results

The results regarding synergy from the two sources will be presented in the upcoming chapters, as they have been manufactured in different ways using different Matlab codes. A closer perspective on how the results have been organized and produced, is located in appendix D.

## 5.3 Optimal Generation Schedule

This chapter will focus on illustrating combined overall production from Achwa 2 Hydroelectric power plant and all designed PV power plants presented in previous chapters. Given the PVsyst simulations for all four cases, dedicated graphs have been produced by using Matlab. Obtained data from those PV simulations consists of one hour intervals and therefore do not represent real life PV production curves. As illustrated in the figure 5.3.1, the power production can change drastically in the matter of minutes. The idealized version of daily power output will be used in this thesis due to the lack of more detailed data sets.

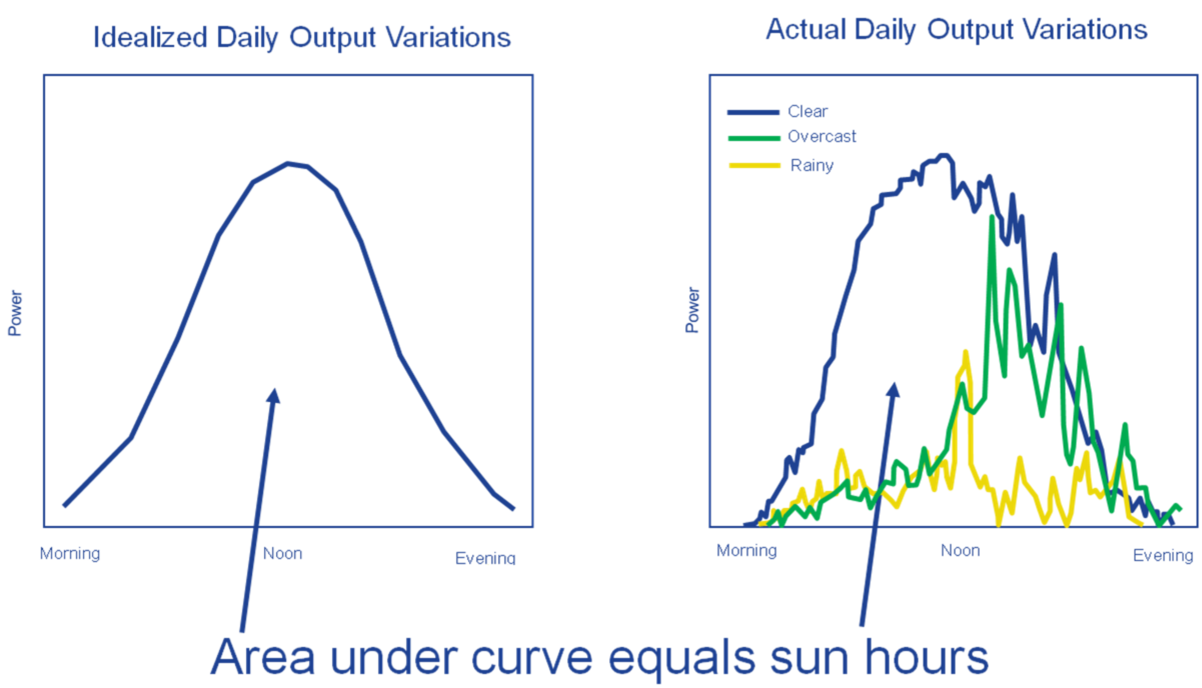


**Figure 5.3.1:** *Difference between theoretical PV production and actual production.[60]*

### 5.3.1 Load consumption

The government of Uganda has in recent years set a new goal to increase the consumption of energy across the country by developing new power plants and constructing high voltage grid networks. It has been reported that the energy demand in Uganda increases with an average 10% annually and will by 2030 peak around 1873 MW nationwide.[3]

Obtained load consumption data from Gulu and Kitgum districts contains daily demand values for five months from February to June with 30 minutes intervals. Since the data set was incomplete, with missing daily and hourly values, the average daily demand for each month has been calculated and later used to define an average annual daily load consumption. A compressed example sheet of the data set for April has been attached in appendix D as figure D.0.1.

As earlier mentioned, the Achwa 2 grid will expand its range to be able to deliver more power further in the region. Since the current grid is limited to a 33 kV substation line, the average load consumption lies around 4 MW, based on gathered information from previously mentioned data set. After the 132 kV line and 30 MVA transformer replace current components further areas will be reached. It is assumed that the load will increase by ten times and as such has been presented in figure 5.3.2.

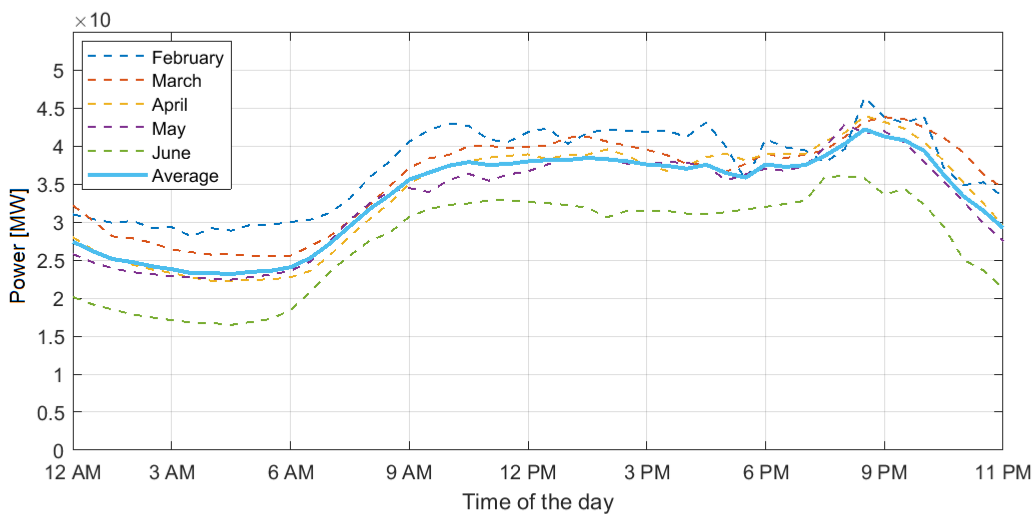


**Figure 5.3.2:** *Calculated average demand after the expansion.*

As the illustration shows, the average daily demand lies at around 40MW, which gives the hydro-electric power plant enough capacity to run fully in the wet season and at the same time distribute enough power as a single power source. That mentioned, it has to be noted that the power production from Achwa 2 power plant is not only controlled by the load curves and electricity exchange prices, but is also influenced by the government of Uganda itself. This means that even though the load consumption in the region can be reached from hydro power production alone, it can be desirable to use other power plants as well.

The annual demand curve presented in later chapters is not an accurate representation of the actual annual load profile in the area. Based on previously mentioned findings, the load profile was showing a decline in value but it was not possible to estimate values for the whole average year. Due to lack of information the simplified demand curve has been created after consultation with an individual working with the Achwa 2 HPP.

### 5.3.2 Potential production forecast

All calculations and simulations presented in previous chapters have been used to forecast power production outlines. All graphs presented in this subchapter are put together from average production values which in reality can change drastically in periods and therefore should not be taken as a final production supply. The annual demand curve, as stated in previous chapter, is an approximation to what a real life demand curve could look like and is in no way an exact presentation of actual load profile in Gulu and Kitgum districts.

To illustrate the average daily production, the month of June was chosen because of its high power production from Achwa 2 HPP which, based on the findings, do not fulfill the created demand curve in this month. Since the power production from the designed PV power plants perform quite similar in the different cases, as well as filling the gap between the load profile and Achwa 2 energy output, it was decided that this month would be most interesting for closer analysis.

Combining two sources significantly helps to close the gap between the demand curve and predict hydroelectric generated power. The difference varies from each case but it can be stated that the PV plant contributes overall positively to power production, especially in the dry season. The power peak is at it highest during wet season period, but varies depending on the case and can be significantly lower due to production differences from Achwa 2 HPP.

It can also be observed that the tracking system helps to increase the power by creating more steep curves at the beginning and end of the day. Energy production rises faster by a significant amount in some, of later presented, cases. In reality the demand curve would be met with other energy sources, in this case in the mornings and evenings.

A short version of the Matlab code used for creation of up-following curves and graphs is presented in the appendix D as listing 2 for annual production, and listing 3 for daily production forecasts.

### Case 1: 15 MWp Monofacial Canadian Solar

Case 1 presents combined hybrid production from Achwa 2 and 15 MWp PV power plant constructed of monofacial Canadian Solar CS3U-375MS 1500 V panels presented in chapter 4.4.1. The annual hybrid production graph consists of photovoltaics with both mounting systems. As demonstrated in the figure 5.3.3, HSAT, increases the power production by a defined red margin in summer months as well as dry season. In the wet season, hybridpower plant can produce up to 55 MW at its peak in August. This production exceeds the load profile with almost 15 MW in value for both fixed tilt and tracking PV system.

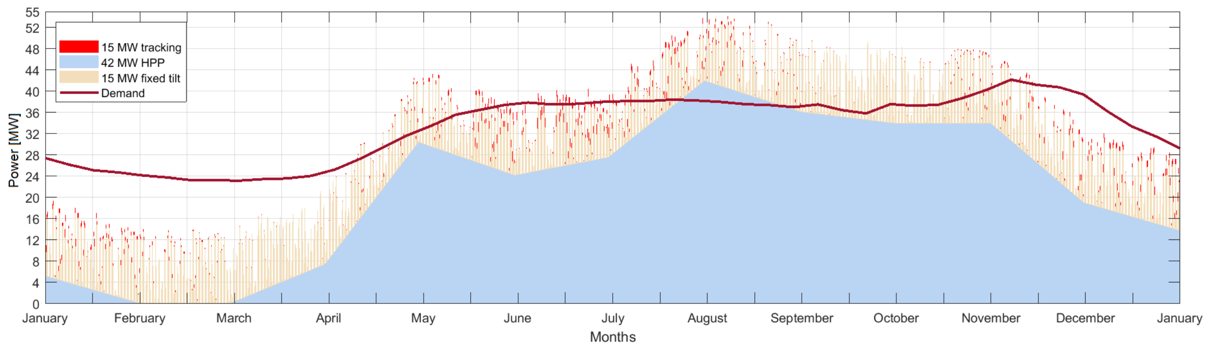


**Figure 5.3.3:** *Annual production from hybrid power plant: 15 MW Canadian Solar.*

Daily power curves have been created for a 15 MWp PV scenario where production from hydropower plant is constant throughout the day. As shown in figure 5.3.4 the PV production helps increasing the total power in the middle of the day when generated solar energy is at its greatest. Regardless of additional energy source the total output was able to reach and exceed the load profile curve only between around 4 A.M. and 8 A.M.

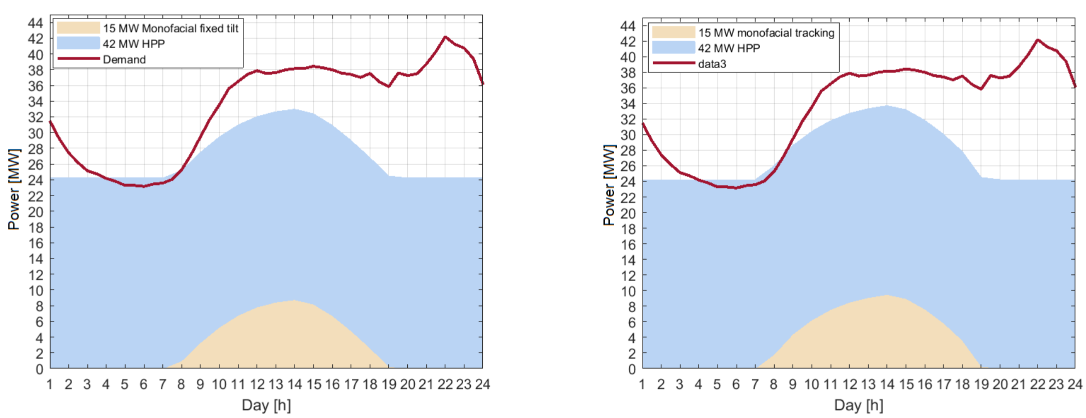


**(a)** *Fixed tilt PV* **(b)** *HSAT PV*

**Figure 5.3.4:** *Daily MW curve in June: monofacial 15 MW power plant.*

### Case 2: 15 MWp Bifacial LG Electronics

The bifacial panels from LG Electronics in Case 2, gain more power from HSAT than the monofacial competitor from Canadian Solar, with the same power peak. This increased production occurs evenly throughout the year, marked with the red coloured area on the figure 5.3.5. The annual hybrid production peak is at 56 MW. The bifacial PV plant contribute similar amount of energy to the system in comparison to its monofacial predecessor. This is shown more clearly in figure 5.3.11 at the end of this chapter.

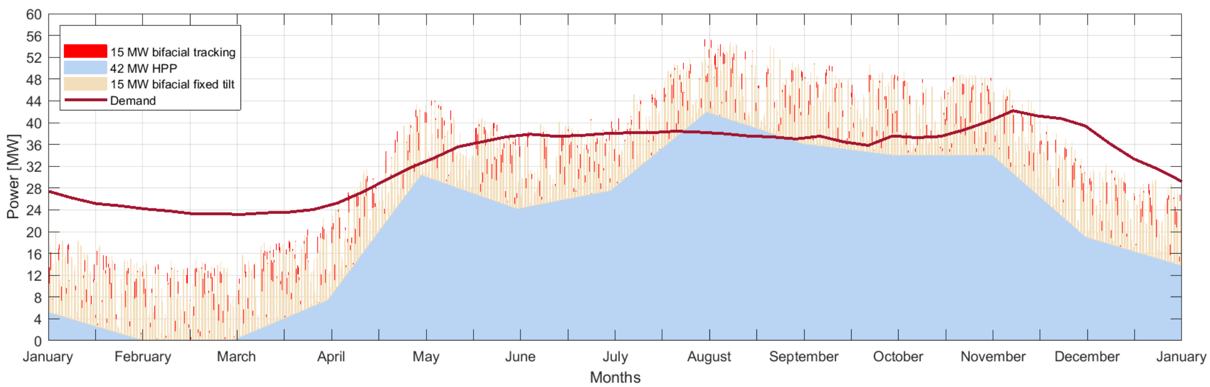


**Figure 5.3.5:** *Annual production from hybrid power plant: 15 MW LG Electronics.*

Power plant with implemented HSAT reaches higher production values faster, than the fixed tilt solution. In the figure 5.3.6(a) the PV generation exceeds 4 MW around 9 A.M., while the tracking system has a value of around 6 MW at the same time spot. Hydropower production is estimated to be stable at 24 MW throughout the day. The HSAT effect is more visible on bifacial panels and thus creates notably enough energy for the demand curve between 4.A.M. and 10 A.M. For detailed hourly production see table 5.3.1.

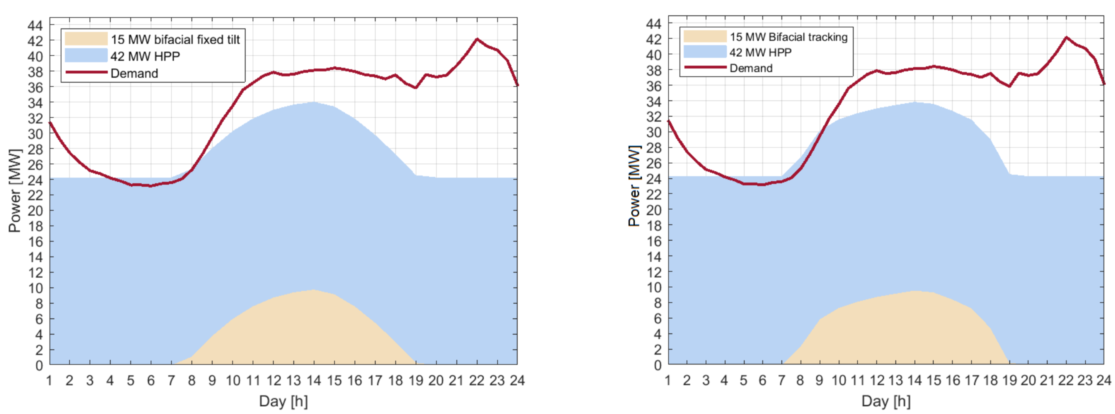


**(a)** *Fixed tilt PV*



**(b)** *HSAT PV*

**Figure 5.3.6:** *Daily power curve in June: bifacial 15 MW power plant.*

### Case 3: 20 MWp Monofacial Canadian Solar

Case 3 presents the combined system with bigger energy capacity at 20 MW for the designed monofacial PV power plant. Similarly to Case 1, the HSAT system increases the output power between the months of May and August, based on the findings presented in figure 5.3.7. Overproduction, relative to calculated load profile occurs from April to November. The annual production from this hybrid power plant surpasses the 56 MW mark at its peak. The generation gain from PV facility is relatively constant throughout the year and therefore quite predictable.

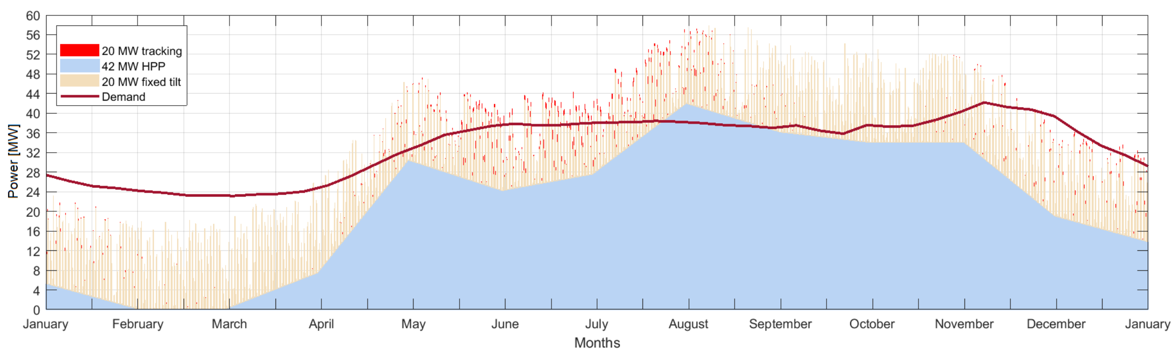


**Figure 5.3.7:** *Annual production from hybrid power plant: 20 MW Canadian Solar.*

As it can be observed in figure 5.3.8, the power peak for the case 3 is significantly higher in the middle of the day, at around 12 MW, compared to prior cases. This is shown to increase the total production to around 36 MW and at the same time, reduce the demand gap. The difference between the two PV mounting systems is noticeable in production, with HSAT fulfilling the load profile in the morning hours more evenly than the fixed tilt construction.

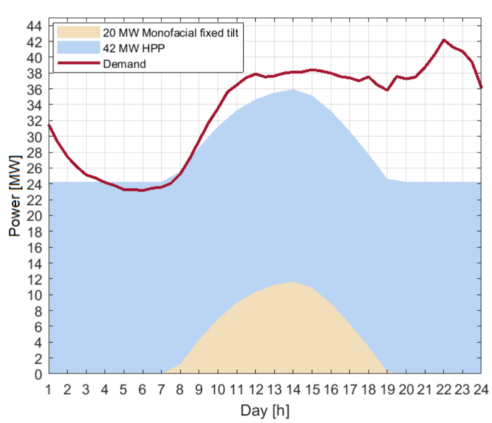


**(a)** *Fixed tilt PV*

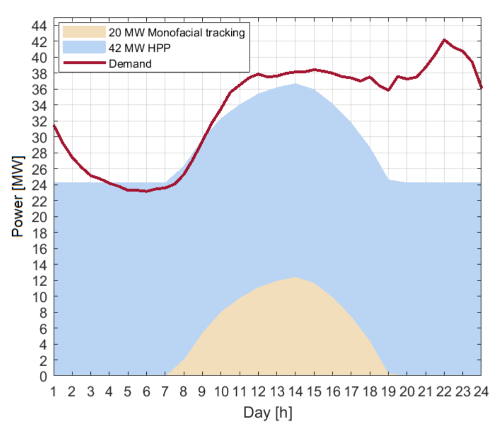


**(b)** *HSAT PV*

**Figure 5.3.8:** *Daily power curve in June: monofacial 20 MW power plant.*

### Case 4: 20 MWp Bifacial LG Electronics

The final case presents hybrid production with implementation of the 20 MW version of the bifacial PV power plant. As shown in the figure 5.3.9 the HSAT system increases the overall production in a noticeable way throughout the year. At its peak, production goes up to 60 MW and fills out most of the load profile gap. The losses due to overproduction are also biggest for this case, ranging from April to November.

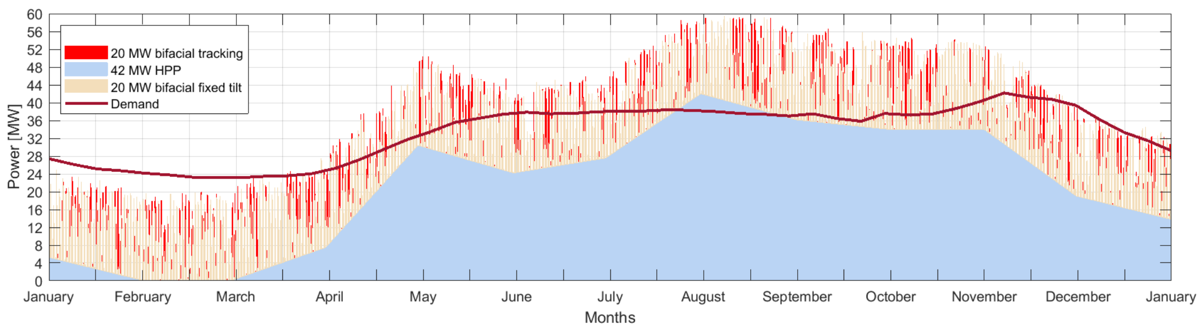


**Figure 5.3.9:** *Annual production from hybrid power plant: 20 MW LG Electronics.*

PV with fixed tilt system, presented in 5.3.10(a) as the yellow area, contributes to smaller hybrid over production at the beginning of the day in contrast to HSAT version of the same plant. Hydropower plant production with implemented tracking system in figure 5.3.10(b) fulfills the demand gap when sun production is at its maximum. HSAT is shown to affect PV production curve by creating even curve with the power peak at around 14MW.

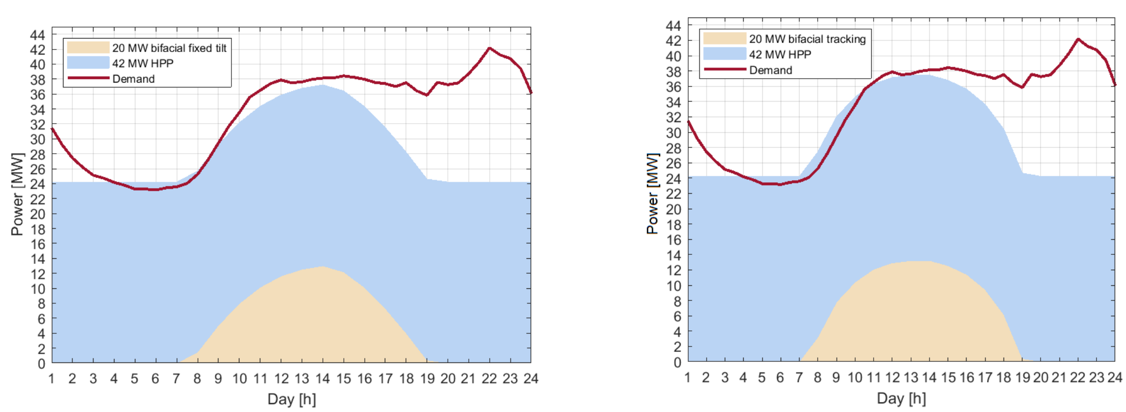


**(a)** *Fixed tilt PV* **(b)** *HSAT PV*

**Figure 5.3.10:** *Daily power curve in June: bifacial 20 MW power plant.*

### Profile comparison

For closer analysis, all PV power contributions to the synergy on the daily charts, have been put together and illustrated in the figure 5.3.11 below. Examination of the following figure reveals detailed structure changes between all designs. As previously observed, using HSAT system results in wider curves and at the same time larger power production with higher peaks.

The production from 15 MW bifacial LG Electronics power plant seem to be most affected by tracking system out of all presented cases. The area (dark green) is noticeably bigger than the fixed tilt version (beige) of the same design.

Daily production schedule shows that the maximal production peak occurs on average between 12 PM and 2 PM. Since the location site is located near the equator, the daytime does not change in any significant way throughout the year. Based on that premise, it is assumed that the average production will start around 6 AM and end before 8 PM.

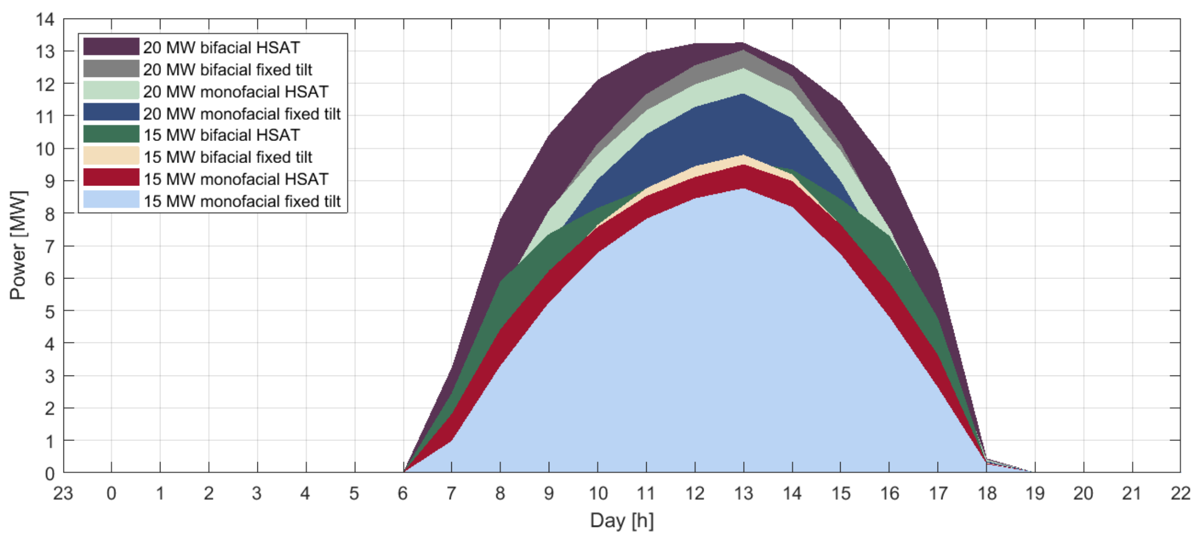


**Figure 5.3.11:** *Daily production in June: different designs.*

The calculated average daily data for June PV production has been presented in the table 5.3.1. The values escalate from the smallest systems on the right to the bigger ones on the left. The table excludes production hours between 7 PM and 6 AM since no production occurs during those hours.

All bifacial power plant designs perform better in given months than their monofacial competitors. Calculations show that a power plant consisting of LG Electronic modules have on average a 11.1% increased daily production in June in comparison to a PV plant consisting out of monofacial modules from Canadian Solar.

**Table 5.3.1:** *Potential average daily power production from PV.*

| | Case 1 fixed tilt | Case 2 fixed tilt | Case 1 HSAT | Case 2 HSAT | Case 3 fixed tilt | Case 4 fixed tilt | Case 3 HSAT | Case 4 HSAT |
|---|---|---|---|---|---|---|---|---|
| Produced Energy [MW] | | | | | | | | |
| 6 AM | 0 | 0 | 0 | 0 | 0 | 0 | 0 | 0 |
| 7 AM | 0.98 | 1.03 | 1.80 | 2.44 | 1.30 | 1.37 | 2.08 | 3.23 |
| 8 AM | 3.29 | 3.42 | 4.41 | 5.88 | 4.39 | 4.56 | 5.44 | 7.80 |
| 9 AM | 5.24 | 5.42 | 6.22 | 7.35 | 6.99 | 7.23 | 8.08 | 10.40 |
| 10 AM | 6.76 | 6.96 | 7.56 | 8.15 | 9.02 | 9.30 | 9.80 | 12.10 |
| 11 AM | 7.81 | 8.03 | 8.51 | 8.75 | 10.42 | 10.69 | 11.15 | 12.92 |
| 12 PM | 8.44 | 8.66 | 9.10 | 9.18 | 11.26 | 11.54 | 11.96 | 13.22 |
| 1 PM | 8.76 | 8.99 | 9.49 | 9.58 | 11.68 | 11.98 | 12.45 | 13.24 |
| 2 PM | 8.18 | 8.41 | 8.97 | 9.33 | 10.91 | 11.20 | 11.71 | 12.56 |
| 3 PM | 6.72 | 6.93 | 7.63 | 8.42 | 8.96 | 9.25 | 9.90 | 11.42 |
| 4 PM | 4.78 | 4.96 | 5.84 | 7.29 | 6.38 | 6.61 | 7.51 | 9.44 |
| 5 PM | 2.61 | 2.72 | 3.60 | 4.74 | 3.48 | 3.63 | 4.44 | 6.20 |
| 6 PM | 0.26 | 0.27 | 0.29 | 0.28 | 0.35 | 0.36 | 0.38 | 0.43 |
| 7 PM | 0 | 0 | 0 | 0 | 0 | 0 | 0 | 0 |

## 5.4 Operation and maintenance

In order to secure a stable year-round production of electricity from the PV plant, proper maintenance is required. It is common to divide the maintenance tasks into three categories - preventative maintenance, corrective maintenance and condition-based maintenance. Tasks associated with preventative maintenance include panel cleaning, vegetation management, water drainage, maintaining site roads and fences as well as inspecting equipment like inverters and generators. Tasks associated with corrective maintenance include on-site monitoring, critical and non-critical repairs as well as enforcing warranties of components. Tasks associated with condition-based maintenance include active monitoring, warranty enforcement and replacements of equipment.[61]

As the tasks linked to operations and maintenance of a PV plant vary in complexity and difficulty, some may be performed by unskilled workers, while other needs the expertise of skilled employees. Due to the varying labor costs worldwide, the total costs of operations and maintenance will differ from one country to another. There are several ways to calculate the O&M costs for a PV plant. One way is to assume that the O&M costs constitutes approximately 1% of the overall investment costs for the PV system. Another way is to assume the expenses based on the installed capacity of the plant. According to the Electric Power Research Institute the costs for operations and maintenance can be expected to range between 10 and 45 USD/kWp per year [61]. As this institute base their costs on U.S. labor costs and conditions, it can be expected to be lower in Uganda, where the cost level is lower. Therefore, it was assumed that O&M-costs were 10 USD/kW per year.

The tilt of the PV panels is 3°. As explained earlier in the thesis, this tilt is the most ideal one for the location and will generate the most power. 3°is a very low angle that is almost level with the ground. It is known phenomenon that the cleaning effect from rainwater is challenged when the tilt of the panels is below 10°. Therefore, the panels must be cleaned manually by hand, or automatically by sprinklers in order to maintain the desired power output. This will have an effect on the OPEX, as the workers employed to maintain the panels have to be paid.

### 5.4.1 Forecasting

Electricity production from photovoltaic sources is known to be sensitive, and may vary considerably in the matter of seconds. All energy created from the panels relies on the stable energy source which can easily be overshadowed by clouds. Since weather conditions play a big role in PV power generation, a real time control performance system is vital for hybrid plant functionality. In order to ensure a stable grid and sufficient delivery of electrical power, forecasting of the production from both sources will be implemented in this project.

Sky cameras, mounted on strategically placed masts, combined with weather sensors enables the possibility of short-term prediction for the photovoltaics. The obtained information would then be used to place the panels in the correct position and maximize energy output. The same data can help regulate inverters output power, given the multiple, drastic fluctuations in production. An example of this is illustrated in figure 5.4.1, where the system output (green line) has been shrunk to be as stable as possible in the afternoon.

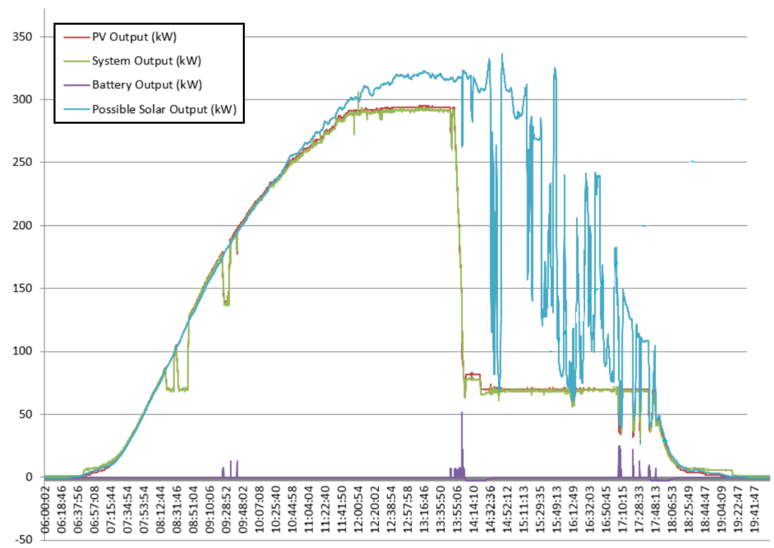


**Figure 5.4.1:** *Example of actual daily PV generation including forecasting and control system.[62]*

The hybrid plant adds production from hydro which can, to some extent, be regulated based on forecasting analysis and meet the required demand. In the event of incoming clouds, the turbines will have to pick up the lost production due to the lack of solar irradiance. In this case pondage storage could also be used if water level is above minimal requirements. This operation would ensure that the frequency of the grid would maintain stable.

### 5.4.2 Hybrid Plant control system

Each component presented in this thesis contributes to the final energy generation output. To operate a secure and reliable power plant, a wide and detailed control system is required. A simplified scheme has been produced and illustrated in the figure 5.4.2. It shows how all main parts within the hybrid power plant communicate with each other. In order to balance production from HPP with PV, a tracking of power supply has to be executed. The information from the PV arrays are therefore sent to SCADA/EMS and presented to plant workers. The information and requests are then sent back to the individual components and PPC which controls the final output to the grid. There is therefore no need for communication between units since all coordination happens on a higher level.

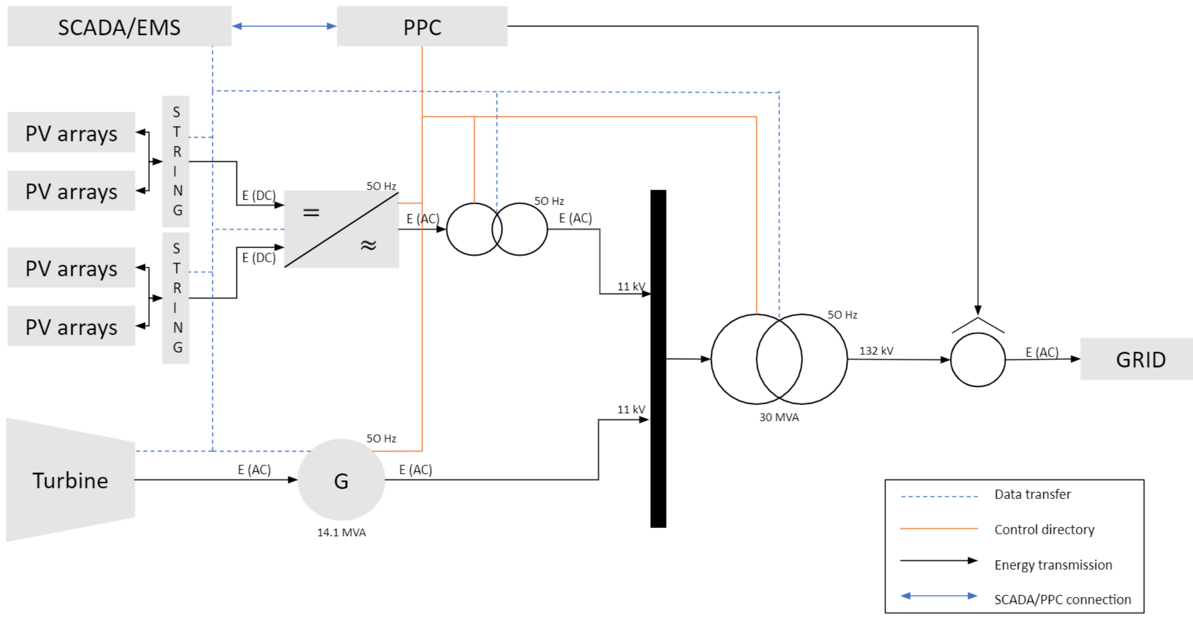


**Figure 5.4.2:** *Hybrid system scheme*

In order to utilize the plant in an efficient and safe manner, one has to create a supervision system structure with different levels of controls. The hierarchy presented in figure 5.4.1 has been created specifically for this thesis and is made up of three levels. Master control takes care of overall operation and optimization of the whole HRES. A few of its main objectives are frequency control, monitoring of performance and ensuring safe electricity output to the grid. It is crucial that all major safety measures are managed on this level, since the vitality of the power plant and grid stability relies on it. The second level contributes with more specific tasks, like holding and optimal water flow through the valves, or identifying the right operation mode for the hybrid plant. On the field level, also called basic control level, all above given assigns are fulfilled. It is on this level the majority of sensors are installed.

**Table 5.4.1:** *Control system hierarchy for hybrid power plant.*

| Control hierarchy | Objectives | Input |
|---|---|---|
| Level 1 | | |
| Master Control | Ensure grid stability<br>- Erase lag<br>- Frequency control<br>- Voltage control<br>- Reactive power control<br>Monitor the control performance<br>Control day/night cycles<br>Generation forecast<br>Meet variations in production; ramp sources<br>Ensure to rotate usage between components<br>Adjust output to follow load profile changes | Available production HPP<br>Available production PV<br>Frequency status<br>Delay time<br>Required demand<br>Transformer capacity<br>Evaluate state of charge if battery is integrated in the plant |
| Level 2 | | |
| Direct control level | Communicate with the master controller<br>Identify the right production strategy mode<br>Prioritize PV<br>Control cooling systems<br>Optimal water flow<br>Load regulation<br>Power curve optimization<br>Maximize combined energy generation | Master control directive<br>Identify water stream flow<br>Pondage reserves<br>Transformer status<br>Weather forecast<br>- Temperature/GHI/rain data |
| Level 3 | | |
| Basic control level HPP | Load rejection<br>Monitor units<br>Pressure control<br>Open/Close valves | Direct control directive<br>Turbine status<br>Flowmeter status |
| Basic control level PV | Maximize power tracking (MPPT)<br>- HSAT control<br>Internal monitoring control of inverter | Direct control directive<br>Sun path<br>Sky camera |

# 6 Economic assessment

One of the aspects of the feasibility study is to investigate the economical viability of the project. In this section, this is examined.

## 6.1 Feed-in-tariffs

In order to increase the production of renewable energy, feed-in tariffs (FIT) have been introduced in several countries, including Uganda. The goal is to stimulate electricity production by offering fixed prices for electricity over a guaranteed time period. This secures the developers a return on the investment. In order to qualify for Uganda Renewable Energy Feed-in Tariff (REFIT), the renewable energy generator must have an installed capacity of 0.5-20 MW.[63] As Achwa 2 has an installed capacity of 42 MW, the feed-in tariff has to be negotiated individually. The feed-in tariff prices for Achwa 2 are listed below, and was obtained by contacting a representative from the hydropower plant.

- 1st year of production: 9.83 US cents/kWh
- 2nd year of production: 10.16 US cents/kWh
- 3rd-15th year of production: 9.97 US cents/kWh
- 16th year of production: 6.96 US cents/kWh
- 17th year of production: 5.09 US cents/kWh
- 18th-21st year of production: 3.48 US cents/kWh
- 22nd year of production and onward: 3.43 US cents/kWh

For the economical analysis of the PV plant in this thesis, it is assumed that the tariff prices are the same as for Achwa 2 hydropower plant.

In the economical calculations, a discount rate of 10% was used, as this was the discount rate used by NREL for PV projects in sub-Saharan Africa.[64]

## 6.2 Cost analysis

**Table 6.2.1:** *High-level CAPEX for PV system in sub-Saharan Africa.*

| Component | USD/kWp | % | USD |
|---|---|---|---|
| PV modules | 300 | 28 | 4,500,000 |
| Mounting system | 210 | 19 | 3,150,000 |
| Inverters | 142 | 13 | 2,130,000 |
| Construction | 110 | 10 | 1,650,000 |
| Transformers | 94 | 9 | 1,410,000 |
| Project execution and commissioning | 86 | 8 | 1,290,000 |
| Grid evacuation | 36 | 3 | 540,000 |
| SCADA | 31 | 3 | 465,000 |
| Cables | 30 | 3 | 450,000 |
| Other official works | 26 | 2 | 390,000 |
| Protective devices | 25 | 2 | 375,000 |
| **Total project investment** | **1090** | **100** | **16,350,000** |

Table 6.2.1 contains high-level CAPEX per kilo watt peak in US dollars. Starting from the left, the first column specifies which type of component the CAPEX is for, the second column specifies the the price per kWp installed, the third column list the percentage of overall investment. The fourth and last column is an example of CAPEX numbers for a PV system with an installed capacity of 15 MW with monofacial panels and no tracking system. It is not specifically for Uganda, but rather a rough estimate for Sub-Saharan Africa, which was provided by Multiconsult.

For the economical evaluation, it was assumed that for bifacial modules, the costs of the PV modules were 5% more expensive than regular PV modules. Additionally, the mounting system for tracking PV plants was assumed to be 10% more expensive than for fixed tilt PV plants. These additional costs were based on the overall experiences from Multiconsult. As mentioned earlier the expanses related to O&M were assumed to be 10 USD/kWp per year. Based on the CAPEX and OPEX numbers, the net present value (NPV) for the different cases could be calculated. The NPV is used to determine the profitability of an investment. The investment costs for the different cases are presented in table 6.2.2.

**Table 6.2.2:** *Investment costs for different cases*

| | 15 MW | | 20 MW | |
|---|---|---|---|---|
| System | Case 1, fixed | Case 1, HSAT | Case 3, fixed | Case 3, HSAT |
| Investment [MUSD] | 16.35 | 16.67 | 21.80 | 22.43 |
| System | Case 2, fixed | Case 2, HSAT | Case 4, fixed | Case 4, HSAT |
| Investment [MUSD] | 16.58 | 16.89 | 22.52 | 22.70 |

It was also assumed that the lifetime of the PV plant was 25 years, as the producers of the panels provide a 25 year warranty. The discount rate used for the calculation of net present value was 10%.

### 6.2.1 NPV

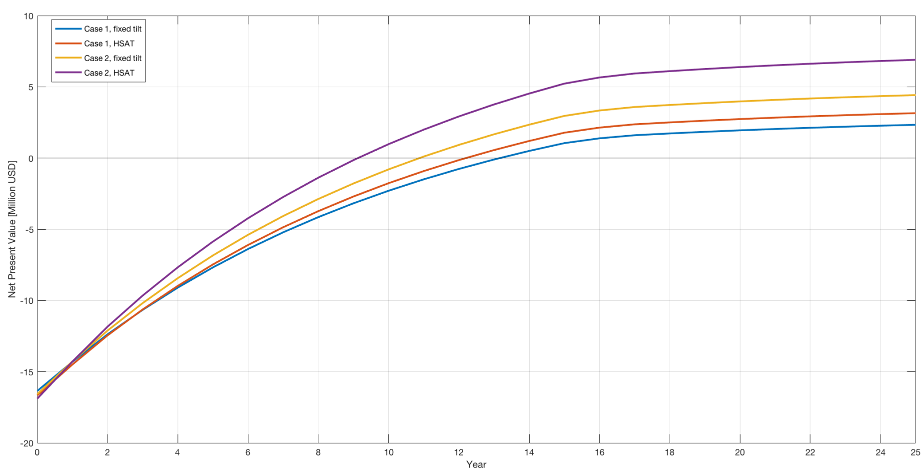


**Figure 6.2.1:** *Net present value for 15MW power plant.*

Figure 6.2.1 shows the net present value for the 4 different panel/mounting technologies for a plant with an installed capacity of 15MW. The bifacial LG panel with horizontal tracking gives the highest NPV out of them at 6.9 million USD, while Canadian Solar with fixed tilt gives the lowest 2.3 million USD. An example of how the calculation of the NPV were made can be found in appendix F, table F.1.

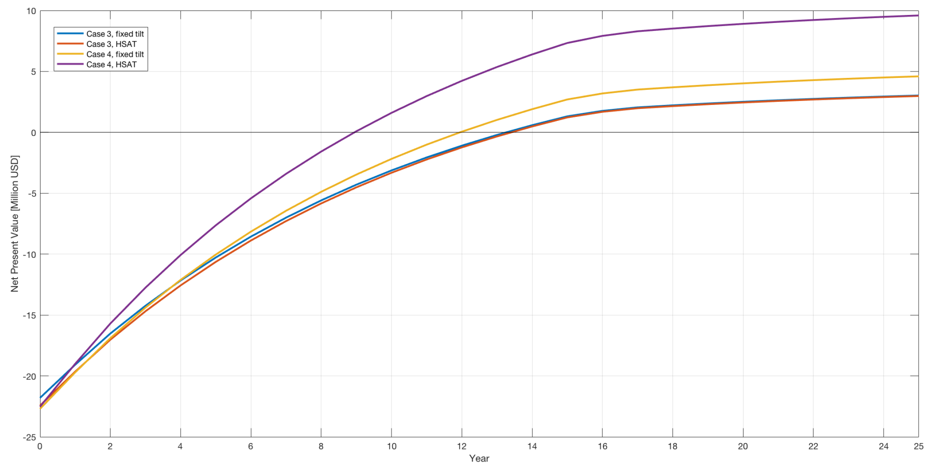


**Figure 6.2.2:** *Net present value for 20MW power plant.*

Figure 6.2.2 shows the net present value for the 4 different panel and mounting technologies for a plant with an installed capacity of 20MW. The bifacial LG panel with horizontal tracking gives the highest NPV out of them at 9.6 million USD, while Canadian Solar with HSAT gives the lowest at 3.0 million USD.

It is interesting to note that every single case gives a positive NPV, reflecting the affordability of solar power.

**Table 6.2.3:** *NPV for 15MW and 20MW*

| | 15 MW | | 20 MW | |
|---|---|---|---|---|
| System | Case 1, fixed | Case 1, HSAT | Case 3, fixed | Case 3, HSAT |
| NPV [Million USD] | 2.33 | 3.15 | 3.02 | 2.98 |
| System | Case 2, fixed | Case 2, HSAT | Case 4, fixed | Case 4, HSAT |
| NPV [Million USD] | 4.42 | 6.90 | 4.60 | 9.60 |

Table 6.2.3 presents the NPV for the different systems after 25 years of operation. The variations in NPV for the same modules, but with different sized power plants can also be compared in this table.

### 6.2.2 LCOE

**Table 6.2.4:** *LCOE for different PV system technologies.*

| | 15MW | | 20MW | |
|---|---|---|---|---|
| System | Case 1, fixed | Case 1, HSAT | Case 3, fixed | Case 3, HSAT |
| LCOE [USD/kWh] | 0.07984 | 0.07692 | 0.08012 | 0.08048 |
| System | Case 2, fixed | Case 2, HSAT | Case 4, fixed | Case 4, HSAT |
| LCOE [USD/kWh] | 0.07250 | 0.06559 | 0.07611 | 0.06482 |

Formula 2.5.3 was used for the LCOE calculations, which were made in order to determine the levelized cost of energy for the different PV system options. When doing the calculations, it was assumed a lifetime of 25 years and a discount rate of 10%. The results from these calculations are presented in table 6.2.4. From this table, it is revealed that case 4 with HSAT results in the lowest LCOE out of all the options. The highest LCOE is achieved in case 3. An example of how the LCOE calculations were made can be found in appendix F, table F.2.

### 6.2.3 EPBT

**Table 6.2.5:** *EPBT for different PV system technologies.*

| | 15MW | | 20MW | |
|---|---|---|---|---|
| System | Case 1, fixed | Case 1, HSAT | Case 3, fixed | Case 3, HSAT |
| EPBT [years] | 5.62 | 5.32 | 5.64 | 5.52 |
| System | Case 2, fixed | Case 2, HSAT | Case 4, fixed | Case 4, HSAT |
| EPBT [years] | 5.10 | 4.53 | 5.22 | 4.48 |

EPBT for the different PV alternatives were calculated using formula 2.5.1, and the results are presented in table 6.2.5. The numerator of the fraction of the equation represents the energy that went into the production of the unit, and for this case that was estimated to be 1731 kWh/m$^2$.[65] The shortest payback time was achieved with case 4 with HSAT, while the longest payback time was achieved in case 3 with fixed tilt.

### 6.2.4 EROI

**Table 6.2.6:** *EROI for different PV system technologies.*

| | 15MW | | 20MW | |
|---|---|---|---|---|
| System | Case 1, fixed | Case 1, HSAT | Case 3, fixed | Case 3, HSAT |
| EROI | 4.45 | 4.70 | 4.43 | 4.53 |
| System | Case 2, fixed | Case 2, HSAT | Case 4, fixed | Case 4, HSAT |
| EROI | 4.90 | 5.52 | 4.79 | 5.58 |

EROI for the different PV plant alternatives were calculated using formula 2.5.2, and the results are presented in table 6.2.6. The alternative with the highest energy return on investment is case 4 with HSAT, while the lowest return is case 3 with fixed tilt. For the EROI calculations, a plant lifetime of 25 years was assumed.

# 7 Discussion

This chapter will provide a further analysis of the thesis and the obtained results from the four chosen cases. The main purpose of this paper is whether the Achwa 2 HPP can be hybridized with supplementing economically viable solar power production, and if the hybridization would minimize the power generation differences. There were four different cases with various technological advancements to find the most optimal PV plant design that could provide substantial synergy between two power plants. Practical challenges and economical aspects of the presented cases and the general power demand in the area, will be discussed.

## 7.1 Natural features of the location

In this subsection, the site of the proposed PV plant itself, is discussed. The location of the proposed PV plant facility have several advantages. Meteorological data have shown that the area has a good potential for photovoltaic power with the mean global horizontal radiation at 217 W/m$^2$. Furthermore, the sunshine duration varied little throughout the day. These data made the location a promising site for a PV plant. In addition to the fact that the climate of the area is characterized by a wet and dry season, which further supported the hybridization of the existing hydro plant. The seasonal weather changes play a major role in both final design of the hybrid power plant but also economical aspects of this project. The results presented in previous chapters show that precipitation has a much higher impact on the HPP production than PV production, as expected.

The location is characterized by being relatively flat, with very few buildings or other types of settlements. This makes shadowing less of a problem than if it was to be built in a mountainous or urban area. The flatness and lack of buildings also makes it an ideal location for a PV plant, as there are few obstructions standing in the way, thus not limiting the physical size of the plant.

Simulations in PVsyst are based on meteorological data produced by Meteonorm. As mentioned in 4.2 this data is not measured on the site of the location, but rather based on interpolation from various meteorological stations in East Africa in addition to satellite data. This leads to the data being influenced by uncertainty, which for the temperature was reported to be 2.4℃, and for the GHI 2.5%. In order to minimize the uncertainty, the meteorological data would have to be recorded on the site over a defined time period. This is the also the case for the albedo, which was solely based on satellite data.

The albedo is not very high, at approximately 0.20 year round. Both technologies are dependent on the albedo, however the bifacial modules rely more heavily on it for great production. If in the near future the need for more PV production becomes a necessity, but not in a way that would require an expansion of the plant, the albedo could be altered. It would be possible to increase the albedo by introducing white sand to the area, as it has a higher albedo factor than the current soil. To avoid possible soiling impact on the panels because of wind, it is also possible to use white rocks or even embed asphalt and paint it white. This investment would increase the power production in a significant way only if the bifacial panels would be implemented in the final design. However, the costs would likely increase considerably, but could be profitable if all the extra electricity would be sold due to the additional income. This is also a cheaper solution than expanding the PV plant because of the increased demand in the future.

Temperature changes throughout the year contribute to the stable thermal losses at around 6.2% for all PV plant designs, presented in this thesis. Generally, the cases with tracking system have higher thermal losses than cases with fixed tilt. A reason for this might be that the tracking systems follows the sun path, and thereby is more directly exposed to the sun at all times. This leads to a temperature rise. Nevertheless, the overall production from HSAT modules is still higher than fixed tilt modules even though the thermal losses are higher.

The temperature losses makes a modest impact on the efficiency naturally due to the warm climate in Uganda, versus had it been in a country with a colder climate, for example Norway. The soiling losses were set to 2.0% in advance, after recommendations from the supervisor in Multiconsult. In the theory, chapter 2.3.7, it is mentioned what it is and what to do to prevent major buildup. Since the tilt on the modules is set to 3° the rainfalls ability to clean is challenged, and therefore requires autonomic cleaning system and manual maintenance. This creates the possibility for workplaces, which could have a positive impact on the society. In addition, the panels would not only be cleaned, but also be naturally cooled by the water, which could decrease the temperature losses moderately. The low tilt of the solar modules makes the environmental losses, such as shading mismatch between them, minimal and is therefore negligible.

As Uganda is a developing country, the job market is quite different than in European countries like for example Germany or Norway. Therefore, the construction of a PV plant would have a significantly higher social impact in Uganda compared to industrialized countries, by the creation of several new jobs for the areas population. These jobs would typically involve maintenance of the plant, where a portion of the tasks involved does not require highly experienced workers.

## 7.2 Components

The components chosen for this pre-feasibility study are presented in section 4.4. Since investigation of multiple PV technologies has been in focus for this project, bifacial solar panels have been chosen for closer analysis and later used in presented cases. The decision of choosing this technology was based on its innovative approach to solar harvesting with usage of both PV panel sides. Bifacials have been in development for years, but are relatively new on the commercial market. It was expected that closer analysis will bring significant variations both in power production and economical assessments. The bifacial module from LG Electronics has been analyzed with a power peak between 395 W and 514 W. This number indicates that by increasing albedo effect the overall power can be much higher, and thus need higher capacity power converters, such as inverters or transformers. The LG Electronics bifacial modules had on average an 11.1% increased daily production compared to their monofacial competitor from Canadian Solar with the same Watt peak and needed approximately between 1000m$^2$ to 2000m$^2$ smaller module area with fewer panels. The ability to generate energy from both sides requires higher elevation from the ground level, so the light can reflect into the rear side. Since the photons are collected from both sides, the panels are easily affected by temperature changes and thus could be in need of innovative cooling system.

The reports on the LG bifacial in the appendix C shows a high albedo loss and view factor for the rear side. The reason for this is most likely because of the facing of the panels on this side, which is towards the ground. Even though the panels are placed 2 m over the ground, the tilt still affects the irradiation, which is unavoidable. If the modules had been placed directly on the ground, the losses would have been even higher. The modules collects an amount of sky diffuse under operation on the rear side, which is biggest for the 15 MW HSAT, and almost zero for the fixed tilts. This could be the case because of the amount of sunlight that hits the rear side is bigger if the modules tracks the sun. Nevertheless, this does not explain the big difference between the 15 MW and 20 MW HSAT modules, which is at approximately 20%. The reason for this could be the choices taken while simulating, such as different components or 3D model placements.

Given the location of the designed PV plant it is beneficial that an efficient cooling system will be implemented in the final design. Water spraying is considered to be the best option given the reliable amount of water from the river nearby. In the wet season, it is accounted for that rain will wash off most of the dirt from the panels if they will be mounted in the efficient enough tilt above 10°. Negative side of the sprinkler based cooling system is how uneven the distribution of water can be, and therefore notable irregularities in production from each cell could be observed.

Analysis of different inverter types concluded that the central inverters connection will work best for all suggested designs, given the size of each plant. As presented earlier in the thesis, central inverters are the most efficient choice for power plants of big sizes. Another design such as string, would increase the costs of the final project and require more BOS components for the final construction. To rise the efficiency of the plant only central inverters with 1500V input were considered. As for publication date of this thesis the 1000V systems still hold the largest market share, the 1500V equivalents are foreseen to become the new standard. This taken into consideration, the 1500V inverters produce more thermal losses given higher voltage.

Because of the high voltage between the PV plant and the connection to the grid, another transformer is needed after the inverter. The reason for this is that the inverter is not suitable to run the high voltage alone, since the voltage would not be high enough to be connected to the transformer already placed there. Another alternative could have been to install a DC-DC converter before the inverter, but that was an disregarded option. The costs of a new transformer will make an impact on the CAPEX-investments, and is fully dependent on the type of inverter chosen for the PV plant.

## 7.3 Economics

As the economical aspect of the project is of great importance, several calculations related to the profitability of the project were made. These results are presented in chapter 6.2. Certain assumptions were appraised when these calculations were made, that have influenced the results both negatively and positively.

When the net present value for the different cases was calculated, the discount rate was assumed to be 10%. Deciding the discount rate was a challenging task, as this varies both from project to project as well as from country to country. A discount rate of 10% means that the shareholders expect a 10% return on the investment each year. This number may be slightly higher than the reality, thus affecting the NPV. If, for instance, the discount rate is reduced to 8% the NPV increases. Additionally, the O&M costs were assumed to be constant every year throughout the lifetime of the PV plant, which may not be the case. Deciding the yearly O&M costs was also a difficult task, as most of the information regarding this matter available online, was usually based on costs in high-income countries in the western sphere. Ultimately, it was decided to use 10 USD/kW per year. This value, however, was the lowest O&M cost in the expected range for U.S. labor costs. Therefore, it may be assumed that the actual O&M costs in Uganda were even lower than this, since Uganda is generally considered to be a low-cost state. As a consequence, the actual NPV would increase due to the decreased OPEX. The income is considered to be credible, as the purchase price of electricity is guaranteed through the Ugandan governments renewable energy feed-in tariffs.

Levelized cost of electricity was also calculated for the different cases that were investigated in this thesis. In general, the LCOE varies little between the cases, at around 8.0 US cents/kWh, with the two tracking bifacial cases being an exception at around 6.5 US cents/kWh. This is surprising, as the investment costs of these cases are significantly higher than the rest of the cases. On the other hand though, the production is far higher, resulting in a higher income due to the extra amount of power sold. It is also worth noting that there is a marginal difference between cases where the same technology, i.e. PV panel and tracking system, is used but the size of the plant is different. This implies that even though the amount of power produced is increased, the added investment cost weaken the profitability, resulting in a slightly higher LCOE. Thus, from an LCOE perspective, it may be wiser to choose a plant size of 15 MW rather than 20 MW.

The energy payback time for the different cases of PV systems were calculated to be in the range 4 to 6 years, and can be found in table 6.2.5. The EPBT is longer than what could be expected for a PV plant in sub-Saharan Africa, which in earlier chapters was said to be in the range of 0.5 to 1.4 years. This may point in the direction that perhaps the value for the embodied energy of the PV system was estimated to be higher than what it actually is. Therefore, the EPBT would increase due to the fact that the produced energy is divided by a larger number. On the other hand, if the embodied energy is assumed to be correct, the amount of power production must be less than what could be expected for the area, which in turn results in a long EPBT. Reasons for a poorer than expected power production may be a result of errors made during PV simulations in PVsyst. The EROI for the different cases are presented in table 6.2.6. From this table it is clear that the 20 MW bifacial system with HSAT has the best results, with the 15 MW bifacial system with HSAT coming second. EROI for these two are 5.58 and 5.52 respectively. A weakness of the EROI calculations is that it does not take into account that the plant may continue to produce electricity after the assumed lifetime of 25 years. If the lifetime would have been longer, the EROI would have been better than what was calculated.

From all of the economical calculations, it is clear that the most optimal case is the 20 MW bifacial system with HSAT. This case yields the highest NPV, the lowest LCOE, the shortest EPBT and the highest EROI. This was somewhat surprising, as this case has the highest investment costs by a significant margin. However, the production is a lot better than the rest of the cases, thus the profitability of this case can be attributed to the large electricity generation being sold. The second best case is the 15 MW bifacial system with HSAT.

The economic model used for the different calculations could be improved in several ways. A rough estimate for the investment costs was provided by Multiconsult. These estimates were not specifically for Uganda, but rather sub-Saharan Africa in general. Therefore, in order to get a more realistic estimate for investment costs, prices should be based on Ugandan conditions. A change in investment costs would affect the different economic parameters that were used for the profit investigation, and could therefore change the outcome of which case is the most profitable. It is reasonable to assume that possible errors made during calculations could influence the values of the economical parameters to both increase and decrease, likewise some may have canceled each other. However, the extent of this can not be quantified at the moment.

Electricity generation is mainly dependent on the amount of irradiation. As earlier mentioned, the meteorological data are not measured on site, and therefore it is reasonable to assume that the actual data will be slightly different. This will affect the yearly power production, thus also affecting the economics. If the electricity generation increases, the NPV will be higher, the LCOE will be lower, the EPBT will be shorter and the EROI will be higher, and the other way around if the generation would decrease.

Diversifying the energy sources is not only positive for the energy stability of a country, but it also affects the finances of an energy company. On one hand, investing in PV would be a significant investment for the owner of Achwa 2 hydropower plant, as the costs of constructing a PV power plant are high. On the other hand, it would secure long term income in the form of sold electricity generated from photovoltaics during dry periods where HPP production is minimal. Thus, securing a year-round income from electricity sale will stabilize the financial balance. All cases are proved to be economically feasible based on the knowledge available today.

## 7.4 Synergy

### 7.4.1 Production

Monthly power generation differences from Achwa 2 are clearly visible on the charts in chapter 3.1.3 and point at the fact that implementing a photovoltaic plant could be a reasonable solution which would help stabilizing monthly power generation. It was at first hypothesized that the PV plant would even the annual hybrid production by creating efficient energy supply in the beginning of the year when precipitation days and amount of the water in the river is low. PVsyst simulations has shown that the PV energy production changes insignificantly throughout the year and by that, increases the maximal power peak in the middle of the wet season. Average monthly generation variations, within each PV design, are under 0.5 GWh. This number indicates a small change at around 15% for each case. The electricity generation from photovoltaics is in fact lowest in June and July, and highest in March and October. Whichever design is chosen, PV has been shown to deliver steady power on the annual perspective.

Given the simulation results, it has been observed that bifacial panels are more responsive to HSAT and generate significantly more power in comparison to their monofacial equivalents. It is assumed that larger photovoltaic collection area on bifacial panels in combination with horizontal single axial tracking system, would provide more stable power source. 20 MW bifacials from LG are proved to be most sensitive to tracking system, and had biggest increase in annual production at around 16% in comparison to 2% from similarly sized Canadian Solar plant with added tracking. Given a smaller photosensitive surface, monofacial panels did not provide the same stability and energy production as theirs competitor, even though they are as feasible as the bifacials. Given the location site, implementation of HSAT is more recommended when investing in bifacial panels.

Calculations regarding daily demand curve have been projected and multiplied ten times to gain a reasonable load profile. Since the actual demand curve is unknown, the values presented are simply an approximation. Since both hydroelectric plants Achwa 1 and Achwa 3 are planned to be finished in upcoming years, it can be hypothesized that the actual demand is much higher for the Kitgum, Pader and Gulu districts, making the overproduction in wet season neglected. In the case where both energy sources are below both daily and annually average demand, the production can run at its maximum, disregarding priority of each system.

Although the overproduction stated in this thesis can be overlooked, given the fact that uncertainty regarding calculated power demand is unknown, it has been decided to discuss hybrid production in those circumstances as a probable real life situation. Additionally it has to be observed that annual electricity usage in Uganda increases each year by a significant amount. This could mean that even though the hybrid production loses the energy by overproducing as for publication of this thesis, in the long term scenario the demand will be considerably higher and thus making space for new energy power plants.

All four designed PV power plant systems have taken into the account that the Achwa 2 HPP is connected to the 132 kV grid, giving it more space for expansion of the plant by increasing the total demand based on the initially obtained data set. Based on previously discussed annual load profile, it has been noticed that overproduction occurs in the similar periods, despite chosen panel and mounting technologies in each design. Generation in facilities from Case 1 and Case 2 go notably over the demand curve from the middle of April up to the beginning of June and again, from the beginning of July to the middle of November. If one would choose a smaller capacity plant, the overall overproduction losses would be significantly reduced. For 20 MW peak designs these losses are even higher. The above mentioned systems would loose energy in much longer period from the beginning of April until the middle of November, just before the beginning of dry season.

### 7.4.2 Operation

Hybrid renewable energy systems are vulnerable for weather changes and therefore require well projected cooperation strategy. Operation of hybrid power plants require accurate control system that would be able to balance both energy sources in one combined system. As presented in the chapter 5.4.2 such control systems would have to maintain maximal production from PV arrays, while at the same time stabilize the energy output by forecasting and regulating turbines from the HPP.

Achwa 2, as a run of the river plant, is especially problematic to cooperate with a photovoltaic power plant giving that its production is fully determined by water flow in the river. This could be a problem because of the limited ability to store energy over longer periods of time. During cloudy conditions, the power output from the PV plant would be drastically reduced compared to clear sky conditions. If there is no available hydropower production to replace the generation from PV, then the stability of the grid is compromised. In a scenario where the demand is not reachable, both power sources should deliver their maximal power potential to repay for investments costs. As such, stabilization of the output power would be controlled and balanced further in the grid.

However if the load profile could be reached, solar source should be favored whereas hydropower would be responsible to deliver the rest of the missing generation. In a situation where frequency increases significantly and overproduction occurs, the power would be lost and the HPP would have to open its valves for discharging. Time used to carry out the changes in production has to be calculated so the stability of the system will be uninterrupted. Photovoltaic addition to the HPP could therefore disturb that production, forcing the turbines to operate below their maximal potential output and thus loosing energy.

As the demand for, and supply of energy in this project does not always harmonize, implementing an energy storage system may be beneficial. In the case of hybridization of Achwa 2 hydropower plant, a battery with right capacity would serve several purposes, and thus needs to be tailored to the specific needs. When the battery is connected to the grid, it can contribute to a stable power distribution, as well as controlling the frequency of the grid. In addition, batteries enable the ability to store excess solar energy for use after sunset. If one would choose to size a battery for the presented hybrid power plant, both the investment and operation costs would rise in a significant way. The designed storage would decrease the overproduction and energy losses attached to that.

However, implementation of a full sized battery for long term energy storage in Achwa 2 would not be feasible based on the power plant size and its high output power. This investment would require both adequate area as well as security measurements, that would increase the operation and maintenance costs. Battery application could not achieve long term energy storage as it would not be cost efficient. Battery usage could be limited to sustain the PV production as it can vary drastically throughout the day.

Alternatively, the existing pondage could be used for short term energy storage giving hydropower plant possibility to use PVs as a main power source and fulfilling the variations from the production. Existing pondage at the site location is able to deliver full, 42 MW production for a span of three hours. Its available capacity will differ during seasons and is possibly neglected when the river stream is weak. On the other hand, despite energy production from the hydro source is equal to zero at the beginning of the year, it is still possible for water to accumulate in the pondage, but requires longer time to reach a wanted volume.

# 8 Conclusion

In Uganda, the electricity demand has been rising at approximately 10% every year. In order to meet the increasing demand, construction of new power plants is necessary, preferably from renewable sources. Since the newly built Achwa 2 run-of-the river HPP in northern Uganda is located in an area characterized by a dry and wet seasons, it could be beneficial to hybridize the facility to secure year round power production. Given the locations flatness, available space and adequate solar irradiance, a PV plant could be a viable solution. In this thesis, synergy between these two energy sources were investigated.

All the cases that were examined proved to be economically feasible, although in varying degrees. In the early stages of this thesis, it was not known whether or not investing in bifacial PV systems would be profitable. However, from the presented results it is clear that the bifacial plants outperformed the monofacial plants. If economics is the basis for determining the best hybrid solution, Case 4 with HSAT is considered to give the best results. Out of all the cases, this one has the lowest LCOE at 6.48 US cents/kWh. The EPBT is also the shortest out of all the cases, at 4.48 years. This reveals that investing in both bifacial modules and tracking systems, despite the larger investment cost, proved profitable.

Based on the results from the simulations, the proposed PV plant would not minimize the annual fluctuations in power production. Generated power from PV during the wet season was larger than initially anticipated. Within each PV design, the average monthly generation variations were less than 0.50 GWh, therefore creating similar annual production variations for the hybrid plant. This resembles the yearly hydropower fluctuations. Generated power was found to exceed the demand for several months of the year, thus wasting potential energy. Identified challenges regarding energy production, were used to create a unique control system hierarchy for given hybrid facility. Detailed supervision scheme has been deducted to be a crucial part of efficient functionality of the hydro-PV hybrid power plant.

In conclusion, hybridizing Achwa 2 with a PV system could contribute to diversifying the power generation sources, thus stabilizing the energy supply in the area. This project would also secure income from electricity sales year round. The location of Achwa 2 is especially attractive for expansion given its increasing load demand in upcoming future. Considering the available grid connection with future plans for expansion, installed elements like SCADA system or switch yard, it can be concluded that implementation of a PV plant at Achwa 2 is economically and technically viable, and therefore recommended.

### Recommendations for further research

- Larger range of the capacity in the different cases.
- Analyze the social- and environmental aspects concerning the location.
- Investigate energy storage solutions.
- Optimization of the hybrid plant in regards to various production factors, for example improvement of the albedo.
- Examine other renewable energy sources for hybridization of Achwa 2.

# References


[1] Fraunhofer Institute for Solar Energy Systems, ISE with support of PSE Conferences & Consulting GmbH (2019): PHOTOVOLTAICS REPORT https://www.ise.fraunhofer.de/content/dam/ise/de/documents/publications/studies/Photovoltaics-Report.pdf (Read 18.01.2019)

[2] The world Bank (2019): Access to electricity (% of population). https://data.worldbank.org/indicator/eg.elc.accs.zs

[3] Energypedia (2019): Uganda Energy Situation. https://energypedia.info/wiki/Uganda_Energy_Situation?fbclid=IwAR2BQvRHmK6WEPTkRYUOlLZP99Kb2UKfuDfb_vH_eTpgoHhryXtoQvUtIAo

[4] International Hydropower Association (2018): Uganda statistics. https://www.hydropower.org/country-profiles/uganda (Read on 08.03.2019)

[5] Store Norske Leksikon (2018): Albedoeffekt. https://snl.no/albedoeffekt (Read 21.01.19)

[6] Geir Wing Gabrielsen (2019): Klimaendringer i Arktis. https://www.researchgate.net/figure/Figur-1-Albedoeffekten-pa-hav-Lys-overflate-is-og-sno-sender-80-90-av-energien_fig7_309962570 (Read 21.01.19)

[7] National Aeronautics and Space Administration (NASA), (2008): Solar Irradiance. https://www.nasa.gov/mission_pages/sdo/science/solar-irradiance.html (Read 04.02.2019)

[8] Timeanddate.com (2019): Altitude & Azimuth: The Horizontal Coordinate System. https://www.timeanddate.com/astronomy/horizontal-coordinate-system.html (Read 11.04.2019)

[9] International Hydropower Association (2019): Types of hydropower https://www.hydropower.org/types-of-hydropower (Read 16.01.19)

[10] Dr.Michael Whiticar, Energy BC (2017): Run of River Power. http://www.energybc.ca/runofriver.html (Read 11.02.2019)

[11] Changing Lanes (2013): Getting off the Grid - Have you considered Hydro-Electric Power? https://hubpages.com/politics/Getting-off-the-Grid-Have-you-considered-Hydro-Electric (Read 16.01.19)

[12] Store norske leksikon (2017): Vannkraftverk. https://snl.no/vannkraftverk (Read 18.01.19)

[13] Tetsuo Soga (2006): Nanostructured Materials for Solar Energy Conversion: Solar Cell https://www.sciencedirect.com/topics/materials-science/solar-cell (Read 18.01.19)

[14] Fraunhofer-Institut für Solare Energiesysteme ISE (2014): New world record for solar cell efficiency at 46% French-German cooperation confirms competitive advantage of European photovoltaic industry. https://web.archive.org/web/20150823133519/http://www.ise.fraunhofer.de/en/press-and-media/press-releases/press-releases-2014/new-world-record-for-solar-cell-efficiency-at-46-percent (read 17.01.2019)

[15] Green Sarawak: Going Solar Chapter 8, Know Your Solar PV Cells and Panels. https://greensarawak.com/things-to-know-before-going-solar/going-solar-chapter-8-know-your-solar-pv-cells-and-panels/

[16] Hanna Langels, Fredrik Gannedahl (2018): BiFacial PV Systems: A technological and financial comparison between BiFacial and standard PV panels, Uppsala University https://uu.diva-portal.org/smash/get/diva2:1218780/FULLTEXT01.pdf

[17] Fraunhofer Institute for Solar Energy Systems (ISE): BIFACIAL PV MODULES–CHARACTERIZATION AND SIMULATION https://www.ise.fraunhofer.de/content/dam/ise/en/documents/information-material/Photovoltaics/16_en_ISE_Flyer_Bifacial_Modules.pdf (Read 28.02.2019)

[18] LG (2018): LG Solar Webinar Series. https://customer.lgsolarusa.com/public/upload/media/images/LG_NeON2_bifacial_Module_for_attendees.pdf

[19] C. Honsberg and S. Bowden (2019): Solar Radiation on a Tilted Surface. https://www.pveducation.org/pvcdrom/properties-of-sunlight/solar-radiation-on-a-tilted-surface

[20] Sara Hoff, Jonathan DeVilbiss (2017): More than half of utility-scale solar photovoltaic systems track the sun through the day. https://www.eia.gov/todayinenergy/detail.php?id=30912

[21] G. Seguier& F. Labrique (1993): Power electronic converters: DC-AC conversion (Electric energy systems and engineering series). Berlin, Germany.

[22] SMA Solar Technology AG: PV Inverters - Basic Facts for Planning PV Systems. https://www.sma.de/en/partners/knowledgebase/pv-inverters-basic-facts-for-planning-pv-systems.html (Read 12.02.2019)

[23] R. Teodorescu, P. Rodriguez & M. Liserre, (2010): Grid converters for photovoltaic and wind power systems, Chichester, West Sussex.

[24] Diez-Mediavilla et al. (2014): Performance of grid-tied PV facilities based on real data in Spain: Central inverter versus string system. Energy Conversion and Management, 86, pp.1128–1133.

[25] Andrew Gong (2018): Understanding PV System Losses, part 1-4. https://blog.aurorasolar.com/understanding-pv-system-losses-part-1

[26] Michael Roy (2015): What is PID and how can you reduce solar power loss? https://blog.hsb.com/2015/09/03/potential-induced-degradation/

[27] David Roberts (2018): Solar power's greatest challenge was discovered 10 years ago. It looks like a duck. https://www.vox.com/energy-and-environment/2018/3/20/17128478/solar-duck-curve-nrel-researcher (Read 11.02.19)

[28] Lisa Cohn (2017): California's Grid Operator Looks at How to Absorb Excess Solar Energy with Storage. https://microgridknowledge.com/excess-solar-energy/ (Read 11.02.19)

[29] Kothari, D. P., and I. J. Nagrath. Electric Machines, page 115. 5th ed. Chennai: McGraw Hill Education (India), 2018. Print.

[30] Energifakta Norge (2019): Stromnettet. https://energifaktanorge.no/norsk-energiforsyning/kraftnett/

[31] Chen, C. Julian. "Energy Storage." Physics of Solar Energy. Hoboken, NJ, USA: John Wiley & Sons, 2011. 253-72. Web.

[32] Dricus (2015): Base Load and Peak Load: understanding both concepts. https://sinovoltaics.com/learning-center/basics/base-load-peak-load/

[33] HOMER Energy (2018): Load following. https://www.homerenergy.com/products/pro/docs/3.11/load_following.html

[34] Inductive Automation (2018): What is SCADA? https://inductiveautomation.com/resources/article/what-is-scada

[35] Integrated Dynamics (2018): Power Plant Controller (PPC) for Grid-Connected Power Plants with Energy Storage https://rdf.idi-software.com/energy/PPC.pdf

[36] TRITEC (2013): Why Solar? http://www.tritec-energy.com/za/why-solar-attractive-pv/

[37] G. Palmer and J. Floyd (2017): An Exploration of Divergence in EPBT and EROI for Solar Photovoltaics. https://link.springer.com/article/10.1007/s41247-017-0033-0

[38] Doe Office Of Indian Energy (2013): Levelized cost of energy (LCOE). https://www.energy.gov/sites/prod/files/2015/08/f25/LCOE.pdf

[39] Investopedia (2019): Capital Expenditures vs. Operating Expenses: What's the Difference? https://www.investopedia.com/ask/answers/020915/what-difference-between-capex-and-opex.asp

[40] Kjell Banken and Else Margrethe Nyhuus: Innføring I Bedriftsøkonomi, page 249. Oslo: Cappelen Akademisk Forl, 1999. Print.

[41] Berkeley Energy (2018): Achwa 2 – Hydro – Uganda. https://www.berkeley-energy.com/project/achwa-2/

[42] African Development Bank Group (2018): ACHWA II HYDROPOWER PLANT. https://www.afdb.org/en/projects-and-operations/project-portfolio/p-ug-fab-007/ (Read 20.05.2019)

[43] Yandex map. https://satellites.pro/Uganda_map#Y3.139075,32.513486,15 (Obtained 20.05.2019)

[44] ATB Riva Calzoni S.p.A. (2018): Work has begun on the HPP2 Uganda Hydropower Plant. https://www.atbrc.com/en/news/2018-02-new-hydropower-plant-in-africa.html

[45] Gulu District Local Government (2013): Statistical Abstract 2012/2013. https://www.ubos.org/onlinefiles/uploads/ubos/Gulu.pdf (Read 07.03.2019)

[46] NASA Prediction Of Worldwide Energy Resources (2018): Frequently Asked Questions. https://power.larc.nasa.gov/#faqs

[47] EU Science Hub (2016): Photovoltaic Geographical Information System (PVGS). https://ec.europa.eu/jrc/en/scientific-tool/pvgis (Read 06.03.2019)

[48] Meteotest AG (2018): Meteonorm Features. https://meteonorm.com/en/meteonorm-features (Read 23.05.19)

[49] The World Bank (2017): Solar resource data: Solargis. https://solargis.com/maps-and-gis-data/download/uganda (Downloaded 07.02.2019)

[50] Meteonorm (2019): Achwa II HPP (Meteorological Report)

[51] Ran Fu, David Feldman, Robert Margolis, Mike Woodhouse, and Kristen Ardani (NREL), (2017): U.S. Solar Photovoltaic System, Cost Benchmark: Q1 2017. https://www.nrel.gov/docs/fy17osti/68925.pdf (Read 25.02.2019)

[52] Eirini Gkoutioudi, Panagiotis Bakas, Antonios Marinopoulos (2013): Comparison of PV systems with maximum DC voltage 1000V and 1500V. https://ieeexplore.ieee.org/abstract/document/6745070 (Read 26.02.2019

[53] Ampt, LLC (2019): Ampt String Optimizers. http://www.ampt.com/wp-content/uploads/2019/02/Ampt_StringOptimizer_Brochure_4pg-51770009-2E-Web.pdf (Read 25.02.2019)

[54] International Technology Roadmap for Photovoltaic (2018): Results 2017 including maturity report 2018, Ninth edition. http://www.itrpv.net/Reports/Downloads/

[55] Mark Z. Jacobson, Vijaysinh Jadhav (2018): World estimates of PV optimal tilt angles and ratios of sunlight incident upon tilted and tracked PV panels relative to horizontal panels. https://web.stanford.edu/group/efmh/jacobson/Articles/I/TiltAngles.pdf (Read 12.03.2019)

[56] Canadian Solar Inc (2018): Datasheet KuMax CS3U-375MS. https://www.canadiansolar.com/upload/cf3b38405d3a3999/b8b58af206ab7fa2.pdf (Read 21.03.19)

[57] LG Electronics (2018): Spec Sheet NeON BiFacial 72 cells. https://www.lg.com/global/business/solar/business-resources/download (Read 21.03.2019)

[58] PVsyst (2018): PVsyst Team. https://www.pvsyst.com/pvsyst-team/ (Read 17.04.2019)

[59] PVsyst (2018): PVsyst 6 Help. http://files.pvsyst.com/help/ (Read 17.04.2019)

[60] PV Education (2019): Solar System Output. https://pveducation.com/solar-concepts/solar-system-output/ (Read 14.04.2019)

[61] Electric Power Research Institute (2015): Budgeting for solar PV plant operations & maintenance: practices and pricing. https://prod-ng.sandia.gov/techlib-noauth/access-control.cgi/2016/160649r.pdf (Read 11.04.2019)

[62] Martin Poole (2016): Cloud detection and prediction for maximising solar PV utilisation in off-grid hybrid power systems Final report: project results and lessons learnt. https://arena.gov.au/assets/2016/11/Fulcrum3D-CloudCAM-ARENA-Public-report.pdf

[63] Electricity Regulatory Authority (2012): Uganda Renewable Energy Feed-in Tariff (REFIT).

[64] National Renewable Energy Laboratory (NREL), (2018): Tariff Considerations for Micro-Grids in Sub-Saharan Africa. https://www.nrel.gov/docs/fy18osti/69044.pdf (Read 02.05.2019)

[65] Hans-Joerg Althaus (2013): Calculation of energy payback time of PV and its determinants (Presentation at the Swiss Photonics Workshop Dübendorf, October 22th 2013) https://www.swissphotonics.net/libraries.files/Althaus.pdf (Read 23.05.2019)

# A Achwa 2 HPP

**Table A.1:** *Switchyard specification*

| | |
|---|---|
| System voltage | 132kV |
| Max. voltage | 145kV |
| Rated frequency | 50Hz +/- 5% |
| Rated short time withstand current | $31.5KA_RMS/1sec.$ |
| 1.2/50 micro second lightning impulse withstand voltage | 650k$V_p$ |
| **132kV Cicuit Breaker** | |
| Type | SF6 three pole operated |
| No. of trip coil | 2 |
| Operating voltage | 110V DC |
| Motor operating voltage | 220-250V AC |
| **132kV Current Transformator** | |
| Type | Single phase outdoor |
| **132kV Isolator/Disconnector** | |
| Type | Gang operated outdoor type |
| Operation | Motorised |
| Motor operating voltage | 220-250V AC |
| **Earth switch** | |
| Operation | Manual |
| **Voltage Transformer** | |
| Type | Single phase, outdoor |
| No. of secondary cores | 3 |
| **Surge arrestor** | |
| Type | Gapless metal oxide |
| Rated voltage | 120k$V_RMS$ |

**Table A.2:** *Specifications of the expected transformer.*

| | |
|---|---|
| Type | Oil filled |
| Rating | 30 MVA, 132/11kV |
| No. of phases | 3 |
| No. of windings | 2 |
| Location | Outdoor |
| Cooling | ONAN |
| System frequency | 50 Hz +/- 5% |
| Rated voltage of LV | 11kV |
| Rated voltage of HV | 132kV |
| Max. voltage LV | 12kV |
| Max voltage HV | 145kV |
| HV winding connection | Star |
| LV winding connection | Delta |
| Neutral | Solidly grounded |
| Vector group | Ynd11 |

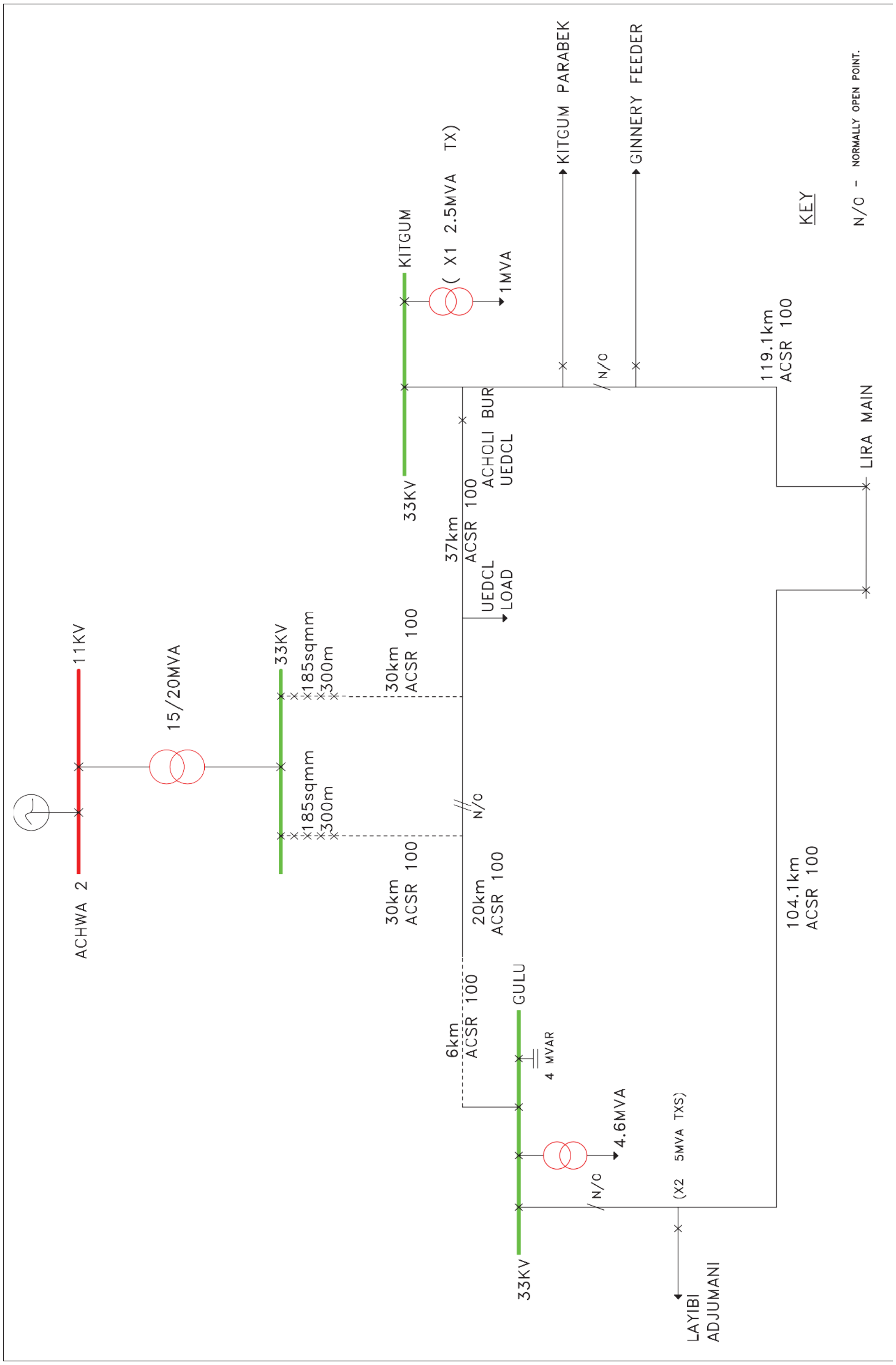


**Figure A.0.1:** *Current grid overview*

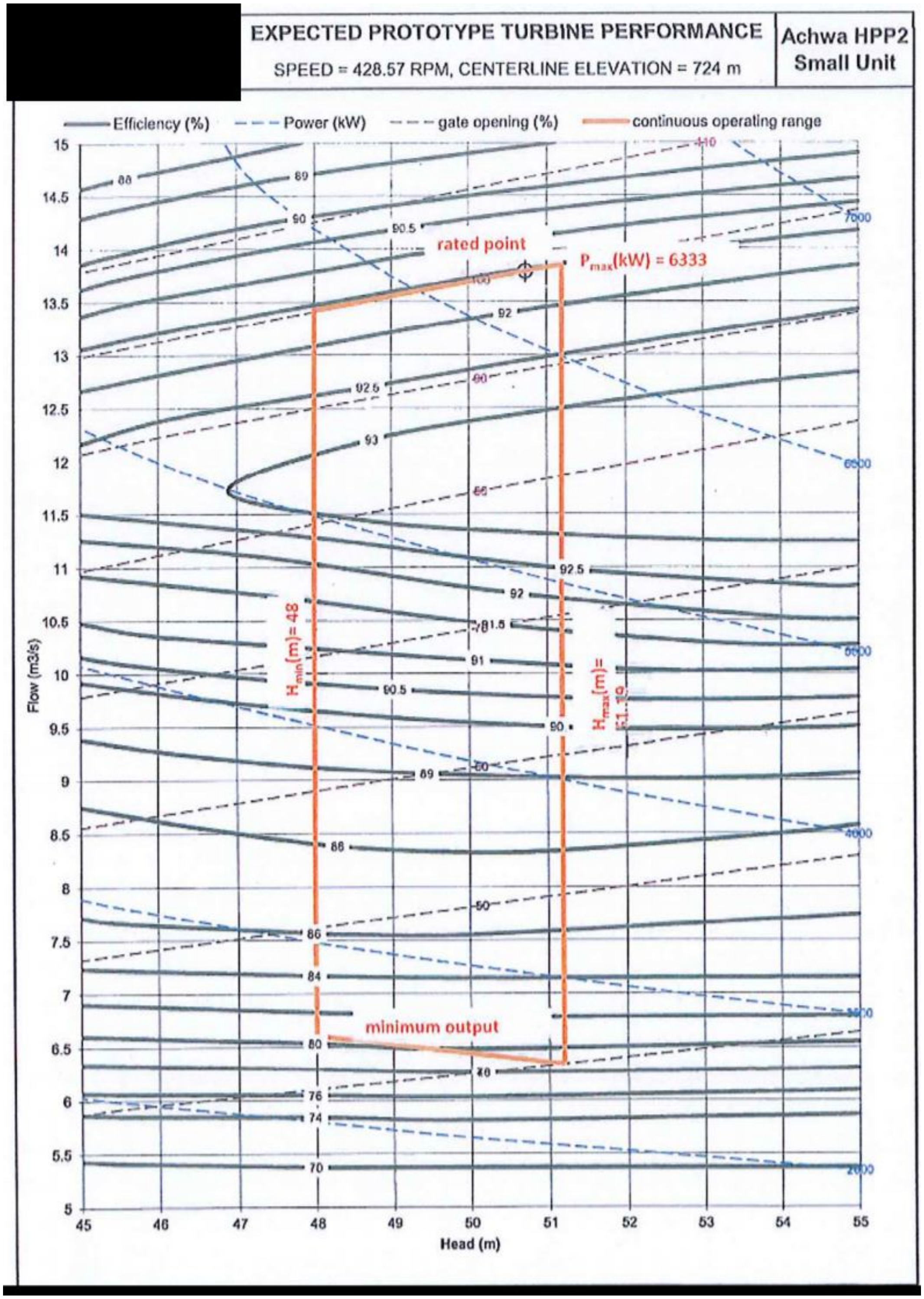


**Figure A.0.2:** *Hill chart for small unit*

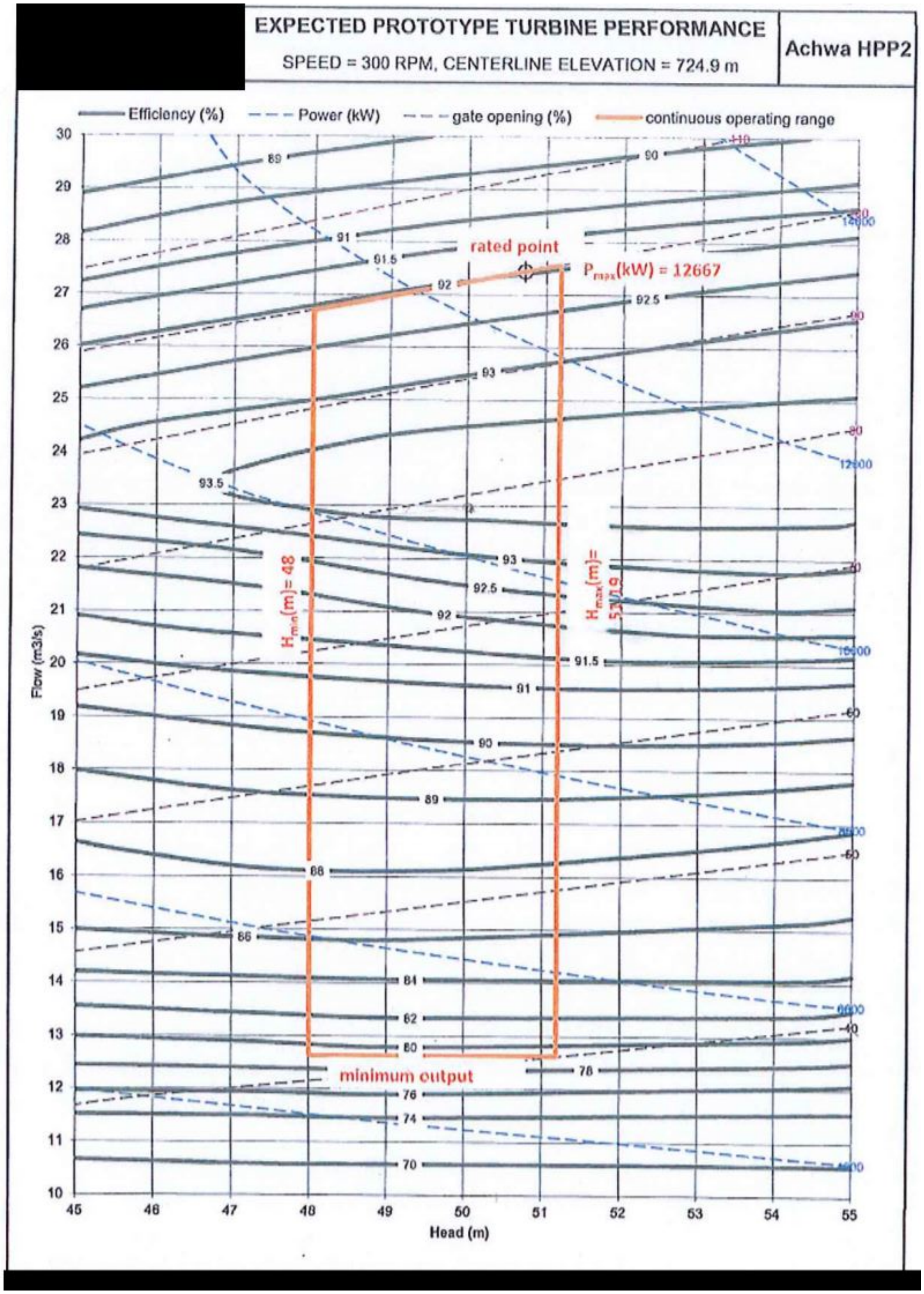


**Figure A.0.3:** *Hill chart for large unit*

**Table A.3:** *Simulated yearly electricity generation 1964 - 2016 [GWh].*

| | | | | | | | | | | | |
|---|---|---|---|---|---|---|---|---|---|---|---|
| 1964 | 187.1 | 1972 | 172.7 | 1980 | 153.3 | 1993 | 155.0 | 2001 | 181.7 | 2009 | 177.8 |
| 1965 | 182.7 | 1973 | 159.2 | 1981 | 149.4 | 1994 | 187.5 | 2002 | 203.1 | 2010 | 174.9 |
| 1966 | 163.1 | 1974 | 172.7 | 1982 | 197.7 | 1995 | 219.8 | 2003 | 181.4 | 2011 | 199.0 |
| 1967 | 183.6 | 1975 | 179.1 | 1983 | 171.2 | 1996 | 183.0 | 2004 | 166.3 | 2012 | 193.5 |
| 1968 | 186.3 | 1976 | 162.6 | 1984 | 166.5 | 1997 | 177.5 | 2005 | 152.1 | 2013 | 193.7 |
| 1969 | 170.1 | 1977 | 199.0 | 1988 | 192.6 | 1998 | 172.9 | 2006 | 200.4 | 2014 | 179.7 |
| 1970 | 169.7 | 1978 | 205.2 | 1990 | 152.4 | 1999 | 171.7 | 2007 | 182.7 | 2015 | 193.7 |
| 1971 | 169.6 | 1979 | 131.4 | 1991 | 148.8 | 2000 | 180.9 | 2008 | 152.2 | 2016 | 148.8 |

**Table A.4:** *Monthly river flow at Gulu Kitgum bridge from 2012 to 2016.*

| YEAR | 2012 | 2013 | 2014 | 2015 | 2016 |
|---|---|---|---|---|---|
| | Q ($m^3/s$) | Q ($m^3/s$) | Q ($m^3/s$) | Q ($m^3/s$) | Q ($m^3/s$) |
| JAN | 10.1 | 9.9 | 14.2 | 8.2 | 18.7 |
| FEB | 3.1 | 3.2 | 6 | 4.2 | 6.1 |
| MAR | 2.0 | 2.1 | 5.2 | 3.4 | 3.2 |
| APR | 27.7 | 22.1 | 8.5 | 16.8 | 11.8 |
| MAY | 130.9 | 62.6 | 31.9 | 82.2 | 79.2 |
| JUN | 55.4 | 24.9 | 102.3 | 71.4 | 32 |
| JUL | 83.3 | 73.7 | 79.6 | 41.9 | 41.6 |
| AUG | 146.5 | 221.3 | 159.5 | 113.6 | 108.3 |
| SEP | 154.6 | 126.7 | 182.5 | 52.7 | 74.6 |
| OCT | 72.1 | 182.3 | 107.2 | 37.3 | 90.6 |
| NOV | 112.3 | 124.3 | 81.4 | 133.2 | 21.2 |
| DEC | 38.8 | 52.9 | 44.5 | 77.7 | 7.3 |
| **AVERAGE** | **69.7** | **75.5** | **68.6** | **53.6** | **41.2** |

### ORIGINAL DATA

| Year | 2012 | 2013 | 2014 | 2015 | 2016 | Avg |
|---|---|---|---|---|---|---|
| JAN | 10.10 | 9.90 | 14.20 | 8.20 | 18.70 | 12.22 |
| FEB | 3.10 | 3.20 | 6.00 | 4.20 | 6.10 | 4.52 |
| MAR | 2.00 | 2.10 | 5.20 | 3.40 | 3.20 | 3.18 |
| APR | 27.70 | 22.10 | 8.50 | 16.80 | 11.80 | 17.38 |
| MAY | 130.90 | 62.60 | 31.90 | 82.20 | 79.20 | 77.36 |
| JUN | 55.40 | 24.90 | 102.30 | 71.40 | 32.00 | 57.20 |
| JUL | 83.30 | 73.70 | 79.60 | 41.90 | 41.60 | 64.02 |
| AUG | 146.50 | 221.30 | 159.50 | 113.60 | 108.30 | 149.84 |
| SEP | 154.60 | 126.70 | 182.50 | 52.70 | 74.60 | 118.22 |
| OCT | 72.10 | 182.30 | 107.20 | 37.30 | 90.60 | 97.90 |
| NOV | 112.30 | 124.30 | 81.40 | 133.20 | 21.20 | 94.48 |
| DEC | 38.80 | 52.90 | 44.50 | 77.70 | 7.30 | 44.24 |
| AVG | 69.73 | 75.50 | 68.57 | 53.55 | 41.22 | m^3/s |

| Year | 2012 | 2013 | 2014 | 2015 | 2016 | Avg |
|---|---|---|---|---|---|---|
| JAN | 10100.00 | 9900.00 | 14200.00 | 8200.00 | 18700.00 | 12220.00 |
| FEB | 3100.00 | 3200.00 | 6000.00 | 4200.00 | 6100.00 | 4520.00 |
| MAR | 2000.00 | 2100.00 | 5200.00 | 3400.00 | 3200.00 | 3180.00 |
| APR | 27700.00 | 22100.00 | 8500.00 | 16800.00 | 11800.00 | 17380.00 |
| MAY | 130900.0 | 62600.00 | 31900.00 | 82200.00 | 79200.00 | 77360.00 |
| JUN | 55400.00 | 24900.00 | 102300.0 | 71400.00 | 32000.00 | 57200.00 |
| JUL | 83300.0 | 73700.0 | 79600.0 | 41900.0 | 41600.0 | 64020.0 |
| AUG | 146500.0 | 221300.0 | 159500.0 | 113600.0 | 108300.0 | 149840.0 |
| SEP | 154600.0 | 126700.0 | 182500.0 | 52700.0 | 74600.0 | 118220.0 |
| OCT | 72100.0 | 182300.0 | 107200.0 | 37300.0 | 90600.0 | 97900.0 |
| NOV | 112300.0 | 124300.0 | 81400.0 | 133200.0 | 21200.0 | 94480.0 |
| DEC | 38800.00 | 52900.00 | 44500.00 | 77700.00 | 7300.00 | 44240.00 |
| AVG | 69733.33 | 75500.00 | 68566.67 | 53550.00 | 41216.67 | kg/s |

| | |
|---|---|
| Efficiency | 0.865 |
| Net head | 50.73 |
| g | 9.81 |
| W→MW | 1000000 |
| h | 8760.00 |
| Capacity factor | 1.00 |
| MW→GW | 1000.00 |

Total capacity (Max GWh production)

| 42MW | 367.92 |
|---|---|

| Year | 2012 | 2013 | 2014 | 2015 | 2016 | Avg | Avg |
|---|---|---|---|---|---|---|---|
| JAN | 4.35 | 4.26 | 6.11 | 3.53 | 8.05 | 5.26 | 3.91 |
| FEB | 1.33 | 1.38 | 2.58 | 1.81 | 2.63 | 1.95 | 1.31 |
| MAR | 0.86 | 0.90 | 2.24 | 1.46 | 1.38 | 1.37 | 1.02 |
| APR | 11.92 | 9.51 | 3.66 | 7.23 | 5.08 | 7.48 | 5.39 |
| MAY | 56.35 | 26.95 | 13.73 | 35.39 | 34.09 | 33.30 | 24.78 |
| JUN | 23.85 | 10.72 | 44.04 | 30.74 | 13.78 | 24.62 | 17.73 |
| JUL | 35.86 | 31.73 | 34.27 | 18.04 | 17.91 | 27.56 | 20.50 |
| AUG | 63.06 | 95.26 | 68.66 | 48.90 | 46.62 | 64.50 | 47.99 |
| SEP | 66.55 | 54.54 | 78.56 | 22.69 | 32.11 | 50.89 | 36.64 |
| OCT | 31.04 | 78.48 | 46.15 | 16.06 | 39.00 | 42.14 | 31.35 |
| NOV | 48.34 | 53.51 | 35.04 | 57.34 | 9.13 | 40.67 | 29.28 |
| DEC | 16.70 | 22.77 | 19.16 | 33.45 | 3.14 | 19.04 | 14.17 |
| AVG | 30.02 | 32.50 | 29.52 | 23.05 | 17.74 | MW | Gwh |
| | | | | | | | 234.07 |
| AVG | 262.96 | 284.71 | 258.56 | 201.94 | 155.43 | GWh | |
| | | | | | | 232.72 | |

### WITH DISCHARGE INTERVAL

| Year | 2012 | 2013 | 2014 | 2015 | 2016 | Avg |
|---|---|---|---|---|---|---|
| JAN | 10.10 | 9.90 | 14.20 | 8.20 | 18.70 | 12.22 |
| FEB | 0.00 | 0.00 | 0.00 | 0.00 | 0.00 | 0.00 |
| MAR | 0.00 | 0.00 | 0.00 | 0.00 | 0.00 | 0.00 |
| APR | 27.70 | 22.10 | 8.50 | 16.80 | 11.80 | 17.38 |
| MAY | 100.00 | 62.60 | 31.90 | 82.20 | 79.20 | 71.18 |
| JUN | 55.40 | 24.90 | 100.00 | 71.40 | 32.00 | 56.74 |
| JUL | 83.30 | 73.70 | 79.60 | 41.90 | 41.60 | 64.02 |
| AUG | 100.00 | 100.00 | 100.00 | 100.00 | 100.00 | 100.00 |
| SEP | 100.00 | 100.00 | 100.00 | 52.70 | 74.60 | 85.46 |
| OCT | 72.10 | 100.00 | 100.00 | 37.30 | 90.60 | 80.00 |
| NOV | 100.00 | 100.00 | 81.40 | 100.00 | 21.20 | 80.52 |
| DEC | 38.80 | 52.90 | 44.50 | 77.70 | 7.30 | 44.24 |
| AVG | 57.28 | 53.84 | 55.01 | 49.02 | 39.75 | m^3/s |

| Year | 2012 | 2013 | 2014 | 2015 | 2016 | Avg |
|---|---|---|---|---|---|---|
| JAN | 10100.00 | 9900.00 | 14200.00 | 8200.00 | 18700.00 | 12220.00 |
| FEB | 0.00 | 0.00 | 0.00 | 0.00 | 0.00 | 0.00 |
| MAR | 0.00 | 0.00 | 0.00 | 0.00 | 0.00 | 0.00 |
| APR | 27700.00 | 22100.00 | 8500.00 | 16800.00 | 11800.00 | 17380.00 |
| MAY | 100000.0 | 62600.00 | 31900.00 | 82200.00 | 79200.00 | 71180.00 |
| JUN | 55400.00 | 24900.00 | 100000.0 | 71400.00 | 32000.00 | 56740.00 |
| JUL | 83300.0 | 73700.0 | 79600.0 | 41900.0 | 41600.0 | 64020.0 |
| AUG | 100000.0 | 100000.0 | 100000.0 | 100000.0 | 100000.0 | 100000.0 |
| SEP | 100000.0 | 100000.0 | 100000.0 | 52700.0 | 74600.0 | 85460.0 |
| OCT | 72100.0 | 100000.0 | 100000.0 | 37300.0 | 90600.0 | 80000.0 |
| NOV | 100000.0 | 100000.0 | 81400.0 | 100000.0 | 21200.0 | 80520.0 |
| DEC | 38800.00 | 52900.00 | 44500.00 | 77700.00 | 7300.00 | 44240.00 |
| AVG | 57283.33 | 53841.67 | 55008.33 | 49016.67 | 39750.00 | kg/s |

| | |
|---|---|
| Efficiency | 0.865 |
| Net head | 50.73 |
| g | 9.81 |
| W→MW | 1000000 |
| h | 8760.00 |
| Capacity factor | 1.00 |
| MW→GW | 1000.00 |

Total capacity (Max GWh production)

| 42MW | 367.92 |
|---|---|

| Year | 2012 | 2013 | 2014 | 2015 | 2016 | Avg | Avg |
|---|---|---|---|---|---|---|---|
| JAN | 4.35 | 4.26 | 6.11 | 3.53 | 8.05 | 5.26 | 3.91 |
| FEB | 0.00 | 0.00 | 0.00 | 0.00 | 0.00 | 0.00 | 0.00 |
| MAR | 0.00 | 0.00 | 0.00 | 0.00 | 0.00 | 0.00 | 0.00 |
| APR | 11.92 | 9.51 | 3.66 | 7.23 | 5.08 | 7.48 | 5.39 |
| MAY | 43.05 | 26.95 | 13.73 | 35.39 | 34.09 | 30.64 | 22.80 |
| JUN | 23.85 | 10.72 | 43.05 | 30.74 | 13.78 | 24.43 | 17.59 |
| JUL | 35.86 | 31.73 | 34.27 | 18.04 | 17.91 | 27.56 | 20.50 |
| AUG | 43.05 | 43.05 | 43.05 | 43.05 | 43.05 | 43.05 | 32.03 |
| SEP | 43.05 | 43.05 | 43.05 | 22.69 | 32.11 | 36.79 | 26.49 |
| OCT | 31.04 | 43.05 | 43.05 | 16.06 | 39.00 | 34.44 | 25.62 |
| NOV | 43.05 | 43.05 | 35.04 | 43.05 | 9.13 | 34.66 | 24.96 |
| DEC | 16.70 | 22.77 | 19.16 | 33.45 | 3.14 | 19.04 | 14.17 |
| AVG | 24.66 | 23.18 | 23.68 | 21.10 | 17.11 | MW | Gwh |
| | | | | | | | 193.45 |
| AVG | 216.01 | 203.04 | 207.44 | 184.84 | 149.90 | GWh | |
| | | | | | | 192.24 | |

### WITH DISCHARGE INTERVAL & MAX CAPACITY OUTPUT

| Year | 2012 | 2013 | 2014 | 2015 | 2016 | Avg |
|---|---|---|---|---|---|---|
| JAN | 10.10 | 9.90 | 14.20 | 8.20 | 18.70 | 12.22 |
| FEB | 0.00 | 0.00 | 0.00 | 0.00 | 0.00 | 0.00 |
| MAR | 0.00 | 0.00 | 0.00 | 0.00 | 0.00 | 0.00 |
| APR | 27.70 | 22.10 | 8.50 | 16.80 | 11.80 | 17.38 |
| MAY | 100.00 | 62.60 | 31.90 | 82.20 | 79.20 | 71.18 |
| JUN | 55.40 | 24.90 | 100.00 | 71.40 | 32.00 | 56.74 |
| JUL | 83.30 | 73.70 | 79.60 | 41.90 | 41.60 | 64.02 |
| AUG | 100.00 | 100.00 | 100.00 | 100.00 | 100.00 | 100.00 |
| SEP | 100.00 | 100.00 | 100.00 | 52.70 | 74.60 | 85.46 |
| OCT | 72.10 | 100.00 | 100.00 | 37.30 | 90.60 | 80.00 |
| NOV | 100.00 | 100.00 | 81.40 | 100.00 | 21.20 | 80.52 |
| DEC | 38.80 | 52.90 | 44.50 | 77.70 | 7.30 | 44.24 |
| AVG | 57.28 | 53.84 | 55.01 | 49.02 | 39.75 | m^3/s |

| Year | 2012 | 2013 | 2014 | 2015 | 2016 | Avg |
|---|---|---|---|---|---|---|
| JAN | 10100.00 | 9900.00 | 14200.00 | 8200.00 | 18700.00 | 12220.00 |
| FEB | 0.00 | 0.00 | 0.00 | 0.00 | 0.00 | 0.00 |
| MAR | 0.00 | 0.00 | 0.00 | 0.00 | 0.00 | 0.00 |
| APR | 27700.00 | 22100.00 | 8500.00 | 16800.00 | 11800.00 | 17380.00 |
| MAY | 100000.0 | 62600.00 | 31900.00 | 82200.00 | 79200.00 | 71180.00 |
| JUN | 55400.00 | 24900.00 | 100000.0 | 71400.00 | 32000.00 | 56740.00 |
| JUL | 83300.0 | 73700.0 | 79600.0 | 41900.0 | 41600.0 | 64020.0 |
| AUG | 100000.0 | 100000.0 | 100000.0 | 100000.0 | 100000.0 | 100000.0 |
| SEP | 100000.0 | 100000.0 | 100000.0 | 52700.0 | 74600.0 | 85460.0 |
| OCT | 72100.0 | 100000.0 | 100000.0 | 37300.0 | 90600.0 | 80000.0 |
| NOV | 100000.0 | 100000.0 | 81400.0 | 100000.0 | 21200.0 | 80520.0 |
| DEC | 38800.00 | 52900.00 | 44500.00 | 77700.00 | 7300.00 | 44240.00 |
| AVG | 57283.33 | 53841.67 | 55008.33 | 49016.67 | 39750.00 | kg/s |

| | |
|---|---|
| Efficiency | 0.865 |
| Net head | 50.73 |
| g | 9.81 |
| W→MW | 1000000 |
| h | 8760.00 |
| Capacity factor | 1.00 |
| MW→GW | 1000.00 |

Total capacity (Max GWh production)

| 42MW | 367.92 |
|---|---|

| Year | 2012 | 2013 | 2014 | 2015 | 2016 | Avg | Avg |
|---|---|---|---|---|---|---|---|
| JAN | 4.35 | 4.26 | 6.11 | 3.53 | 8.05 | 5.26 | 3.91 |
| FEB | 0.00 | 0.00 | 0.00 | 0.00 | 0.00 | 0.00 | 0.00 |
| MAR | 0.00 | 0.00 | 0.00 | 0.00 | 0.00 | 0.00 | 0.00 |
| APR | 11.92 | 9.51 | 3.66 | 7.23 | 5.08 | 7.48 | 5.39 |
| MAY | 42.00 | 26.95 | 13.73 | 35.39 | 34.09 | 30.43 | 22.64 |
| JUN | 23.85 | 10.72 | 42.00 | 30.74 | 13.78 | 24.22 | 17.44 |
| JUL | 35.86 | 31.73 | 34.27 | 18.04 | 17.91 | 27.56 | 20.50 |
| AUG | 42.00 | 42.00 | 42.00 | 42.00 | 42.00 | 42.00 | 31.25 |
| SEP | 42.00 | 42.00 | 42.00 | 22.69 | 32.11 | 36.16 | 26.04 |
| OCT | 31.04 | 42.00 | 42.00 | 16.06 | 39.00 | 34.02 | 25.31 |
| NOV | 42.00 | 42.00 | 35.04 | 42.00 | 9.13 | 34.03 | 24.50 |
| DEC | 16.70 | 22.77 | 19.16 | 33.45 | 3.14 | 19.04 | 14.17 |
| AVG | 24.31 | 22.83 | 23.33 | 20.93 | 17.02 | MW | Gwh |
| | | | | | | | 191.15 |
| AVG | 212.95 | 199.98 | 204.38 | 183.31 | 149.13 | GWh | |
| | | | | | | 189.95 | |

| Final Capacity factor | 0.51628079 |
|---|---|

**Figure A.0.4:** *Production calculations in Excel*

# B Meteorological Data

**Listing 1:** *Exammple of matlab code for finding Solar irradiance*

```
JAN(:,1)=table2array(Book_JAN(1:24,1));
JAN(:,2)=table2array(Book_JAN(25:48,1));
JAN(:,3)=table2array(Book_JAN(49:72,1));
JAN(:,4)=table2array(Book_JAN(73:96,1));
JAN(:,5)=table2array(Book_JAN(97:120,1));
JAN(:,6)=table2array(Book_JAN(121:144,1));
JAN(:,7)=table2array(Book_JAN(145:168,1));
JAN(:,8)=table2array(Book_JAN(169:192,1));
JAN(:,9)=table2array(Book_JAN(193:216,1));
JAN(:,10)=table2array(Book_JAN(217:240,1));
JAN(:,11)=table2array(Book_JAN(241:264,1));
JAN(:,12)=table2array(Book_JAN(265:288,1));
JAN(:,13)=table2array(Book_JAN(289:312,1));
JAN(:,14)=table2array(Book_JAN(313:336,1));
JAN(:,15)=table2array(Book_JAN(337:360,1));
JAN(:,16)=table2array(Book_JAN(361:384,1));
JAN(:,17)=table2array(Book_JAN(385:408,1));
JAN(:,18)=table2array(Book_JAN(409:432,1));
JAN(:,19)=table2array(Book_JAN(433:456,1));
JAN(:,20)=table2array(Book_JAN(457:480,1));
JAN(:,21)=table2array(Book_JAN(481:504,1));
JAN(:,22)=table2array(Book_JAN(505:528,1));
JAN(:,23)=table2array(Book_JAN(529:552,1));
JAN(:,24)=table2array(Book_JAN(553:576,1));
JAN(:,25)=table2array(Book_JAN(577:600,1));
JAN(:,26)=table2array(Book_JAN(601:624,1));
JAN(:,27)=table2array(Book_JAN(625:648,1));
JAN(:,28)=table2array(Book_JAN(649:672,1));
JAN(:,29)=table2array(Book_JAN(673:696,1));
JAN(:,30)=table2array(Book_JAN(697:720,1));
JAN(:,31)=table2array(Book_JAN(721:744,1));
for K=1:24
        AVG_JAN(K)=mean(JAN(K,:));
end
for k=1:31
        WORST_JAN(k)=mean(JAN(:,k));
end
[a_worst_JAN, b_worst_JAN]=min(WORST_JAN)
[a_best_JAN, b_best_JAN]=max(WORST_JAN)
```

# Achwa II HPP
Location name

3.135
Latitude [°N]

32.521
Longitude [°E]

776
Altitude [m a.s.l.]

V, 2
Climate region

Standard
Radiation model

Standard
Temperature model

Perez
Tilt radiation model

2000–2009
Temperature period

1991–2010
Radiation period

## Additional information

Uncertainty of yearly values: Gh = 5%, Bn = 10%, Ta = 2,4 °C
Trend of Gh / decade: -
Variability of Gh / year: 2,5%
Radiation interpolation locations: Gulu (1971-1980, 48 km), Paraa (139 km), Arua (178 km), Masindi (184 km), Soroti (199 km) (Share of satellite data: 71%)
Temperature interpolation locations: KISUMU (437 km), Eldoret (422 km), Meru (663 km), NAKURU (548 km), Nairobi/Jomo Kenyatt (695 km), Garissa (886 km)
P90 and P10 of yearly Gh, referenced to average: 96,5%, 102,6%

| Month | G_Gh | G_Dh | Ta | FF |
|---|---|---|---|---|
| | [W/m2] | [W/m2] | [°C] | [m/s] |
| January | 223 | 96 | 22.6 | 3.1 |
| February | 227 | 99 | 23.5 | 3.4 |
| March | 226 | 106 | 23.0 | 3.2 |
| April | 209 | 97 | 22.3 | 2.5 |
| May | 218 | 99 | 21.9 | 2.3 |
| June | 207 | 94 | 21.2 | 2.3 |
| July | 196 | 100 | 20.9 | 2.3 |
| August | 206 | 93 | 21.1 | 2.4 |
| September | 228 | 110 | 21.7 | 2.6 |
| October | 231 | 90 | 22.4 | 2.7 |
| November | 222 | 90 | 22.1 | 2.7 |
| December | 217 | 91 | 22.5 | 3.0 |
| Year | 217 | 97 | 22.1 | 2.7 |

Ta: Air temperature
FF: Wind speed
G_Gh: Mean irradiance of global radiation horizontal
G_Dh: Mean irradiance of diffuse radiation horizontal

Meteonorm

*Meteonorm V7.3.0.26247* 1/3

**Figure B.0.1:** *Meteonorm meteorological report*

# C Solar panels

**ENGINEERING DRAWING (mm)**

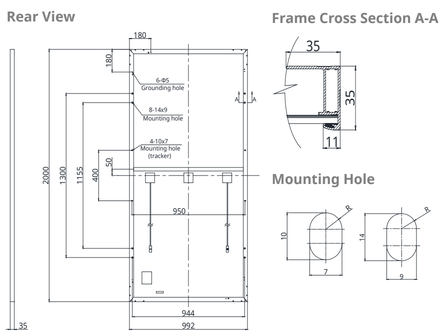


**CS3U-375MS / I-V CURVES**

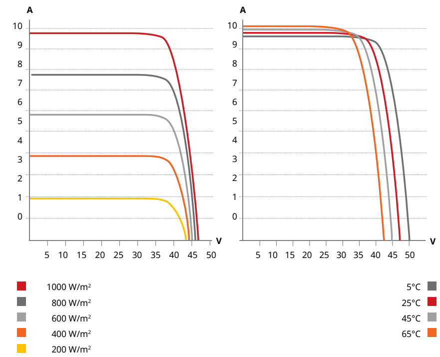


**ELECTRICAL DATA | STC***

| CS3U | 375MS | 380MS | 385MS | 390MS | 395MS |
|---|---|---|---|---|---|
| Nominal Max. Power (Pmax) | 375 W | 380 W | 385 W | 390 W | 395 W |
| Opt. Operating Voltage (Vmp) | 39.8 V | 40.0 V | 40.2 V | 40.4 V | 40.6 V |
| Opt. Operating Current (Imp) | 9.43 A | 9.50 A | 9.58 A | 9.66 A | 9.73 A |
| Open Circuit Voltage (Voc) | 47.6 V | 47.8 V | 48.0 V | 48.2 V | 48.4 V |
| Short Circuit Current (Isc) | 9.93 A | 10.01 A | 10.09 A | 10.17 A | 10.25 A |
| Module Efficiency | 18.90% | 19.15% | 19.41% | 19.66% | 19.91% |
| Operating Temperature | -40°C ~ +85°C | | | | |
| Max. System Voltage | 1500V (IEC/UL) or 1000V (IEC/UL) | | | | |
| Module Fire Performance | TYPE 1 (UL 1703) or CLASS C (IEC 61730) | | | | |
| Max. Series Fuse Rating | 30 A | | | | |
| Application Classification | Class A | | | | |
| Power Tolerance | 0 ~ + 5 W | | | | |

* Under Standard Test Conditions (STC) of irradiance of 1000 W/m², spectrum AM 1.5 and cell temperature of 25°C.

**ELECTRICAL DATA | NMOT***

| CS3U | 375MS | 380MS | 385MS | 390MS | 395MS |
|---|---|---|---|---|---|
| Nominal Max. Power (Pmax) | 280 W | 284 W | 287 W | 291 W | 295 W |
| Opt. Operating Voltage (Vmp) | 36.9 V | 37.1 V | 37.3 V | 37.5 V | 37.7 V |
| Opt. Operating Current (Imp) | 7.58 A | 7.64 A | 7.70 A | 7.76 A | 7.82 A |
| Open Circuit Voltage (Voc) | 44.8 V | 45.0 V | 45.1 V | 45.3 V | 45.5 V |
| Short Circuit Current (Isc) | 8.01 A | 8.07 A | 8.14 A | 8.20 A | 8.26 A |

* Under Nominal Module Operating Temperature (NMOT), irradiance of 800 W/m², spectrum AM 1.5, ambient temperature 20°C, wind speed 1 m/s.

**MECHANICAL DATA**

| Specification | Data |
|---|---|
| Cell Type | Mono-crystalline |
| Cell Arrangement | 144 [2 X (12 X 6) ] |
| Dimensions | 2000 X 992 X 35 mm (78.7 X 39.1 X 1.38 in) |
| Weight | 22.5 kg (49.6 lbs) |
| Front Cover | 3.2 mm tempered glass |
| Frame | Anodized aluminium alloy, crossbar enhanced |
| J-Box | IP68, 3 bypass diodes |
| Cable | 4 mm² (IEC), 12 AWG (UL) |
| Cable Length (Including Connector) | Portrait: 400 mm (15.7 in) (+) / 280 mm (11.0 in) (-); landscape: 1250 mm (49.2 in);leap-frog connection: 1670 mm (65.7 in)* |
| Connector | T4 series |
| Per Pallet | 30 pieces |
| Per Container (40' HQ) | 660 pieces |

* For detailed information, please contact your local Canadian Solar sales and technical representatives.

**TEMPERATURE CHARACTERISTICS**

| Specification | Data |
|---|---|
| Temperature Coefficient (Pmax) | -0.37 % / °C |
| Temperature Coefficient (Voc) | -0.29 % / °C |
| Temperature Coefficient (Isc) | 0.05 % / °C |
| Nominal Module Operating Temperature | 41 ± 3°C |

**PARTNER SECTION**

* The specifications and key features contained in this datasheet may deviate slightly from our actual products due to the on-going innovation and product enhancement. Canadian Solar Inc. reserves the right to make necessary adjustments to the information described herein at any time without further notice. Please be kindly advised that PV modules should be handled and installed by qualified people who have professional skills and please carefully read the safety and installation instructions before using our PV modules.

**CANADIAN SOLAR INC.**
545 Speedvale Avenue West, Guelph, Ontario N1K 1E6, Canada, www.canadiansolar.com, support@canadiansolar.com



**Figure C.0.1:** *Canadian Solar CS3U-375MS 1500 V specification.[56]*

# LG NeON® 2 *BiFacial*

LG395N2T-A5 | LG390N2T-A5

## Electrical Properties (STC*)

| | | LG395N2T - A5 | Bifaical Gain** | | | | LG390N2T - A5 | Bifacial Gain** | | | |
|---|---|---|---|---|---|---|---|---|---|---|---|
| | | | 5% | 10% | 20% | 30% | | 5% | 10% | 20% | 30% |
| Maximum Power (Pmax) | [W] | 395 | 415 | 435 | 474 | 514 | 390 | 410 | 429 | 468 | 507 |
| MPP Voltage (Vmpp) | [V] | 41.8 | 41.8 | 41.8 | 41.9 | 41.9 | 41.4 | 41.4 | 41.4 | 41.5 | 41.5 |
| MPP Current (Impp) | [A] | 9.46 | 9.92 | 10.39 | 11.31 | 12.26 | 9.43 | 9.90 | 10.36 | 11.28 | 12.22 |
| Open Circuit Voltage (Voc) | [V] | 49.3 | 49.3 | 49.3 | 49.4 | 49.4 | 49.2 | 49.2 | 49.2 | 49.3 | 49.3 |
| Short Circuit Current (Isc) | [A] | 10.19 | 10.70 | 11.21 | 12.23 | 13.25 | 10.15 | 10.15 | 11.17 | 12.18 | 13.20 |
| Module Efficiency | [%] | 18.7 | 19.6 | 20.6 | 22.4 | 24.3 | 18.5 | 19.4 | 20.3 | 22.1 | 24.0 |
| Operating Temperature | [°C] | -40 ~ +90 | | | | | | | | | |
| Maximum System Voltage | [V] | 1,500(UL) / 1,000(IEC) | | | | | | | | | |
| Maximum Series Fuse Rating | [A] | 20 | | | | | | | | | |
| Pmax Bifaciality Coefficient*** | [%] | 76 | | | | | | | | | |
| Power Tolerance | [%] | 0 ~ +3 | | | | | | | | | |

The nameplate power output is measured and determined by LG Electronics at its sole and absolute discretion.
* STC (Standard Test Condition): Irradiance 1,000 W/m², cell temperature 25 °C, AM 1.5(Measurement Tolerance : ±3%, Electrical Parameter Tolerance : ±5%)
** Bifacial Gain: The additional gain from the back side compared to the power of the front side at the standard test condition. It depends on installation condition.
*** Pmax Bifaciality Coefficient 25years warranty based on front output warranty. tolerance±7%

## Mechanical Properties

| | |
|---|---|
| Cells | 6 x 12 |
| Cell Type | Monocrystalline / N-type |
| Cell Dimensions | 161.7 x 161.7 mm / 6 inches |
| # of Busbar | 12(Multi Wire Busbar) |
| Dimensions (L x W x H) | 2,064 x 1,024 x 40 mm |
| | 81.26 x 40.31 x 1.57 in |
| Front Load | 5,400 Pa / 113 psf* |
| Rear Load | 4,300 Pa / 90 psf* |
| Weight | 22.0 kg / 48.72 lb |
| Connector Type | MC4 (MC), PV-JM601A (JMTHY) |
| Junction Box | IP68 with 3 Bypass Diodes |
| Cables | 1,200 mm x 2 ea / 47.24 in x 2 ea |
| Glass | High Transmission Tempered Glass |
| Frame | Anodized Aluminium |

* Please refer to the installation manual for the details

## Electrical Properties (NOCT*)

| Model | | LG395N2T-A5 | LG390N2T-A5 |
|---|---|---|---|
| Maximum Power (Pmax) | [W] | 292 | 289 |
| MPP Voltage (Vmpp) | [V] | 38.7 | 38.3 |
| MPP Current (Impp) | [A] | 7.55 | 7.54 |
| Open Circuit Voltage (Voc) | [V] | 46.0 | 45.9 |
| Short Circuit Current (Isc) | [A] | 8.20 | 8.17 |

* NOCT (Nominal Operating Cell Temperature): Irradiance 800 W/m², ambient temperature 20 °C, wind speed 1 m/s

## Characteristic Curves

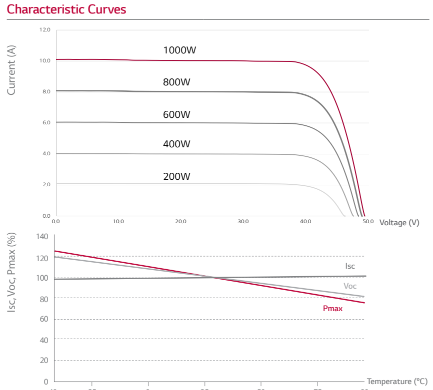


## Certifications and Warranty

| | |
|---|---|
| Certifications | UL 1703 |
| | IEC 61215, IEC 61730-1/-2 |
| | IEC 61701 (Salt mist corrosion test) |
| | IEC 62716 (Ammonia corrosion test) |
| | ISO 9001 |
| Module Fire Performance | Type 1(UL 1703) |
| Fire Resistance Class | Class C (ULC/ORD C1703, IEC 61730) |
| Product Warranty | 25 Years |
| Output Warranty of Pmax | Linear Warranty* |

* 1) 1st year: 98%, 2) After 1st year: 0.5% annual degradation, 3) 86% for 25 years

## Temperature Characteristics

| | | |
|---|---|---|
| NOCT | [ °C ] | 45 ± 3 |
| Pmax | [%/°C] | -0.36 |
| Voc | [%/°C] | -0.27 |
| Isc | [%/°C] | 0.03 |

## Dimensions (mm / inch)

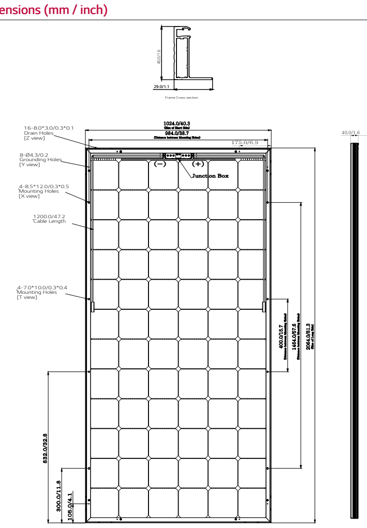


*Thedistancebetweenthecenterofthemounting/groundingholes.

LG Life's Good

LG Electronics Inc.
Solar Business Division
LG Twin Towers, 128 Yeoui-daero, Yeongdeungpo-gu, Seoul 07336, Korea
www.lg-solar.com

Product specifications are subject to change without notice.
DS-T5-72-W-G-P-EN-80510



**Figure C.0.2:** *LG Electronics LG390N2T-A5 1500 V (Bifacial) specification.[57]*

# D Production forecast

| TIME | | April | 1 | | 2 | | 15 | | 16 | | 29 | | 30 | | | AVERAGE |
|---|---|---|---|---|---|---|---|---|---|---|---|---|---|---|---|---|
| 01.04.2018 | 12:00:00 AM | 12:30:00 AM | 2883.32 | 3476.56 | 2800.7 | 3175.16 | 2926.46 | 4162.74 | 2797.92 | 3811.3 | 3054.42 | 4309.46 | 2696.82 | 4568.98 | | 2800.007586 |
| 01.04.2018 | 12:30:00 AM | 1:00:00 AM | 2340.48 | 2783.36 | 2614.14 | 2996.16 | 2735.32 | 3621.3 | 2634.22 | 3596.9 | 2974.38 | 4161.06 | 2665.62 | 4653.78 | | 2637.631034 |
| 01.04.2018 | 1:00:00 AM | 1:30:00 AM | 2396.88 | 3088.68 | 2480.06 | 2877.7 | 2588.04 | 3511.56 | 2495.7 | 3464.92 | 2962.14 | 4211.16 | 2500.32 | 4437.7 | | 2519.855862 |
| 01.04.2018 | 1:30:00 AM | 2:00:00 AM | 2483.64 | 3136.94 | 2390.64 | 2791.04 | 2519.34 | 3399.54 | 2461.38 | 3411.9 | 2821.32 | 4116.36 | 2554.98 | 4622.34 | | 2440.2 |
| 01.04.2018 | 2:00:00 AM | 2:30:00 AM | 2462.76 | 3111.36 | 2263.62 | 2649.6 | 2395.14 | 3203.46 | 2440.2 | 3399.42 | 2751 | 4053.12 | 2533.68 | 4620.92 | | 2376.022759 |
| 01.04.2018 | 2:30:00 AM | 3:00:00 AM | 2363.04 | 3005.88 | 2194.2 | 2601.96 | 2286.24 | 3042.3 | 2381.94 | 3362.1 | 2717.4 | 4022.16 | 2518.92 | 4555.98 | | 2329.224828 |
| 01.04.2018 | 3:00:00 AM | 3:30:00 AM | 2187.78 | 2679 | 2127.3 | 2550.36 | 2035.14 | 2648.04 | 2397.3 | 3375.36 | 2588.28 | 3833.34 | 2475.36 | 4547.38 | | 2271.736552 |
| 01.04.2018 | 3:30:00 AM | 4:00:00 AM | 1949.88 | 2374.08 | 2117.16 | 2529.06 | 2039.7 | 2657.76 | 2380.74 | 3370.08 | 2505.18 | 3821.22 | 2456.22 | 4554.12 | | 2227.324138 |
| 01.04.2018 | 4:00:00 AM | 4:30:00 AM | 2002.26 | 2423.4 | 2104.8 | 2504.22 | 2316.06 | 3306.24 | 2362.98 | 3401.1 | 2497.86 | 3805.92 | 2408.52 | 4440.18 | | 2226.384828 |
| 01.04.2018 | 4:30:00 AM | 5:00:00 AM | 1993.92 | 2421.42 | 2239.14 | 2802.96 | 2164.62 | 3081.3 | 2404.62 | 3446.1 | 2555.7 | 3915.72 | 2365.2 | 4398.64 | | 2239.874483 |
| 01.04.2018 | 5:00:00 AM | 5:30:00 AM | 1987.86 | 2398.98 | 2317.14 | 2892 | 2254.02 | 3205.44 | 2448.6 | 3487.38 | 2556.48 | 3881.46 | 2326.68 | 4373.48 | | 2245.870345 |
| 01.04.2018 | 5:30:00 AM | 6:00:00 AM | 2048.52 | 2477.7 | 2329.62 | 2885.1 | 1867.5 | 2567.28 | 2500.14 | 3552.66 | 2521.86 | 3861.84 | 2320.38 | 4290.36 | | 2273.141379 |
| 01.04.2018 | 6:00:00 AM | 6:30:00 AM | 2184.84 | 2579.76 | 2358.6 | 2909.82 | 1978.08 | 2780.04 | 2577.84 | 3606.24 | 2599.14 | 3949.56 | 2417.88 | 4336.2 | | 2357.246897 |
| 01.04.2018 | 6:30:00 AM | 7:00:00 AM | 2316.48 | 2701.36 | 2494.8 | 3047.76 | 2343.54 | 3703.92 | 2678.76 | 3724.46 | 2799.06 | 4192.32 | 2643 | 4465.84 | | 2564.752414 |
| 01.04.2018 | 7:00:00 AM | 7:30:00 AM | 2500.32 | 2878.14 | 2705.46 | 3319.86 | 2625.96 | 4109.46 | 2912.14 | 4043.48 | 2967.88 | 4382.96 | 2925.68 | 4710.68 | | 2816.002759 |
| 01.04.2018 | 7:30:00 AM | 8:00:00 AM | 2732.8 | 3109.34 | 2873.94 | 3549.92 | 2828.02 | 4305.28 | 3110.1 | 4268.64 | 3251.22 | 4715.66 | 3171.72 | 4885.98 | | 3038.98069 |
| 01.04.2018 | 8:00:00 AM | 8:30:00 AM | 3032.76 | 3458.9 | 3226.36 | 3986.36 | 3011.86 | 4460.1 | 3352.84 | 4566.84 | 3416.82 | 4932.22 | 3290.72 | 5003.54 | | 3247.257931 |
| 01.04.2018 | 8:30:00 AM | 9:00:00 AM | 3470.3 | 4085.84 | 3462.2 | 4256.08 | 3203.4 | 4666.2 | 3585.46 | 4813.98 | 3513.3 | 5088.8 | 3445.98 | 5168.76 | | 3507.945517 |
| 01.04.2018 | 9:00:00 AM | 9:30:00 AM | 3684.96 | 4355.66 | 3779.24 | 4664.1 | 2779.88 | 4274 | 3721.88 | 4974.2 | 3467.82 | 5110.02 | 3544.9 | 5300.34 | | 3639.222759 |
| 01.04.2018 | 9:30:00 AM | 10:00:00 AM | 3243.24 | 3734.72 | 3909.88 | 4840.96 | 2871.14 | 4414.56 | 3854.44 | 5152.36 | 3485.18 | 5138.14 | 3612.6 | 5405.58 | | 3744.108571 |
| 01.04.2018 | 10:00:00 AM | 10:30:00 AM | 3315.04 | 3833.94 | 3964.96 | 4925.9 | 2414.88 | 3957.54 | 3902.98 | 5265.6 | 3456.66 | 5168.32 | 3720.26 | 5516.26 | | 3796.607143 |
| 01.04.2018 | 10:30:00 AM | 11:00:00 AM | 3445.64 | 3990.18 | 3946.4 | 4990.38 | 2404.38 | 3946.62 | 3944.48 | 5341.82 | 3485.08 | 5235.52 | 3694.18 | 5484.02 | | 3845.485 |
| 01.04.2018 | 11:00:00 AM | 11:30:00 AM | 3683.86 | 4404.58 | 4052.96 | 5161.4 | 2395.38 | 3949.8 | 3977.26 | 5387.16 | 3520.8 | 5280.98 | 3678.14 | 5448.6 | | 3870.81 |
| 01.04.2018 | 11:30:00 AM | 12:00:00 PM | 3891.32 | 4703.68 | 3938.36 | 5068 | 2369.34 | 3897.96 | 3952.94 | 5354.76 | 3609.58 | 5405.38 | 3791 | 5526.44 | | 3888.924286 |
| 01.04.2018 | 12:00:00 PM | 12:30:00 PM | 3648.16 | 4339.94 | 3990.92 | 5190.16 | 2352.84 | 3900.3 | 4037.14 | 5438 | 3534.7 | 5336.78 | 3989.02 | 5718.18 | | 3825.24 |
| 01.04.2018 | 12:30:00 PM | 1:00:00 PM | 3448.24 | 4032.28 | 4028.2 | 5261.44 | 2351.58 | 3910.2 | 4022.02 | 5424.78 | 3652.16 | 5432.02 | 4049.54 | 5785.7 | | 3886.145714 |
| 01.04.2018 | 1:00:00 PM | 1:30:00 PM | 3461.94 | 4036.9 | 4096.44 | 5390.6 | 2380.86 | 3944.64 | 2737.24 | 3980.54 | 3698.52 | 5440.24 | 4056.16 | 5793.38 | | 3887.276429 |
| 01.04.2018 | 1:30:00 PM | 2:00:00 PM | 3468.86 | 4054.88 | 4086.56 | 5398.52 | 2377.68 | 3922.62 | | | 3666.82 | 5438.38 | 3807.1 | 5557.14 | | 3954.618519 |
| 01.04.2018 | 2:00:00 PM | 2:30:00 PM | 3495.82 | 4154.32 | 3859.46 | 5201.14 | 2355.42 | 3856.68 | | | 3419.88 | 5234.74 | 3754.28 | 5468.4 | | 3871.517857 |
| 01.04.2018 | 2:30:00 PM | 3:00:00 PM | 3457.52 | 4127.6 | 2828.82 | 4065.54 | 2358.24 | 3741.36 | | | 3218.92 | 5039.46 | 3860.98 | 5599.38 | | 3750.642143 |
| 01.04.2018 | 3:00:00 PM | 3:30:00 PM | 3351.42 | 4005.84 | 3700.94 | 5096.58 | 2295.84 | 3409.32 | | | 3299.58 | 5194.72 | 3821.12 | 5558.98 | | 3673.108571 |
| 01.04.2018 | 3:30:00 PM | 4:00:00 PM | 3307.4 | 3962.28 | 2609.02 | 3896.88 | 2430 | 3535.56 | | | 3497.44 | 5278.1 | 3983.84 | 5679.92 | | 3736.437931 |
| 01.04.2018 | 4:00:00 PM | 4:30:00 PM | 3202.9 | 3865.7 | 3607.32 | 5037.8 | 2940.4 | 4055.7 | | | 3679.66 | 5384.98 | 4168.72 | 5788.6 | | 3852.245517 |
| 01.04.2018 | 4:30:00 PM | 5:00:00 PM | 3108.54 | 3762.64 | 3558.88 | 4945.16 | 3183.92 | 4259.86 | | | 3821.7 | 5521.12 | 4101.6 | 5693.94 | | 3896.864828 |
| 01.04.2018 | 5:00:00 PM | 5:30:00 PM | 3022.16 | 3659.22 | 3449.48 | 4817.6 | 3701.74 | 4797.48 | | | 3884.86 | 5563.64 | 3745.82 | 5289.84 | | 3807.802069 |
| 01.04.2018 | 5:30:00 PM | 6:00:00 PM | 3030.32 | 3652.52 | 3605.7 | 4964.66 | 3872.24 | 4909.76 | | | 4025.8 | 5617.12 | 4062.62 | 5578.96 | | 3895.266897 |
| 01.04.2018 | 6:00:00 PM | 6:30:00 PM | 3027.86 | 3644.44 | 3711.62 | 5058.1 | 3973.42 | 5005.66 | 2501.22 | 3741.98 | 4147.36 | 5685.08 | 4142.94 | 5612.42 | | 3894.269655 |
| 01.04.2018 | 6:30:00 PM | 7:00:00 PM | 3109.34 | 3712.34 | 3743.34 | 5044.66 | 4007.42 | 5026.46 | 2590.04 | 3812.62 | 4234.42 | 5715.72 | 3951 | 5202.04 | | 3894.081379 |
| 01.04.2018 | 7:00:00 PM | 7:30:00 PM | 3281.54 | 3843.18 | 3968.8 | 5223.44 | 4195.08 | 5137.5 | 3828.88 | 5076.26 | 4059.32 | 5248.74 | 4130.96 | 5281.44 | | 4060.191333 |
| 01.04.2018 | 7:30:00 PM | 8:00:00 PM | 3546.82 | 4026.04 | 4249.44 | 5432.9 | 4279.1 | 5180.22 | 4394.12 | 5963.04 | 4342.04 | 5656.74 | 4609 | 5910.7 | | 4172.862 |
| 01.04.2018 | 8:00:00 PM | 8:30:00 PM | 3809.52 | 4267.48 | 4405.32 | 5701.76 | 4424 | 5314.64 | 4679.68 | 6136.64 | 4486.84 | 5834.44 | 4607.46 | 5839.5 | | 4395.145333 |
| 01.04.2018 | 8:30:00 PM | 9:00:00 PM | 3989.94 | 4390.44 | 4608.08 | 6072.94 | 4491.26 | 5352.92 | 4813.88 | 6215.56 | 3637.58 | 5064.72 | 4450.98 | 5733.06 | | 4314.555333 |
| 01.04.2018 | 9:00:00 PM | 9:30:00 PM | 3923.16 | 4297.82 | 4500.6 | 5936.52 | 4410.42 | 5304.26 | 4726.66 | 6126.72 | 3871.42 | 5115 | 4284.24 | 5566.54 | | 4228.317333 |
| 01.04.2018 | 9:30:00 PM | 10:00:00 PM | 3826.88 | 4190.6 | 4322.28 | 5733.16 | 4238.98 | 5166.66 | 4546.14 | 5868 | 3555 | 4768.66 | 3981.54 | 5304.54 | | 4048.566 |
| 01.04.2018 | 10:00:00 PM | 10:30:00 PM | 3654.94 | 4039.28 | 4048.24 | 5442.94 | 3990.7 | 4902.88 | 4424.58 | 5702.46 | 3478.1 | 4910.82 | 3631.52 | 4965.46 | | 3803.933333 |
| 01.04.2018 | 10:30:00 PM | 11:00:00 PM | 3413.14 | 3785.88 | 3743.52 | 5100.74 | 3720.86 | 4694.44 | 4221.02 | 5372.46 | 3074.2 | 4538.9 | 3143.76 | 4396.5 | | 3515.115333 |
| 01.04.2018 | 11:00:00 PM | 11:30:00 PM | 3231.76 | 3587.78 | 3479.02 | 4785.5 | 3377.36 | 4338.08 | 3880.38 | 4806.52 | 2668.02 | 3993.9 | 2639.3 | 3869.88 | | 3242.998667 |
| 01.04.2018 | 11:30:00 PM | 12:00:00 PM | 2998.02 | 3376.14 | 3211.44 | 4099.46 | 3080.36 | 4063.78 | 2471.36 | 3344.76 | 2753.4 | 4523.46 | 2378.22 | 3636.84 | | 2953.153333 |

**Figure D.0.1:** *Example of demand calculations from daily data made in Excel.*

**Listing 2:** *Example of matlab code for finding combined annual production.*

```
y1 = [5260429.23939000,0];
x1 = [0,744];
plot (x1,y1)
i =[1:744];
  hpp_1a = −7070.469408;
  hpp_1b = 5260429.239;
hpp_1 = (hpp_1a*i + hpp_1b)';
hold on
y2 = [0,0];
x2 = [0,672];
plot (x2,y2)
i =[1:672];
  hpp_2a = 0;
  hpp_2b = 0;
hpp_2 = (hpp_2a*i + hpp_2b)';
hold on
.
.
.
area (all_bi_b_t)
hold on
area (all_bi_b_f)
hold on
dem_v = [27418724.0991662,26165302.8337808,25124412.4234669,24728103.8269060,
24170583.1443737,23788897.6922005,23273747.8439285,23279252.4912392,
23154273.1077555,23447553.2039359,23580935.2809722,24057813.0593726,
25262958.8294847,27203120.2601192,29464106.3499684,31709020.1063699,
33522527.2537740,35577018.2142063,36492276.4069968,37399328.8761905,
37869040.2095238,37506894.9904762,37620099.3024631,37967074.1576355,
38131037.4476191,38152436.3809524,38423190.2957394,38239849.6545809,
37975386.4686717,37554345.9523810,37384195.4095238,37005352.5287356,
37517125.6059113,36441891.8680015,35825881.5381700,37569298.2893814,
37249778.8140144,37482358.6367569,38718123.8335624,40277600.1481481,
42185986.6188769,41242482.2843489,40738420.0334528,39386883.3691756,
36183314.0501792,33366556.7108093,31480303.7077475,29204258.9605735];

dem_h = [0,186.3829787,372.7659787,559.1489787,745.5319787,931.9149787,
1118.297979,1304.680979,1491.063979,1677.446979,1863.829979,2050.212979,
2236.595979,2422.978979,2609.361979,2795.744979,2982.127979,3168.510979,
3354.893979,3541.276979,3727.659979,3914.042979,4100.425979,4286.808979,
4473.191979,4659.574979,4845.957979,5032.340979,5218.723979,5405.106979,
5591.489979,5777.872979,5964.255979,6150.638979,6337.021979,6523.404979,
6709.787979,6896.170979,7082.553979,7268.936979,7455.319979,7641.702979,
7828.085979,8014.468979,8200.851979,8387.234979,8573.617979,8760];
plot (dem_h,dem_v)
```

**Listing 3:** *Example of matlab code for finding combined daily production.*

```
june_bi_b_f_DAILY(:,1)=(june_bi_b_f(1:24,1));
june_bi_b_f_DAILY(:,2)=(june_bi_b_f(25:48,1));
.
.
.
june_bi_b_f_DAILY(:,29)=(june_bi_b_f(673:696,1));
june_bi_b_f_DAILY(:,30)=(june_bi_b_f(697:720,1));

for K=1:24
        AVG_june_bi_b_f(K)=(mean(june_bi_b_f_DAILY(K,:)));
end

AVG_june_bi_b_f = (AVG_june_bi_b_f)';

june_bi_b_f_combined(:,1)=(AVG_june_bi_b_f(1:24,1));
june_bi_b_f_combined(:,2)=(hpp_prod(1:24,1));

area (june_bi_b_f_combined)
hold on

dem_v = [31480303.7077475,29204258.9605735,27418724.0991662,
26165302.8337808,25124412.4234669,24728103.8269060,24170583.1443737,
23788897.6922005,23273747.8439285,23279252.4912392,23154273.1077555,
23447553.2039359,23580935.2809722,24057813.0593726,25262958.8294847,
27203120.2601192,29464106.3499684,31709020.1063699,33522527.2537740,
35577018.2142063,36492276.4069968,37399328.8761905,37869040.2095238,
37506894.9904762,37620099.3024631,37967074.1576355,38131037.4476191,
38152436.3809524,38423190.2957394,38239849.6545809,37975386.4686717,
37554345.9523810,37384195.4095238,37005352.5287356,37517125.6059113,
36441891.8680015,35825881.5381700,37569298.2893814,37249778.8140144,
37482358.6367569,38718123.8335624,40277600.1481481,42185986.6188769,
41242482.2843489,40738420.0334528,39386883.3691756,36183314.0501792,
33366556.7108093];
dem_h = [1,1.5,2,2.5,3,3.5,4,4.5,5,5.5,6,6.5,7,7.5,8,8.5,9,9.5,10,
10.5,11,11.5,12,12.5,13,13.5,14,14.5,15,15.5,16,16.5,17,17.5,18,18.5,
19,19.5,20,20.5,21,21.5,22,22.5,23,23.5,24,24.5];
plot (dem_h,dem_v)
axis([1 24 0 45000000])
xticks([1,2,3,4,5,6,7,8,9,10,11,12,13,14,15,16,17,18,19,20,21,22,23,24])
xticklabels({'1','2','3','4','5','6','7','8','9','10','11','12','13','14','15','16'
    ,'17','18','19','20','21','22','23','24'})
xlabel ('Day [h]')
ylabel ('MW')
grid on
hold off
```

# E PVsyst reports: loss overview

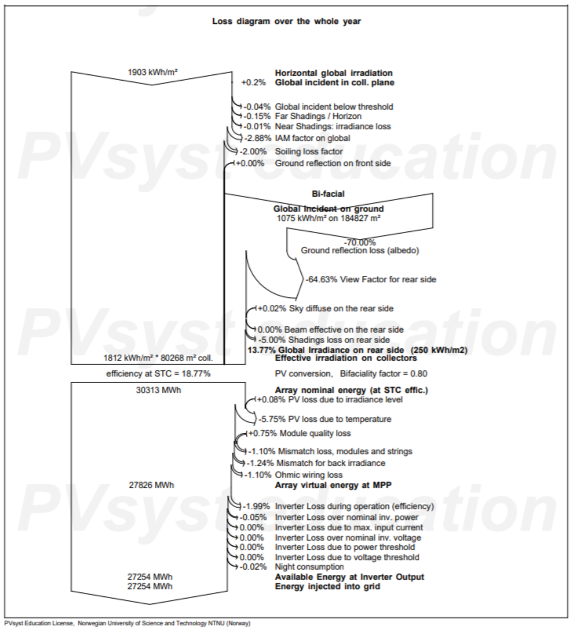


**(a)** *15 MW*

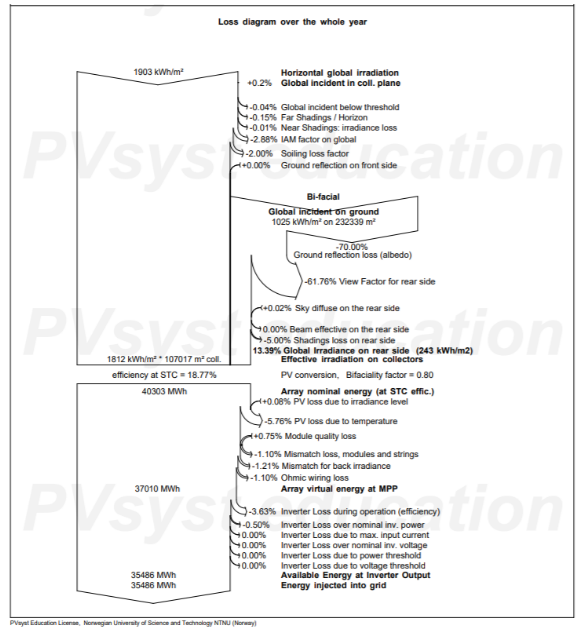


**(b)** *20 MW*

**Figure E.0.1:** *LG fixed tilt*

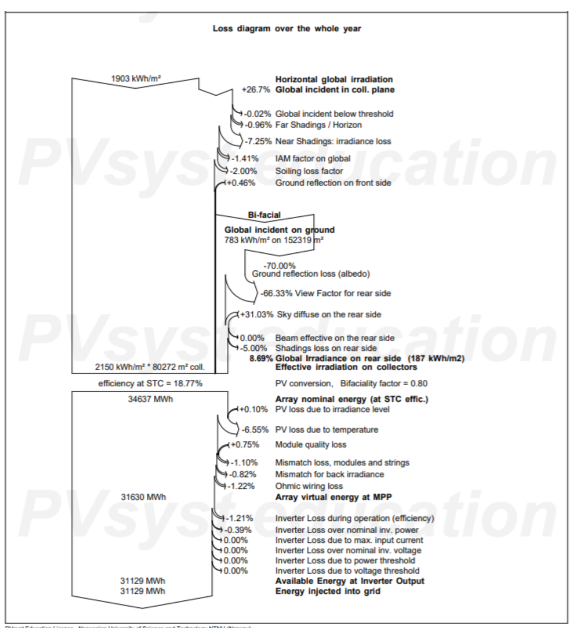


**(a)** *15 MW*

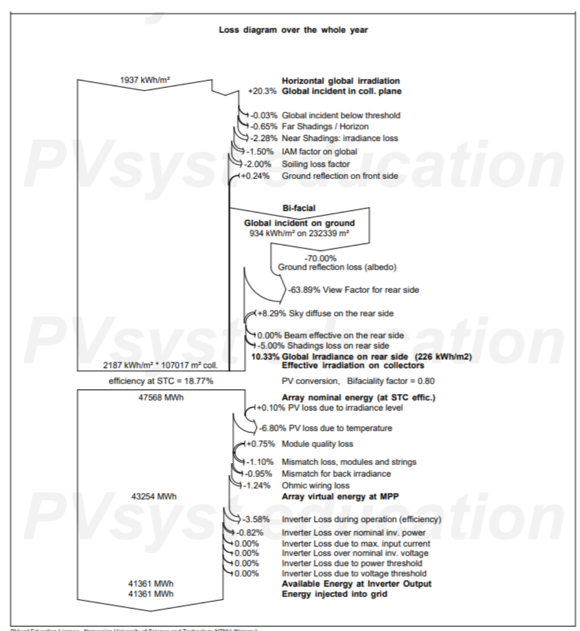


**(b)** *20 MW*

**Figure E.0.2:** *LG HSAT*

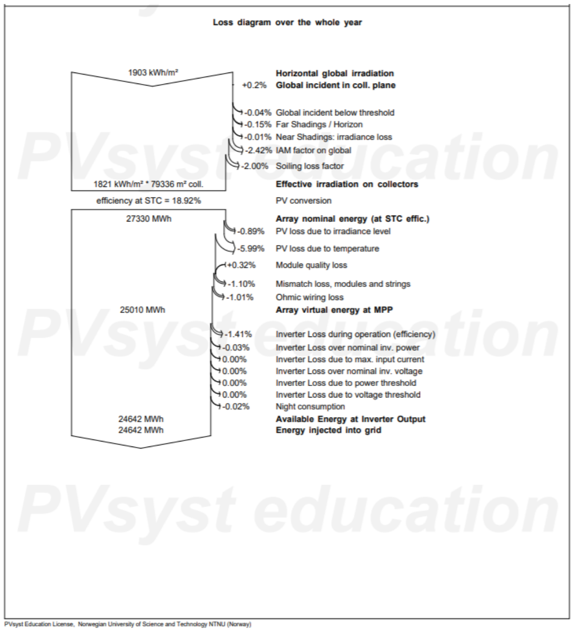


**(a)** *15 MW*

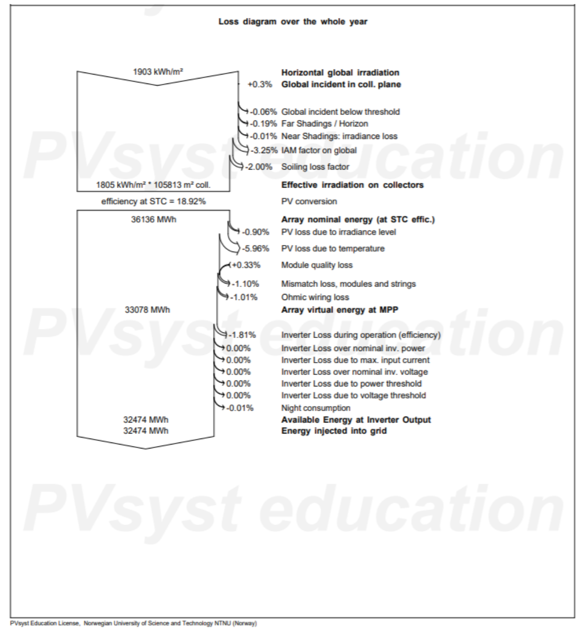


**(b)** *20 MW*

**Figure E.0.3:** *Canadian Solar fixed tilt*

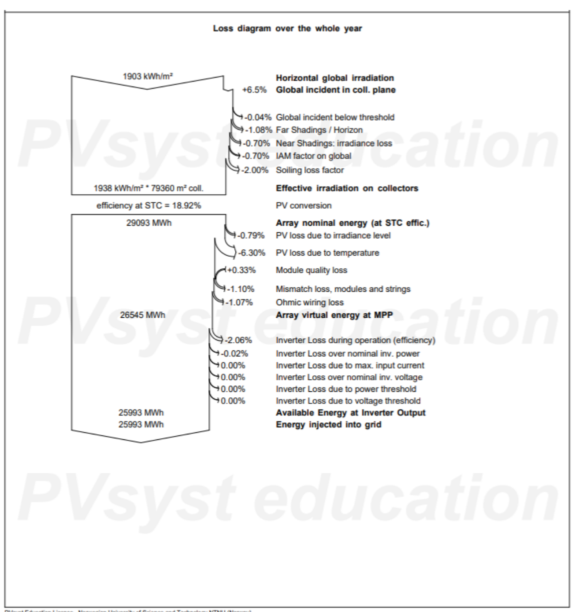


**(a)** *15 MW*

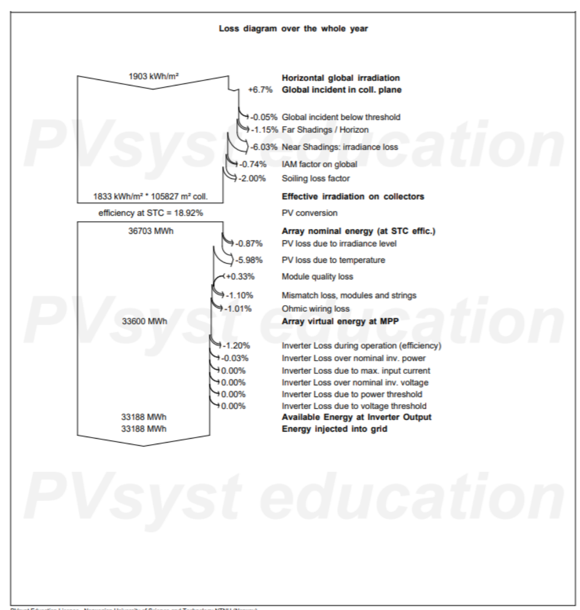


**(b)** *20 MW*

**Figure E.0.4:** *Canadian Solar HSAT*

# F Economics calculations

## NPV

**Table F.1:** *NPV calculations for case 1 with fixed tilt.*

| Year | Price per kWh | Earned |
|---|---|---|
| 1 | 0,0983 | 2252255,4 |
| 2 | 0,1016 | 2332900,8 |
| 3 | 0,0997 | 2286468,6 |
| 4 | 0,0997 | 2286468,6 |
| 5 | 0,0997 | 2286468,6 |
| 6 | 0,0997 | 2286468,6 |
| 7 | 0,0997 | 2286468,6 |
| 8 | 0,0997 | 2286468,6 |
| 9 | 0,0997 | 2286468,6 |
| 10 | 0,0997 | 2286468,6 |
| 11 | 0,0997 | 2286468,6 |
| 12 | 0,0997 | 2286468,6 |
| 13 | 0,0997 | 2286468,6 |
| 14 | 0,0997 | 2286468,6 |
| 15 | 0,0997 | 2286468,6 |
| 16 | 0,0696 | 1550884,8 |
| 17 | 0,0509 | 1093894,2 |
| 18 | 0,0348 | 700442,4 |
| 19 | 0,0348 | 700442,4 |
| 20 | 0,0348 | 700442,4 |
| 21 | 0,0348 | 700442,4 |
| 22 | 0,0343 | 688223,4 |
| 23 | 0,0343 | 688223,4 |
| 24 | 0,0343 | 688223,4 |
| 25 | 0,0343 | 688223,4 |
| | 1,8929 | 42508690,2 |
| **Avg. Price** | 0,075716 | |

| Year | Value | Sum |
|---|---|---|
| 0 | -16350000 | -16350000 |
| 1 | 2047504,909 | -14302495,09 |
| 2 | 1928017,19 | -12374477,9 |
| 3 | 1717857,701 | -10656620,2 |
| 4 | 1561688,819 | -9094931,381 |
| 5 | 1419717,108 | -7675214,273 |
| 6 | 1290651,917 | -6384562,356 |
| 7 | 1173319,924 | -5211242,432 |
| 8 | 1066654,477 | -4144587,955 |
| 9 | 969685,8877 | -3174902,068 |
| 10 | 881532,6252 | -2293369,442 |
| 11 | 801393,2957 | -1491976,147 |
| 12 | 728539,3597 | -763436,787 |
| 13 | 662308,5088 | -101128,2781 |
| 14 | 602098,6444 | 500970,3662 |
| 15 | 547362,404 | 1048332,77 |
| 16 | 337517,7187 | 1385850,489 |
| 17 | 216421,1358 | 1602271,625 |
| 18 | 125980,7225 | 1728252,347 |
| 19 | 114527,9295 | 1842780,277 |
| 20 | 104116,2996 | 1946896,576 |
| 21 | 94651,18142 | 2041547,758 |
| 22 | 84545,47361 | 2126093,231 |
| 23 | 76859,52146 | 2202952,753 |
| 24 | 69872,29224 | 2272825,045 |
| 25 | 63520,26567 | 2336345,311 |
| | 2336345,311 | |

| Yearly production | 25-year production |
|---|---|
| 24438000 | 610950000 |

| Investment cost |
|---|
| 16350000 |

| O&M |
|---|
| 150000 |

## LCOE

**Table F.2:** *LCOE calculations for case 1 with fixed tilt.*

| 15 MW | Production | Investmentcost | O&M-costs | | Discount rate | Life of system |
|---|---|---|---|---|---|---|
| Mono, fix | 24438000 | 16350000 | 150000 | | 1,1 | 25 |
| Mono, track | 25818000 | 16665000 | 150000 | | | |
| Bifacial, fix | 27254000 | 16575000 | 150000 | | | |
| Bifacial, track | 30658000 | 16890000 | 150000 | | | |

| | | Mono, fixed | Mono, track | Bifacial, fixed | Bifacial, track |
|---|---|---|---|---|---|
| Year | Discounted O&M | Discounted prod | Discounted prod | Discounted prod | Discounted prod |
| 1 | 136363,6364 | 22216363,64 | 23470909,09 | 24776363,64 | 27870909,09 |
| 2 | 123966,9421 | 20196694,21 | 21337190,08 | 22523966,94 | 25337190,08 |
| 3 | 112697,2201 | 18360631,1 | 19397445,53 | 20476333,58 | 23033809,17 |
| 4 | 102452,0183 | 16691482,82 | 17634041,39 | 18614848,71 | 20939826,51 |
| 5 | 93138,19846 | 15174075,29 | 16030946,72 | 16922589,74 | 19036205,92 |
| 6 | 84671,08951 | 13794613,9 | 14573587,93 | 15384172,49 | 17305641,75 |
| 7 | 76973,71773 | 12540558,09 | 13248716,3 | 13985611,35 | 15732401,59 |
| 8 | 69976,10703 | 11400507,36 | 12044287,54 | 12714192,14 | 14302183,26 |
| 9 | 63614,64276 | 10364097,6 | 10949352,31 | 11558356,49 | 13001984,78 |
| 10 | 57831,49341 | 9421906,907 | 9953956,646 | 10507596,81 | 11819986,17 |
| 11 | 52574,08492 | 8565369,916 | 9049051,497 | 9552360,736 | 10745441,97 |
| 12 | 47794,62266 | 7786699,923 | 8226410,452 | 8683964,306 | 9768583,609 |
| 13 | 43449,65696 | 7078818,112 | 7478554,956 | 7894513,005 | 8880530,554 |
| 14 | 39499,68815 | 6435289,193 | 6798686,324 | 7176830,005 | 8073209,595 |
| 15 | 35908,80741 | 5850262,902 | 6180623,931 | 6524390,914 | 7339281,45 |
| 16 | 32644,37037 | 5318420,82 | 5618749,028 | 5931264,467 | 6672074,045 |
| 17 | 29676,70034 | 4834928,019 | 5107953,662 | 5392058,606 | 6065521,859 |
| 18 | 26978,81849 | 4395389,108 | 4643594,238 | 4901871,46 | 5514110,781 |
| 19 | 24526,19862 | 3995808,28 | 4221449,307 | 4456246,782 | 5012827,983 |
| 20 | 22296,5442 | 3632552,982 | 3837681,188 | 4051133,438 | 4557116,348 |
| 21 | 20269,58564 | 3302320,892 | 3488801,08 | 3682848,58 | 4142833,044 |
| 22 | 18426,89604 | 3002109,902 | 3171637,346 | 3348044,164 | 3766211,858 |
| 23 | 16751,72367 | 2729190,82 | 2883306,678 | 3043676,513 | 3423828,962 |
| 24 | 15228,8397 | 2481082,564 | 2621187,889 | 2766978,648 | 3112571,783 |
| 25 | 13844,39973 | 2255529,603 | 2382898,081 | 2515435,134 | 2829610,712 |
| **Sum** | **1361556,003** | **221824704** | **234351019,2** | **247385648,7** | **278283892,9** |

| 15MW | LCOE (USD/kWh) |
|---|---|
| Mono, fix | 0,079844831 |
| Mono, track | 0,076921176 |
| Bifacial, fix | 0,072504432 |
| Bifacial, track | 0,065586103 |

NTNU
Norwegian University of
Science and Technology